Visual Impairments Following Birth Asphyxia:

Unravelling the Role of Retinopathy

Suna Jung

Integrated Program in Neuroscience

Faculty of Medicine

McGill University, Montreal

February, 2018

A thesis submitted to McGill University in partial fulfillment of the requirements

of the degree of Ph.D.

TABLE OF CONTENTS

CHAPTER V: REFERENCES

CHAPTER VI: APPENDICES

PREFACE

PART I

ABSTRACT

Birth asphyxia (i.e., insufficient delivery of oxygen and blood to the organs around the time of birth) is a leading cause of childhood visual impairments and blindness in developed countries. Visual impairments following birth asphyxia have been attributed primarily to injury to the visual pathways within the brain. Much like the brain, adequate oxygen and blood supply is critical for the development and maintenance of the retinal function and structure. Despite this, potential retinal contribution to visual impairments remains understudied in term asphyxiated newborns. The purpose of my thesis was to investigate the effects of neonatal hypoxia-ischemia on the function and structure of the retina in rats at term-equivalent age. Hypoxia-ischemia was induced in postnatal day 10 (P10) male Long-Evans rats by a unilateral ligation of the left common carotid artery followed by a 2-hour exposure to 8% oxygen. Retinal function was assessed using the flash electroretinogram (ERG) at P30 and P60, while the structure was assessed by retinal histology at P60. Retinocortical function and brain structure were evaluated by flash visual evoked potential (VEP) and histology, respectively, at P60. Hypoxia-ischemia induced a retinopathy, which manifested mainly in the inner retina (attenuated ERG b-wave amplitude and decreased inner retinal thickness) while sparing the outer retina (no change in the ERG a-wave and slightly increased outer nuclear layer thickness). The VEP P100 amplitude was also found to be attenuated; however, there was no correlation between the severity of retinal injury and brain injury at the level of function and structure, suggesting a potential independent contribution of retina and brain injury to the development of visual impairments following birth asphyxia.

The second purpose of my thesis was to determine if sildenafil could rescue retinal changes resulting from neonatal hypoxia-ischemia as described above. Sildenafil is a

phosphodiesterase type-5 inhibitor that has been shown to have a neuroprotective and neurorestorative role in animal models of neurologic diseases, such as ischemic stroke, Alzheimer's disease and multiple sclerosis. Vehicle or sildenafil (2, 10 or 50 mg/kg) was administered by oral gavage twice daily for 7 consecutive days, with a 12-hour delay following the induction of hypoxia-ischemia in P10 male Long-Evans rats. Flash ERG recordings at P29 revealed a dose-dependent improvement of the affected ERG amplitudes (scotopic a- and b-wave, photopic b-wave and photopic negative response) in rats subjected to hypoxia-ischemia. Retinal histology from these rats also showed corroborating normalization of retinal layer thicknesses with increasing doses of sildenafil at P30. Sildenafil did not have an effect on the normal retinal function as assessed in the sham control as well as the fellow eyes of the rats subjected to hypoxia-ischemia.

In conclusion, using a rat model of term neonatal hypoxic-ischemic encephalopathy, I demonstrate that function and structure of the retina are susceptible to hypoxic-ischemic injury and that the outcome of injury can be improved by oral sildenafil. These findings suggest a role of retinal injury as opposed to brain injury alone in the development of visual impairments following birth asphyxia and a potential therapeutic role of sildenafil in treating this disease. Cellular and molecular mechanisms underlying the pathophysiology of retinopathy as well as the beneficial effects of sildenafil remain to be elucidated.

RÉSUMÉ

L'asphyxie à la naissance (c.-à-d. l'apport insuffisant d'oxygène et de sang aux organes au moment de la naissance) est une des principales causes de déficience visuelle et de cécité chez les enfants dans les pays développés. Les déficiences visuelles à la suite de l'asphyxie à la naissance ont été attribuées principalement à une lésion des voies visuelles dans le cerveau. Tout comme le cerveau, l'apport adéquat d'oxygène et de sang est essentiel au développement et au maintien de la fonction et des structures rétiniennes. Malgré cela, la contribution rétinienne potentielle aux déficiences visuelles reste sous étudiée chez les nouveau-nés asphyxiés à terme. Le but de ma thèse était d'étudier les effets de l'hypoxie-ischémie néonatale sur la fonction et la structure de la rétine chez des rats d'âge équivalent à terme. L'hypoxie-ischémie a été induite 10 jours après la naissance (P10) chez des rats mâles Long-Evans par une ligature unilatérale de l'artère carotide commune gauche, suivie d'une exposition de 2 heures à 8% d'oxygène. La fonction rétinienne a été évaluée en utilisant l'électrorétinogramme flash (ERG) à P30 et P60, alors que la structure a été évaluée par histologie rétinienne à P60. La fonction rétinocorticale et la structure cérébrale ont été évaluées par des potentiels évoqués visuels par flash (PEV) et par histologie, respectivement, à P60. L'hypoxie-ischémie a induit une rétinopathie qui se manifeste principalement dans la rétine interne (l'amplitude de l'onde-b de l'ERG est atténuée et l'épaisseur rétinienne interne est diminuée), tout en épargnant la rétine externe (pas de changement de l'onde-a de l'ERG et l'épaisseur de la couche nucléaire externe légèrement augmentée). L'atténuation de l'amplitude du P100 du PEV a aussi été constatée; Cependant, il n'y avait aucune corrélation entre la gravité des lésions rétiniennes et des lésions cérébrales au niveau de la fonction et de la structure, suggérant une contribution indépendante potentielle de la rétine et

des lésions cérébrales au développement d'une déficience visuelle suite à l'asphyxie à la naissance.

Le second objectif de ma thèse était de déterminer si le sildénafil pouvait sauver les changements rétiniens résultant de l'hypoxie-ischémie néonatale comme décrit ci-dessus. Le sildénafil est un inhibiteur de la phosphodiestérase de type 5 qui a été démontré pour avoir un rôle neuroprotecteur et neurorestauratif dans les modèles animaux de maladies neurologiques, telles que les accidents vasculaires cérébraux ischémiques, la maladie d'Alzheimer et la sclérose en plaques. Le véhicule ou le sildénafil (2, 10 ou 50 mg/kg) a été administré par gavage oral deux fois par jour pendant 7 jours consécutifs, avec un délai de 12 heures après l'induction d'une hypoxie-ischémie chez des rats Long-Evans mâles à P10. Les enregistrements d'ERG flash à P29 ont révélé une amélioration dose-dépendante des amplitudes d'ERG affectées (ondes-a et-b scotopiques, onde-b photopique et la réponse photopique négative) chez les rats soumis à une hypoxie-ischémie. L'histologie rétinienne de ces rats a également montré une normalisation correspondante de l'épaisseur de la couche rétinienne avec des doses croissantes de sildénafil à P30. Le sildénafil n'a pas eu d'effet sur la fonction rétinienne normale tel que démontré dans le groupe placebo, ainsi que sur les yeux controlatéraux des rats soumis à une hypoxie-ischémie.

En conclusion, en utilisant un modèle d'encéphalopathie hypoxique-ischémique néonatale chez le rat à terme, je démontre que la fonction et la structure de la rétine sont sensibles à une lésion hypoxique-ischémique et que les conséquences de ce traumatisme peuvent être améliorées par le sildénafil oral. Ces résultats suggèrent un rôle des lésions rétiniennes par opposition aux lésions cérébrales seules dans le développement de déficiences visuelles à la suite d'une asphyxie à la naissance et un rôle thérapeutique potentiel du sildénafil dans le traitement de cette maladie.

Les mécanismes cellulaires et moléculaires sous-jacents à la physiopathologie de la rétinopathie ainsi que sur les effets bénéfiques du sildénafil restent à élucider.

ACKNOWLEDGMENTS

I would like to express my sincere gratitude to my supervisor, Dr. Pia Wintermark and co-supervisor, Dr. Pierre Lachapelle for giving me the opportunity to pursue my graduate studies under their supervision and for their excellent supervision, guidance and support throughout my Master's and PhD journey. Their input was invaluable to the completion of my PhD thesis as well as to my growth as a scientist and a person. They will forever be my scientific mom and dad, and I will always carry with me the precious skills, lessons, values and memories I learned/formed during my training as I move forward in life.

I would also like to thank the members of my advisory committee, Dr. John M Little and Dr. Sylvain Chemtob for providing me with their helpful advice, feedback and support. I also am grateful to my IPN mentor, Dr. Thomas Stroh and the external examiner, Dr. Aimee Ryan for their presence and input at my doctoral candidacy exam.

I would like to acknowledge the instrumental training and assistance provided by the past and present members of the Wintermark and Lachapelle Laboratories, as well as the collaborators and the staff of the RI-MUHC platforms, which made my animal research possible. I thank Dr. Anna Polosa for training me in all techniques, analyses and presentation of data related to the retina, and for helping me with the collection of some ERG and VEP data and the rat tissues. I thank her also for her critical reading of the first manuscript. I thank Zehra Khoja for her invaluable assistance in carotid ligation surgery and hypoxia, sildenafil administration, tissue collection, and brain and eye cryo-sectioning and Aaron Johnstone for training me in carotid ligation surgery and hypoxia, and for performing surgery/hypoxia, sildenafil administration, and tissue collection for the sildenafil study, as well as his critical reading of the second manuscript. I

thank Xiaojuan Yang for her assistance in tissue collection and for training me in retina and RPE/choroid/sclera flatmount techniques and Armin Yazdani for his help with perfusion and tissue collection. I thank Hyba Bessaklia for her assistance in collecting some long-term ERG and VEP data points, Laurel Stephens for her technical assistance in tissue collection and retinal sectioning for the sildenafil study, and Laura Dale for her technical assistance in tissue collection for the sildenafil study. I also am grateful to Dr. Sylvain Chemtob and the members of his laboratory, Dr. José Carlos Rivera and Dr. Tianwei Ellen Zhou for sharing their retina and RPE/choroid/sclera flatmount and staining protocols. I thank Dr. Emmanuel Rampakakis for his contribution to the statistical analysis of the data in the second manuscript. I thank Wayne Ross Egers for his professional English editing of the first and second manuscripts. I thank RI-MUHC Histopathology Platform for their service on the staining of the brain sections for the first manuscript. I thank Dr. Min Fu and Shi-Bo Feng at the RI-MUHC Molecular Imaging Platform for their training and assistance in confocal imaging. Finally, I thank staff of the RI-MUHC Animal Facility for taking good care of my rats.

Although the data from the human study were only briefly introduced in my discussion, I would like to acknowledge the invaluable help and effort put into the study by numerous people. First and most, I am grateful to the babies and their families who participated in our study. It was a privilege to interact and work with them. Next, I would like to thank everyone who was involved in the eye exams. I thank Dr. John Little for examining the newborns and sharing his expert knowledge and Dr. Allison Dorfman for recording the ERG/VEP in newborns and helping with the interpretation of the data. Without their help, the study would not have been possible. I also thank Philippe Lamer, NNP for helping with the fundus imaging. In addition, I thank the ophthalmology residents, orthoptists and administrative staff at the Ophthalmology Clinic at the

Montreal Children's Hospital for their assistance during the ophthalmic exams. I am grateful to the clinical and administrative teams of the Neonatal Intensive Care Unit at the Montreal Children's Hospital (neonatologists, residents, nurse managers, bed nurses, transport nurses, nurse assistants, pharmacists and unit coordinators) for helping with the countless behind-the-scene steps from recruitment to getting to the exams. I thank the nurse managers, assistant nurse managers, and Dr. Denis Leduc at the Maternity Care Unit of the Royal Victoria Hospital for helping us to recruit healthy babies in our study. I also thank the MRI team at the Montreal Children's Hospital. Last but not least, I thank each and every one of the past and present members of the NeoBrain Lab who was involved in the human eye exam study. Special thanks to Elodie Boudes, Megan Sheppard, Arjun Paliwal and Saskia Kwan for their contribution before I came on board, and Elodie Boudes and Megan Sheppard for training me for a smooth transition into the project. Big thanks to Priscille-Nice Sanon for her help during the eye exams and with scheduling of the follow-up exams and Eric Xu for always extending his helping hands when I needed them. I thank Armin Yazdani, Parissa Owji, Annie Poon, Eric Xu, Bianca Olivieri, Alexandra Bélanger and Palig Balian for the excellent teamwork and help with enrolling and organization processes.

I must acknowledge the tremendous moral support I received from my supervisors and lab mates. From the Wintermark lab: Elodie Boudes, Aaron Johnstone, Zehra Khoja, Priscille-Nice Sanon, Armin Yazdani, Annie Poon, Parissa Owji, Eric Xu, Bianca Olivieri, Alexandra Bélanger and Palig Balian; from the Lachapelle Lab: Anna Polosa, Allison Dorfman, Mathieu Gauvin, Samaneh Chaychi, Xiaojuan (Joanna) Yang, Antoine Brassard Simard, Hyba Bessaklia, Mina Ghabraie, Thaina Rosinvil, Shasha Lv and Mercedes Gauthier; and from our neighbour Dr.

Sébire's lab, Marie-Julie Allard. I thank them for all the scientific and non-scientific discussions, therapy sessions, activities, conferences and etc., and most of all their friendship that made my graduate student life enjoyable and special. I also thank summer students and undergraduate students that came and went for each making their contribution and helping me become a better teacher.

I would like to thank Dr. Giamal Luheshi and Dr. Argel Aguilar-Valles for giving me the first opportunity in research as an undergraduate co-op student and helping me develop my interest in neuroscience research and Dr. Shernaz Bamji and Dr. Stefano Brigidi for taking me under their supervision for my honours thesis and helping me take my interest further.

I would like to thank my friends near and far for their support and for always being there for me. Lastly, I would like to thank my relatives and family for believing in me and cheering me on throughout my studies. To my mom and dad and my brother, thank you for your unconditional love and support. You are my biggest role models and source of strength and inspiration.

I thank my supervisors for reading my thesis and Google and Mercedes Gauthier for the French translation of the abstract.

My graduate studies were supported by the CIHR Master's Award: Frederick Banting and Charles Best Canada Graduate Scholarship, RI-MUHC Foundation of Stars Studentship, IPN Returning Student Fellowship, Green Cross Scholarship – Korean Canadian Scientists

Scholarship Foundation, and the Vanier Canada Graduate Scholarship (CIHR). I extend my sincere thanks to their generous contributions.

PREFACE

PART II

PREFACE

Visual impairments following birth asphyxia of term babies have been attributed to brain injury for the most part, and few studies exist on the impact of birth asphyxia on the retina. This thesis aims to narrow the knowledge gap by first identifying the functional and structural consequences of neonatal hypoxia-ischemia on the retina in a widely used rat model of term neonatal hypoxic-ischemic encephalopathy, namely the Vannucci model. The main contribution of this thesis includes a demonstration of retinal injury in this model and a detailed description of how the retinopathy manifests. At short-term (up to P60), retinal injury was mostly limited to the function and structure of the inner retina, while the outer retina appeared to be resistant to injury. We characterized inter-individual variability in the severity of inner retinal injury, and described the heterogenous distribution of injury with respect to retinal eccentricity; these novel findings prompted further questions as to what regional or individual factors are at play in the development of these injuries. The second part of this thesis explores the potential role of sildenafil as a novel therapy to treat the retinopathy described in the first part. We showed that oral sildenafil improved in a dose-dependent manner both the functional and the structural outcome of the retinopathy induced following neonatal hypoxia-ischemia. We also showed that our treatment regimen did not have an adverse effect on the development of normal retinal function. We are the first to explore and demonstrate the beneficial effects of sildenafil on the function and structure of the retina in a neonatal hypoxia-ischemia model. This represents a step forward from assessing only the acute effects of sildenafil on retinal function or ocular blood flow in the context of side effects of the drug, and a possibility of new treatment option for other ischemic or degenerative retinopathies. This thesis also provides some preliminary evidence of vascular anomaly and long-term degeneration of the outer retina in this animal model, as well as

evidence of abnormal retinal function in human asphyxiated newborns treated with hypothermia, all of which are considered as original scholarship.

CONTRIBUTION OF AUTHORS ON CO-AUTHORED PAPERS

1. Manuscript 1 (Chapter II)

Jung S, Polosa A, Lachapelle P, Wintermark P (2015) Visual impairments following term neonatal encephalopathy: do retinal impairments also play a role? Invest Ophthalmol Vis Sci 56(9):5182-5193.

PW, PL and I designed the study. I performed HI induction in rats, ERG and VEP recording and analysis, tissue (retina and brain) collection, retinal histology and analysis, brain surface area measurements, and statistical analyses. AP trained me in ERG, VEP, and retinal histology techniques and helped me with the tissue collection. I prepared the tables and figures, and wrote the first draft of the manuscript. AP, PL, PW and I revised the manuscript. All of the work was done under the supervision of PL and PW.

2. Manuscript 2 (Chapter III)

Jung S, Johnstone A, Khoja Z, Rampakakis E, Lachapelle P, Wintermark P (2016) Sildenafil improves functional and structural outcome of retinal injury following term neonatal hypoxia-ischemia. Invest Ophthalmol Vis Sci 57(10): 4306-4314.

PW, AJ, PL, and I designed the study. AJ and ZK performed HI induction and sildenafil administration in rats and collected the tissues. I performed ERG, retinal histology, and

respective data analyses. ER performed the statistical analysis. I prepared the tables and figures, and wrote the first draft of the manuscript. AJ provided critical review of the manuscript. PL, PW and I revised the manuscript. All of the work was done under the supervision of PL and PW.

CHAPTER I

INTRODUCTION

AND

LITERATURE REVIEW

INTRODUCTION

Despite improvements in neonatal care, neonatal hypoxia-ischemia (HI), which refers to insufficient delivery of oxygen and blood to the body's tissues around the time of birth, remains a serious condition that causes significant mortality and long-term morbidity, such as cerebral palsy, mental retardation and visual impairments (AAP, 1992; Al-Macki et al., 2009). Although neonatal HI and resulting hypoxic-ischemic encephalopathy (HIE) in *term* newborns have been extensively investigated, relatively few studies have explored its impact on vision, despite birth asphyxia being one of the major causes of pediatric visual impairments in developed countries (Hoyt, 2003). Up to now, visual impairments in asphyxiated newborns have been attributed primarily to brain injury along the visual pathways, especially those occurring on the posterior pathway (i.e., optic radiations, primary visual cortex, visual associative cortical areas, and/or visual attention pathways) (Foster, 1988; Eken et al., 1995; Hoyt, 2003, 2007; Huo et al., 1999). However, abnormalities on the anterior pathway, such as optic nerve atrophy, optic nerve hypoplasia and retinal atrophy, also have been reported (McCulloch et al., 1991; Muttitt et al., 1991). Yet in these studies, ophthalmic exams were performed when patients were older, and subsequently the authors were unable to conclude whether the abnormalities were a direct consequence of the HI insult or were secondary to the brain HI injury through retrograde degeneration (McCulloch et al., 1991). Ophthalmic exams as well as exams of visual function is not part of the standard monitoring practice of asphyxiated newborns, which makes it difficult to identify visual impairments early on as well as to determine whether retinal injury plays a role.

The retina has high metabolic demands and consumes the greatest level of oxygen per volume of tissue in the body (Flammer et al., 2013). It is therefore reasonable to suspect that a disruption of blood flow and oxygen would have direct negative consequences on the retina.

Evidence for retinal susceptibility to HI is well documented in ischemic retinopathy in adults and premature infants (retinopathy of prematurity), as well as animal models of such conditions (Osborne et al., 2004; Dorfman et al., 2008; Rey-Funes et al., 2013; Huang et al., 2012). **Thus, I hypothesized that visual impairments following term neonatal HI could be due to retinal injury in addition to brain injury.** One way we can investigate the effect of neonatal HI on the retina is to use an animal model of term neonatal HIE, the Vannucci model (Rice et al., 1981). In this model, postnatal day (P) 10 (i.e., the age at which the developmental stage of the central nervous system in rats is similar to that in humans at term) rat pups are subjected to a unilateral ligation of the common carotid artery (ischemia) followed by a 2-hour exposure to 8% oxygen (hypoxia), which produces brain injury on the hemisphere ipsilateral to the ligation. This model allows us to study the effect of HI also on the retina, since the common carotid artery gives rise to the arteries that supply the retina. **The first aim of my thesis, therefore, was to determine the effects of neonatal HI on the structure and function of the retina in the rat model of term neonatal HIE.**

If my first hypothesis holds true, it would be imperative to find a treatment that could rescue the retinal injury. Currently, hypothermia remains the sole standard therapy for newborns with neonatal encephalopathy resulting from birth asphyxia. It is a neuroprotective strategy aimed at preventing reperfusion injury and is shown to improve neurologic outcome when the treatment is initiated within 6 hours of life (Azzopardi et al., 2009; Gluckman et al., 2005; Shankaran et al., 2005). Unfortunately, hypothermia only benefits 1 in 6 treated newborns (Edwards et al., 2010; Shah, 2010; Jacobs et al., 2013). In addition, the requirement of a tertiary care setting and relatively short treatment window further limit those who can potentially benefit from the treatment. Taken together, a novel therapy is needed. Sildenafil is a potent vasodilator

that is widely used to treat erectile dysfunction and pulmonary hypertension in adults and is also used to treat persistent pulmonary hypertension in newborns (Goldstein et al., 1998; Barnett et al., 2006; Shah et al., 2011). Interestingly, it is emerging as a neuroprotective and/or neurorestorative agent based on studies done in animal models of neurologic diseases, such as stroke, Alzheimer's disease and multiple sclerosis (Bednar et al., 2008; Chen et al., 2014; Nunes et al., 2012; Zhang et al., 2005; Zhang et al., 2012; Zhang et al., 2013). In these studies, sildenafil promoted neuronal survival as well as neurogenesis, synaptogenesis and angiogenesis, and decreased neuroinflammation, leading to improved outcome. Whether the benefits of such effects extend to injured neurons in immature brain and retina in neonatal HI has not been widely tested. Sildenafil acts by inhibiting phosphodiesterase type-5 (PDE5), thereby increasing the level of cyclic guanosine monophosphate (cGMP). Based on the above findings in the brain and given the expression of PDE5 in several retinal layers and blood vessels (Foresta et al., 2008), **I hypothesized that sildenafil would have therapeutic effects on retinal neuronal injury following neonatal HI. Hence, the second aim of my thesis was to assess the ability of sildenafil to alleviate the effects of neonatal HI on retinal function and structure (if any) in the rat model of term neonatal HIE.** In the following section, I will provide a literature review of the relevant topics.

REVIEW OF THE RELEVANT LITERATURE

1. The Primary Visual Pathway

The primary visual pathways begin at the retina, where the photoreceptors transduce light into electrical signals, which are relayed to the bipolar cells, and subsequently to the retinal ganglion cells (RGCs) (Figure 1). Furthermore, the horizontal cells make contacts with the photoreceptors

and bipolar cells while the amacrine cells make contacts with the bipolar cells and the RGCs; the horizontal and amacrine cells contribute to the lateral flow of information (Tessier-Lavigne, 2000). The RGCs generate action potentials that are transmitted along their axons that form the optic nerve. The optic nerve synapses onto the neurons at the lateral geniculate nucleus (LGN) in the thalamus. These neurons send signals to the primary visual cortex in the occipital lobe via the optic radiations (Wurtz and Kandel, 2000).

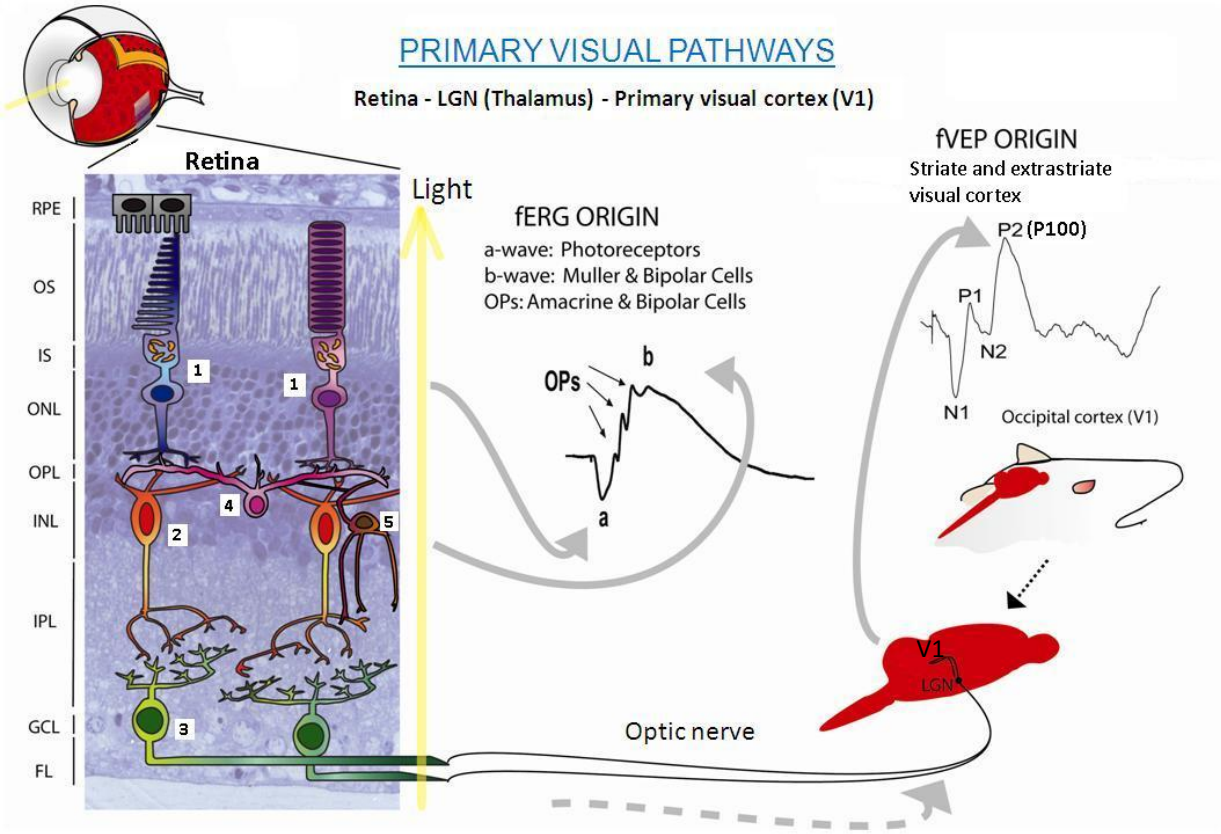

Figure 1. The primary visual pathways and the origins of the flash electroretinogram (fERG) and visual evoked potential (fVEP). Cartoon representation of the (1) cone and rod photoreceptors, (2) bipolar cells, (3) retinal ganglion cells, (4) horizontal cells, and (5) amacrine cells overlaid on retinal histology. RPE, retinal pigment epithelium; OS. outer segment; IS, inner segment; ONL, outer nuclear layer; OPL, outer plexiform layer; INL, inner nuclear layer; IPL, inner plexiform layer; GCL, ganglion cell layer; FL, fiber layer. The function of the retina and the primary visual pathways can be assessed using fERG and fVEP, respectively. The origins of the major components of fERG and fVEP of rats are illustrated. *©Anna Polosa, the figure was reproduced with modifications with the permission of the original author.*

Function of the retina and the primary visual pathways can be assessed by electrophysiological techniques, such as electroretinograms (ERGs) and visual evoked potentials (VEPs), respectively (Brown, 1968; Aminoff and Goodin, 1994) (Figure 1). The flash ERGs (fERGs) represent the global electrical activity of the retina in response to flashes of light. A typical mixed rod-cone ERG waveform of a mature rat is composed of a negative a-wave, which originates from the photoreceptors (Granit, 1933; Granit and Riddel, 1934; Penn and Hagins, 1969; Hood and Birch, 1990), followed by a positive b-wave which is thought to originate from the bipolar cells and Müller cells (Miller, 1973; Stockton and Slaughter, 1989; Knapp and Schiller, 1984). The flash VEPs (fVEPs) in turn represent the electrical activities of the visual cortex in response to flashes of light. The origins of the fVEP components are less clear but they are thought to be generated from the striate and extrastriate visual cortices (Siegel et al., 1996; Di Russo et al., 2001).

2. Normal Development of the Retina and its Vasculature

2.1. Development of the retina in rats

The eye forms from an out-pouching of the neural tube, which grows and folds inwards to form an optic cup (Galli-Resta et al., 2008). During this early stage of development, the optic cup consists of two proliferating cell layers – a retinal pigment epithelium (RPE) on the outside or apical side, and a retinal neuroepithelium on the inside or basal side (Galli-Resta et al., 2008). The neuroblasts in the latter layer give rise to all types of retinal neurons as well as Müller glia. The neurogenesis of the rat retina begins around embryonic day (E) 10 and is complete near P12, following a specific temporal and spatial sequence (Rapaport et al., 2004). The RGCs are the first to be generated and migrate basally to form a ganglion cell layer (GCL). The horizontal

cells, cones, and amacrine cells are subsequently generated during the embryonic period (Rapaport et al., 2004). The cones and horizontal cells remain in the neuroblastic layer (NBL), whereas the amacrine cells migrate to the basal side of the NBL, forming a rudiment of the inner nuclear layer (INL) that is continuous with the NBL, or towards the GCL (Galli-Resta et al., 2008). The dentritic processes of the amacrine cells start to form the inner plexiform layer (IPL). The birth of the rods, bipolar cells and Müller glia begin during the late embryonic period (E16 for rods and E20 for bipolar cells and Müller glia) and continues postnatally until around P7 (Rapaport et al., 2004). Spatially, the generation of each cell type begins centrally and spreads peripherally (Rapaport et al., 2004). At P5, the outer plexiform layer (OPL) first appears at the central retina as the horizontal cell to photoreceptor synapses begin to form, and subsequently spreads to the retinal periphery by P7, separating the NBL to outer and inner portions which become the outer nuclear layer (ONL) and the INL, respectively (Braekevelt and Hollenberg, 1970). At P7, the inner segment (IS) and outer segment (OS) of the photoreceptor start to elongate and reach mature lengths between P10–14 (Weidman and Kuwabara, 1968). Also, the developing bipolar cell processes make synaptic connections with the photoreceptor axonal endings between P10–14 (Weidman and Kuwabara, 1968). At P9, all of the retinal layers are present from the retinal centre to periphery and the inner and outer plexiform layers have thickened (Braekevelt and Hollenberg, 1970). At around P10, the IPL also becomes more compact as developing Müller cell processes fill the space (Weidman and Kuwabara, 1968), essentially achieving adult-like retinal cell morphologies and laminar positioning (Reese, 2011). However, it is not until P12 that the bipolar to RGC synapses form in the IPL, which coincides with the appearance of recordable ERGs (Weidman and Kuwabara, 1986). The rats open their eyes at P14 and the retina continues to undergo structural and functional maturation until around

P30 (Weidman and Kuwabara, 1986; Dorfman et al., 2008).

2.2. Development of the retinal and choroidal vasculature in rodents

The retina is nourished by two major blood supplies, the retinal and choroidal vasculatures, which arise from the ophthalmic artery, which is one of the branches of the internal carotid artery. The choroidal vasculature sits above the RPE and indirectly supplies oxygen and nutrients to the RPE and underlying photoreceptors while the retinal vasculature directly supplies the inner retina (Osborne et al., 2004). Although the development of both vasculatures is primarily directed by a potent angiogenic factor, vascular endothelial growth factor (VEGF), , the timing and sequence of their development differ.

The development of the choroid in rodents depends on the expression of VEGF by the RPE during the embryonic period (Marneros et al., 2005). Hence, the choroid vessels are already quite well developed at birth. The retina at this point is supported by the choroid vasculature as well as the hyaloid vasculature in the vitreous, with the latter regressing once the retinal vasculature is in place (Yi et al., 1998; Marneros et al., 2005). VEGF is weakly expressed in the RPE throughout life, which appears to be important in the maintenance of the choroid (Yi et al. 1998).

In contrast, the development of the retinal vasculature occurs after birth and is thought to be driven by the increasing metabolic demands (“physiological hypoxia”) of the neural retina that undergoes differentiation and maturation (Chan-Ling and Stone, 1993). This in turn, acts as a signal to induce VEGF expression by the glial cells. The retinal vasculature is organized in three parallel layers of capillary network that are interconnected. The superficial plexus is the first to be formed as the VEGF-expressing astrocytes spread along the inner limiting membrane from the optic disc (P0–3) to periphery (P7). The deep plexus is formed by radial sprouting of

the superficial vessels into the outer margin of the INL, starting at the optic disc (P7) and spreading horizontally towards the retinal periphery (P11–12) (Stone et al., 1995). Formation of the deep plexus is guided by the VEGF expression of the INL cells. Finally, the intermediate plexus is formed by sprouting of the deep vessels to the inner margin of the INL, starting at around P11–12 in the central retina to reach the periphery at around P17 (Fruttiger, 2007). Recent studies have reported a close association between the horizontal and amacrine cells and the deep and intermediate plexus vessels, respectively, and suggested a role for these cells, rather than Müller cells, in guiding the deep and intermediate plexus formation (Usui et al., 2015). Newly formed retinal vessels retain plasticity for remodelling and pruning until they obtain pericyte coating (Benjamin et al., 1998). Unlike the RPE, Müller cells and astrocytes cease to express VEGF once the vessels are formed, and an excessive expression of VEGF in later ages are associated with pathological conditions, such as neovascularization (Yi et al., 1998).

2.3. Postnatal development of the retina and visual pathway in humans

In humans, differentiation and vascularization of the retina is almost complete at term (Horsten and Winkelman, 1962; Michaelson, 1948). The retina and the primary visual pathways are also functional at birth (Kriss and Russell-Eggitt, 1992). However, rapid maturational changes occur during the first four months of life. Structural changes include elongation of the rod and cone photoreceptor outer segments, differentiation of the fovea, thickening of the myelin sheath around the optic nerve and optic radiation, maturation of synaptic connections in the lateral geniculate bodies and visual cortex, and increase in the volume of primary and secondary visual cortices (Kriss and Russell-Eggitt, 1992). Functional development of the retina is characterized by increasing flash ERG amplitudes and sensitivity that reach adult values at around 6–12 months of age (Fulton and Hansen, 1985; Kriss and Russell-Eggitt, 1992). On the other hand, the

maturation of flash VEP is characterized by a progressive decrease in the latency of the main positive component, which is around 200 ms after the stimulus onset in newborns versus 100 ms in adults (Kriss and Russell-Eggitt, 1992).

3. Neonatal HI and Visual Impairments

Neonatal HIE is estimated to occur in 1.5 per 1000 live full-term births (Kurinczuk et al., 2010). Among affected newborns, about 15–20% die in the postnatal period and an additional 25% develop severe long-term neurological sequelae, including cerebral palsy, mental retardation, learning difficulties, and visual impairments (Kurinczuk et al., 2010).

In *term* asphyxiated newborns, the frontal and parieto-occipital cortices (the watershed areas between the anterior and middle cerebral arteries and between the posterior and middle cerebral arteries, respectively) as well as thalami, posterior putamen, hippocampus and corticospinal tracts have been found to be particularly vulnerable to HI (Hoyt, 2003). With respect to the visual system, damages to the primary and associative visual cortices have been associated with visual impairments in term asphyxiated newborns (Hoyt, 2003, 2007). However, it is not uncommon that these newborns also show damages to the lateral geniculate bodies and the optic radiations (Hoyt, 2003). Furthermore, changes in the optic nerve and the retina have also been noted, although the latter less frequently in term asphyxiated infants (McCulloch et al., 1991; Muttitt et al., 1991; Hoyt, 2007). These findings highlight the fact that visual problems resulting from neonatal HI is multifaceted, involving multiple structures along the visual pathway.

Functional integrity of the visual pathways in term asphyxiated newborns has been evaluated using electrophysiological recordings before hypothermia treatment became available.

One study reported subnormal flash ERG responses in 7- to 12-month-old asphyxiated infants, which normalized by 3 to 4 years of age (Nickel and Hoyt, 1982). According to McCulloch et al. (1991), 9 out of 25 term asphyxiated infants showed abnormal VEPs in the first week of life, and of those, 3 resolved while 6 remained abnormal at 2.5 to 4.5 years of age. Muttitt et al. (1991) also reported similar findings in term asphyxiated infants, where abnormal VEPs throughout the first week of life persisted to later ages. Although ERGs were simultaneously recorded with VEPs in both studies, only Muttitt and colleagues (1991) mentioned that they were normal. Furthermore, normative data in such young infants are sparse, making it difficult to determine what "normal" is.

4. HI and Retinal Damage

4.1. Susceptibility of the adult retina to HI injury

The retina has the highest metabolic demand in the body, and failure to meet such demand, as happens under prolonged ischemic conditions, leads to tissue damage. As such, retinal ischemia is a common cause of visual impairments and blindness implicated in diseases, such as central retinal artery occlusion (CRAO), glaucoma, diabetic retinopathy, ophthalmic artery occlusion and carotid insufficiency (Osborne et al., 2004).

The effects of ischemia on the retina have been extensively studied using adult rat models, such as two-vessel occlusion (2VO) (i.e., transient or permanent bilateral carotid artery occlusion), four-vessel occlusion (4VO) (i.e., permanent bilateral vertebral artery occlusion combined with transient bilateral carotid artery occlusion), central retinal artery occlusion (CRAO) and increased intraocular pressure (IOP) (Block and Schwarz, 1998; Osborne et al., 2004). In these models, the inner retina shows a greater susceptibility to ischemia than the outer

retina, as demonstrated by a significant attenuation of the ERG b-wave while the a-wave is unaffected or only slightly attenuated (Block and Schwarz, 1998). Furthermore, the duration of ischemia plays an important role in determining the reversibility of the functional impairment. For example, transient 2VO of 24 minutes, 4VO of 20 minutes, CRAO of 50 minutes, and increased IOP of 50 minutes all result in suppression of the b-wave which completely recovers during reperfusion, whereas prolonged ischemia (permanent 2VO, CRAO and increased IOP exceeding 90 minutes) results in irreversible attenuation of the b-wave amplitude accompanied by structural changes in the inner retina (Block and Schwarz, 1998). Finally, the degree of ischemia (i.e., reduction in blood flow) correlates with the degree of reduction in b-wave amplitude. That is, unilateral common carotid artery occlusion (~25% reduction in cerebral blood flow, CBF) produces no retinal changes while bilateral common carotid artery occlusion (~50% reduction in CBF) leads to partial attenuation of the b-wave, and 4VO (complete blockage of CBF) leads to complete abolition of the b-wave (Block and Schwarz, 1998).

4.2 Susceptibility of the developing retina to HI injury

Susceptibility of the developing retina to fluctuating oxygen levels have been extensively studied in animal models of retinopathy of prematurity (ROP), where retinal ischemia that occurs as a result of vaso-obliteration (following hyperoxic exposure) plays an important role in producing permanent structural and functional damages to the retina (Chen and Smith, 2007; Sapieha et al., 2010).

Detrimental effects of HI on the immature retina have also been described in rat models of perinatal asphyxia, recently. Kaur et al. (2009) exposed 1-day-old rats to hypoxia (5% oxygen) for 2 hours and found increased levels of vasoactive substances in the retina which were accompanied by INL cell death, ganglion cell and Müller cell swelling and leaky retinal vessels.

Another rat model of birth asphyxia involves hysterectomy at the onset of delivery and submersion of the uterine horns to 37°C water bath for 20 minutes, after which the pups are resuscitated (Loidl et al., 2000). Using this model, Rey-Funes et al. (2013) demonstrated that perinatal asphyxia caused gliosis and angiogenesis in the innermost layer of the retina, which in turn increased the thickness of this layer. Using a similar model, however, Kiss et al. (2009) reported thinning of the ONL and INL as well as ganglion cell loss. The effects of HI on the immature retina has also been demonstrated using the most commonly used rat model of neonatal HIE, i.e., the Vannucci model. Here, HI was induced in 7-day-old rats by unilateral common carotid artery ligation followed by 2-hour hypoxia (8% oxygen) (Rice et al., 1981). Rats subjected to this model showed irreversible functional (the b-wave attenuation) and structural (INL, IPL and ganglion cell layer thinning) damage as well as microglia and Müller cell activation in the inner retina of the eye ipsilateral to the carotid ligation (Huang et al., 2012).

Developmental stages of the central nervous system in the aforementioned models, however, correspond to those of prematurely born infants. The effect of neonatal HI on the rat retina at human term equivalent age remains to be elucidated.

4.3. Vannucci model as an animal model of term neonatal HIE

One of the most commonly used rodent models of neonatal HIE is the Vannucci model (Rice et al. 1981), which was adapted from the Levine model, an adult rat model of hypoxic-ischemic brain damage (Levine, 1960). The original procedure included a permanent unilateral ligation of the common carotid artery followed by a period of hypoxia produced by exposure to 8% oxygen/balance nitrogen at a controlled temperature in 7-day-old rats. The unilateral ligation does not affect the CBF to the level that would produce appreciable injury, as the Circle of Willis is able to compensate. During hypoxia, however, the mean blood pressure drops by 25–30% and

the CBF in the ipsilateral hemisphere decreases to 40–60% of control (Vannucci et al., 1998; Patel et al. 2014); this leads to damage in the ipsilateral hemisphere. Over the years, the effect of age at which hypoxia-ischemia is induced on the pattern and extent of brain injury has been studied in detail. This, combined with the studies looking at the developmental stage of the central nervous system with regards to anatomy and function (EEG and aEEG) at different age of the rats, concluded that P10–12 rats rather than P7 rats were more appropriate to model term human newborns (Towfighi et al., 1997; Romjin et al., 1991; Tucker et al., 2000; Cuaycong et al., 2011). The pattern of brain injury produced at this age, i.e., deep grey matter (hippocampus and thalamus) and cortical injury, also is more representative of that of term-born infants (Towfighi et al., 1997).

We can utilize the P10 Vannucci model to study the effect of HI on the brain and retina simultaneously as the common carotid artery gives rise to the ophthalmic artery, which in turn gives rise to the central retinal artery and posterior ciliary artery that supply the retinal and choroidal circulation, respectively. Thus, the ipsilateral retina will be subjected to hypoxia-ischemia in this model.

5. Mechanisms Underlying HI-Induced Brain and Retinal Injury and Therapeutic Targets

Common mechanisms of brain and retinal injury following HI include excitotoxicity, inflammation, and oxidative stress by free radicals (Osborne et al., 2004; Kaur et al., 2008, 2009; Lai and Yang, 2011; Shankaran, 2012). HI leads to energy failure, resulting in a decrease in adenosine triphosphate (ATP) production and thus a failure of the ATP-dependent Na+/K+ pumps. This leads to membrane depolarization, which causes increased glutamate release and further membrane depolarization. A shift in ion balance causes the cells to swell and die from

necrosis in the early phase. Prolonged membrane depolarization and increased extracellular glutamate also raise intracellular calcium to toxic levels, by the activation of the N-methyl-D-aspartate (NMDA) receptors and voltage-gated calcium channels. Increased intracellular calcium leads to cascades of events that induce mitochondrial damage, free radical production and proinflammatory cytokine induction, which can all lead to apoptotic cell death (Osborne et al., 2004). Furthermore, HI leads to induction of vasoactive substances such as VEGF and nitric oxide synthase, which may cause vessel leakage and thereby further spreading of the damage (Kaur et al., 2008). In this regard, selective vulnerability of certain structures in the brain and retina – cortex, hippocampus, retinal ganglion cells, bipolar cells and horizontal cells, for example – have been suggested to stem from their abundant expression of glutamate receptors (Hoyt, 2003; Osborne et al., 2004).

6. Therapeutic Strategies

6.1. Current therapy

Currently, the only available treatment for neonatal HIE is hypothermia, which reduces the core body temperature of an affected infant to 33–34°C for 72 hours (Shankaran et al., 2005; Azzopardi et al., 2009). Hypothermia aims to reduce secondary brain injury by slowing down the metabolism, reducing edema, inhibiting inflammation and suppressing free radical activity (Shankaran, 2012). Hypothermia has also been shown to prevent retinal injury in a premature rat model of perinatal asphyxia by reducing nitric oxide production and preventing gliosis and angiogenesis (Rey-Funes et al., 2011, 2013). Although hypothermia treatment improves outcome in some infants, it is far from optimal, as 44 to 53% of treated infants will still suffer mortality or moderate to severe disability (Shankaran et al., 2005; Azzopardi et al., 2009).

6.2. Other neuroprotective therapies

Pre-treatment with glutamate receptor blockers, anti-inflammatory mediators and free radical scavengers have shown some promises in reducing brain or retinal HI injury in animal models; however, the effect is hardly translated to humans due to challenges associated with choosing a safe and effective dose, timing of the treatment and existence of confounding variables (Block and Schwarz, 1998; Lees, 2001; Osborne et al., 2004; Lai and Yang, 2011).

Several agents that are known to work on the abovementioned pathways have shown synergistic effects with hypothermia in improving histological and functional outcomes in animal models of neonatal HIE. These include Xenon, melatonin, N-acetylcysteine, and erythropoietin (Epo) (Wintermark, 2011; Cilio and Ferriero, 2010). However once again, the exact timing and dose of the drugs that are safe and effective need to be refined. One particularly interesting therapy that has gone to clinical trials to treat neonatal encephalopathy is Epo. In animal studies, Epo was demonstrated to enhance neuroregeneration in addition to preventing neuronal death (Xiong et al., 2011; Traudt et al., 2013; Yan et al., 2016). According to a recent phase II trial, high-dose Epo appears to offer additional benefits to hypothermia in reducing brain injury and improving 1-year neurodevelopmental outcome in term infants with neonatal encephalopathy (Wu et al., 2016). In line with this, neurorestorative therapies that can potentiate endogenous repair processes, such as neurogenesis, synaptogenesis and angiogenesis, while limiting apoptosis and inflammation, are gaining traction in research. Such therapies include Epo as mentioned above, stem cell therapy, and sildenafil. Our laboratory is particularly interested in sildenafil.

7. Sildenafil as a Potential Neuroprotective/Neurorestorative Therapy for Retinal Injury Induced by Neonatal HI.

7.1. Overview

Sildenafil is a potent vasodilator that acts by inhibiting the phosphodiesterase type-5 (PDE5) enzyme, which breaks down cyclic guanosine monophosphate (cGMP) (Terrett et al., 1996). Therefore, sildenafil increases the level of cGMP, a secondary messenger, which in turn activates protein kinase G (PKG) and its multiple downstream effectors. Sildenafil has been widely used to treat erectile dysfunction in adults and pulmonary hypertension in both adults and newborns (Goldstein et al., 1998; Barnett et al., 2006; Shah et al., 2011). More recently, an accumulating body of literature has demonstrated the neuroprotective and/or neurorestorative roles of sildenafil in animal models of neurologic diseases, such as ischemic stroke, multiple sclerosis and Alzheimer's disease (Bednar et al., 2008; Chen et al., 2014; Nunes et al., 2012; Zhang et al., 2005; Zhang et al., 2012; Zhang et al., 2013).

7.2. Sildenafil in animal models of neurologic diseases

In rat models of adult stroke, sildenafil has been shown to promote neurogenesis, angiogenesis and synaptogenesis, and improve functional outcome with or without an accompanying reduction in infarct size, even with a delayed administration of up to a week post-stroke (Zhang et al., 2005; Bednar, 2008). Furthermore, sildenafil has been shown to decrease neuroinflammation in animal models of other neurologic diseases, such as Alzheimer's disease and multiple sclerosis (Zhang et al, 2013; Nunes et al., 2012; Pifarre et al., 2013).

Therapeutic effects of sildenafil on immature brain with HI injury have been tested in rat and mouse models (Charriaut-Marlangue et al., 2014; Moretti et al., 2016; Yazdani et al., 2016; Engels et al., 2017). Charriaut-Marlangue et al. reported decreased neuronal and endothelial cell

apoptosis, astrogliosis and microglia/macrophage activation at 72 hours and 7 days post-HI after a single intraperitoneal administration of sildenafil following HI in P7 rats. At the latter time-point (7 days post-HI), they also observed decreased tissue loss and improved motor recovery. In a neonatal stroke model of P9 mice, sildenafil treatment did not show a change in infarct volume at 72 hours after permanent middle cerebral artery occlusion, but a significant reduction 8 days after the occlusion (Moretti et al., 2016). The authors argued that the microglia/macrophage profile supported an anti-inflammatory effect of sildenafil in limiting the expansion of lesion. Finally, our group used the P10 Vannucci model of neonatal HIE in Long-Evans rats and demonstrated that 7 days of oral sildenafil administration, beginning 12-hour post-HI, improved the motor outcome, ipsilateral brain hemisphere size and the number of neurons at P30 (Yazdani et al., 2016).

Despite the accumulating evidence of neuroprotective and/or neurorestorative role of sildenafil in the brain, its therapeutic potential has been rarely explored in the context of retinal diseases.

7.3. Sildenafil and the retina

7.3.1. Expression of PDE5 in the retina

PDE5 is expressed in the endothelial cells and the smooth muscles of the retinal vasculature, the choroidal vasculature, and the ophthalmic artery (Foresta et al., 2008). In the human retina, PDE5 was shown to be expressed in the INL and the ganglion GCL; however, its role in these structures remains unclear. Of interest, PDE6, on which sildenafil has a mild inhibitory effect, is abundantly expressed by rod and cone photoreceptors.

7.3.2. Effects of sildenafil on choroidal and retinal circulation

There is some inconsistency in the literature regarding the effects of sildenafil on ocular blood

flow and vessel diameters (Harris et al., 2008). In general, a single 50–100 mg dose of oral sildenafil in healthy adults have been shown to transiently increase the blood flow in the ophthalmic artery and choroid, but not in the retinal vessels (Harris et al., 2008; Paris et al., 2001; Dundar et al., 2001; Foresta et al., 2008). Sildenafil has been shown to increase the diameter of the retinal artery and vein; however, a lack of blood velocity measurements in these vessels make it inconclusive as to whether there was any blood flow change (Pache et al., 2002). A study by Polak et al. (2003) reported an increase in retinal vein diameter and venous blood flow in healthy subjects after sildenafil. More recent studies using optical coherence tomography (OCT) angiography reported increased choroidal thickness after a single dose of sildenafil, presumably resulting from choroidal vasodilation (Kim et al., 2013; Berrones et al., 2017). While the choroidal blood flow was also found to be elevated in Kim et al.'s study, Berrones et al. did not find any change in the choroidal blood flow, which could be due to the difference in the techniques used. Again, the retinal blood flow was not found to be affected in the latter study. In a study by Vatansever et al. (2003), male rats fed 8 mg/kg/day of sildenafil every other day for 4 weeks showed a thickening of the choriocapillaries but not of the retinal vessels on histology. The difference in response of choroid and the retinal circulation to sildenafil could be due to the difference in innervation and local autoregulation (Harris et al., 2008; Berrones et al., 2017).

7.3.3. Effects of sildenafil on retinal function and structure

Some of the vision related side effects of sildenafil in the adult population include changes in color and light perception, blurred vision and photophobia (Berrones et al., 2017; Moschos and Nitoda, 2016). These effects are thought to be mediated by the inhibition of PDE6 in photoreceptors by sildenafil, and subsequent disruption of the phototransduction pathway. As such, many studies have investigated the effect of sildenafil on retinal function using full-field

ERGs in humans and animals.

In healthy human adults, slight transient changes in ERG amplitudes and/or peak times have been reported to occur 1–2 hours following a single dose of sildenafil (50–200 mg). The changes involved both rod and cone pathways and outer and inner retina function (Jagle et al., 2004, 2005; Luu et al., 2001). Patients treated with sildenafil for erectile dysfunction also showed acute changes in ERG 1 hour after a 50 mg dose, particularly a higher rod V_{max} and increased sensitivity, which may explain photosensitivity experienced by some patients after taking sildenafil (Gabrieli et al., 2001). The effects of chronic high dose sildenafil have been looked at in patients with pulmonary arterial hypertension, who had been on 120–300 mg/day of sildenafil for 1–4 years (Zoumalan et al., 2009). Upon being tested 1 hour after a dose, patients showed a delayed cone b-wave peak time but no change in the amplitudes. Taken together, acute or chronic sildenafil does not seem to pose serious risk for retinal health in humans.

An intravenous (i.v.) injection of sildenafil (0, 1, 3, and 10 mg/kg) in healthy monkeys demonstrated transient ERG changes that returned to baseline within 24 hours (Kinoshita et al., 2015). Specifically, the b-waves were delayed and/or attenuated at a lower dose than the a-waves, and the sensitivity of the cones appeared to be affected more than that of the rods. No fundus changes were noted.

Behn and Potter (2001) showed that an intraperitoneal (i.p.) injection of 2.9 mg/kg and 14.3 mg/kg (2 and 10 times the maximum recommended dose, respectively, for a 70-kg human) sildenafil had no effect on the ERG of wild type mice. Mice that were heterozygous for rod PDE6 (i.e., a model of retinitis pigmentosa), however, showed a dose-dependent decrease in a- and b-wave amplitudes, which returned to baseline values within 48 hours. Using higher doses of sildenafil (7.25–72.5 mg/kg, i.p.), Nivison-Smith et al. (2014) showed a reversible attenuation of

ERG a- and b-wave amplitudes in the wild type. Mice heterozygous for rd1 (another type of retinitis pigmentosa carrier) showed a reduced a-wave and supernormal b-wave that took 2 weeks to recover. These studies raise possible adverse effect of sildenafil on retinas with a compromised photoreceptor PDE6 system; however, the dose used in these studies far exceeded the maximum dose and even then the effects were mostly reversible.

Similar results were obtained with studies using the isolated or *ex vivo* retina. Luke et al. (2005) showed a dose-dependent and reversible attenuation of ERG a- and b-wave amplitudes after sildenafil on isolated superfused bovine retina. Again, the b-wave began to be affected at a lower dose than the a-wave and showed a greater attenuation than the a-wave. They also showed slower and partial recovery following washout after higher doses. Martins et al. (2015) demonstrated that sildenafil on *ex vivo* retina decreased and delayed the ON- and OFF-RGC response to light in a reversible and dose-dependent manner.

In summary, sildenafil alters retinal function but the effect is mostly transient and occurs only at doses far above the recommended maximum. Human studies also suggest that sildenafil does not cause any significant adverse effect on the retina, even at a high dose or after chronic use. Interestingly, all of the above studies suggested that sildenafil may have direct effects on inner retinal cells, as demonstrated by the changes in the b-wave that exceeds what was expected from the consequence of a change in the a-wave alone. Sildenafil likely affects the inner retina through the inhibition of PDE5.

7.3.4. Sildenafil and retinopathy of prematurity

A few case studies reported the development of retinopathy of prematurity (ROP) in preterm infants treated with sildenafil for persistent pulmonary hypertension (Marsh et al., 2004; Fuwa et al., 2017). However, these cases did not establish a causal relationship, and retrospective studies

with a larger cohort reported no adverse ocular findings in association with sildenafil (Kehat et al., 2010; Fang et al., 2013; Samiee-Zaarghandy et al., 2016).

There is only one study looking at the effect of sildenafil on retinal vascular changes in a mouse oxygen-induced retinopathy (OIR) model, a model for retinopathy of prematurity (Fawzi et al., 2014). They reported that sildenafil administration during exposure to hyperoxia significantly decreased retinal vaso-obliteration through HIF-α stabilization. At a later time point, they also observed decreased neovascularization, which normally develops when the pups are returned to room air which is relatively hypoxic to vaso-obliterated retinas. Although they did not look at the retinal structure or function, this study provides evidence of a beneficial role of sildenafil in the OIR.

Given that vasodilation and angiogenesis can either help or worsen the HI injury, and that the adequate angiogenic signalling is critical for normal development and maintenance of the retinal vasculature and the retina, it would be important to test the effect of sildenafil in the context of neonatal HI, both in terms of safety and efficacy.

PREFACE TO CHAPTER II

Previous animal studies report that the immature retina is susceptible to hypoxic-ischemic injury. The affected retinal layers as well as the extent of injury vary depending on the model and the age of the animals used. In general, however, the inner retina is more susceptible to injury than the outer retina. The effect of HI on the rat model of neonatal HI at term equivalent age has not yet been investigated. In this chapter, we used the P10 Vannucci model to study the effect of hypoxia-ischemia on retinal function (ERG) and structure (histology) in detail. In particular, we examined the histology of the retina along the entire superior-inferior axis at the level of the optic disc in order to characterize the distribution of injury not only from outer to inner retina, but also from center to periphery. We found that there are differences in the severity of injury with respect to depth as well as eccentricity. We also looked at the functional integrity of the primary visual pathway using VEP and investigated the relationship between the brain and retinal injury at the level of function and structure. Our results demonstrate that retinal injury may develop independently from brain injury as a result of HI.

CHAPTER II

MANUSCRIPT 1

Suna Jung, Anna Polosa, Pierre Lachapelle, Pia Wintermark. Visual Impairments Following Term Neonatal Encephalopathy: Do Retinal Impairments Also Play a Role? Invest Ophthalmol Vis Sci 2015; 56(9): 5182-5193.

ABSTRACT

Purpose: To investigate the effects of term neonatal encephalopathy on retinal function and structure.

Methods: A rat model of term neonatal hypoxic-ischemic encephalopathy (Vannucci model) was used. Hypoxia-ischemia was induced by a left common carotid ligation followed by a 2-hour period of hypoxia (8% oxygen) in Long-Evans rat pups at postnatal day 10 (P10). Sham operated rats served as controls.. Retinal function was assessed at P30 and P60 by electroretinograms (ERGs), after which retinal histology was performed. Retino-cortical function was assessed with visual evoked potentials (VEPs) at P60 and subsequently brain histology was performed.

Results: The ERGs of the HI animals at P30 and P60 demonstrated a significant reduction in the scotopic and photopic b-wave amplitudes, but a preserved a-wave amplitude. The retinal histology of the HI animals confirmed that the photoreceptor layer remained intact, whereas the inner layers of the retina were damaged. The HI animals also showed reduced VEP P100 amplitudes, which correlated with reduced left cerebral hemisphere surfaces. There was no correlation between the severities of retinal versus cerebral injuries.

Conclusions: Our findings suggest that term neonatal encephalopathy resulting from hypoxia-ischemia induces functional and structural damages to the inner retina, while relatively sparing the photoreceptors. These findings raise the possibility that retinal injuries may contribute to visual impairments with or without the presence of brain injury in term asphyxiated newborns and thus warrant further studies with humans and animals to better understand the disease process.

INTRODUCTION

Despite improvements in neonatal care, birth asphyxia remains a serious condition that causes significant mortality and long-term morbidity, such as cerebral palsy, mental retardation, and visual impairments (including blindness).[1,2] Although birth asphyxia and the resulting neonatal encephalopathy in term newborns have been extensively studied, relatively few studies have explored their impact on the retina and visual function. However, loss of vision following birth asphyxia is one of the most common causes of pediatric visual impairments in developed countries. These visual impairments have been largely attributed to injuries along the intra-cerebral visual pathways (i.e., the optic nerves, optic radiations, primary visual cortex, visual associative cortical areas, and/or visual attention pathways) rather than injuries to the retina, although in some studies abnormal ocular findings have been reported.[3-11] One study reported transient subnormal electroretinogram findings within 1 year following birth asphyxia,[12] while other studies found normal electroretinogram with abnormal visual evoked potentials in asphyxiated newborns.[13,14] All of the above make it difficult to appreciate if the retina is at risk of direct hypoxic-ischemic injury in asphyxiated newborns.

The retina is the organ that has the highest oxygen consumption per volume in the body.[15] In addition, much like the brain, the developing retina is highly sensitive to variation in oxygen levels, as demonstrated by the abundant literature on the retinopathy of prematurity, including the animal model (i.e., oxygen-induced retinopathy) of this disease,[16,17] as well as by several studies using different premature animal models of hypoxia-ischemia, which have reported functional and/or structural damages to the retina.[18-20]

The Vannucci model (unilateral common carotid ligation followed by hypoxia), which was originally developed to study brain injury in the context of neonatal hypoxic-ischemic

encephalopathy, must also be a valid model to simultaneously study the effect of hypoxia-ischemia on the retina, since the occlusion of the common carotid artery also disturbs the blood supply to the retina. Thus, we hypothesized that in addition to the brain injury, hypoxia-ischemia in this animal model will also induce injury to the retina. Furthermore, we hypothesized that the retinal injury will be most pronounced in the inner retina, based on the findings obtained in other hypoxic or ischemic retinopathy models, such as the oxygen-induced retinopathy. The present study was designed to investigate the detailed effects of neonatal hypoxia-ischemia on retinal function and structure and compare them to the retino-cortical visual function and brain structure using a rat model of term neonatal hypoxic-ischemic encephalopathy.

MATERIALS AND METHODS

1. Animals

All experiments were conducted in accordance with the Association for Research in Vision and Ophthalmology Statement for the use of animals in ophthalmic and vision research, and were approved by the local animal care committee. Adult female Long-Evans rats with their male-only litters (Harlan Laboratories) were received in the animal facility, housed under standard environment and allowed food and water *ad libitum*. Rat pups remained with their mother until weaning at postnatal day 21 (P21).

2. Induction of Term Neonatal HIE

A well-established rat model of term neonatal HIE (Vannucci model),[21-26] combining a unilateral common carotid artery ligation and a 2-hour exposure to hypoxia in 10-day-old rat pups, was used for the experiments, since this model is recognized to mimic the brain injuries observed in

human term asphyxiated newborns.[27-29] The common carotid artery gives rise to the ophthalmic artery, which feeds the two major blood vessels supplying the retina, i.e., the choroidal and retinal arteries.[30] For the ligation, 10-day-old male Long-Evans rat pups were weighed and then deeply anesthetized with an intraperitoneal injection of fentanyl (0.2 mg/kg) and midazolam (1 mg/kg) to the point of unresponsiveness to noxious stimulation. Anesthesia was reversed with an intraperitoneal injection of naloxone (0.1 mg/kg) and flumazenil (1 mg/kg). Pups were allowed to recover for approximately 1.5 hours after surgery, and were then placed in a sealed hypoxia chamber (Plastic Concepts, North Billerica, MA, USA). The chamber was gradually filled with nitrogen until a level of 8% oxygen was reached, which was maintained for 2 hours. Pups were then allowed to recover for 30 minutes and returned to their mother. Rats undergoing the whole procedure were considered as the hypoxic-ischemic (HI) group (n = 14). Sham operated rats (identical procedure as the HI group, but not the ligation and the hypoxia) served as the control group (n = 10). Rats undergoing the carotid ligation but not the hypoxia served as the ischemia-only group (n = 4), while the right eyes of HI rats served as the hypoxia-only group.

3. Retinal Function

Full-field flash electroretinograms (ERGs) were recorded at P30 (acute effect) from the left (i.e., ipsilateral to the carotid ligation) and right (i.e., controlateral to the carotid ligation) eyes of HI animals, and from the left eyes of the control and ischemic-only animals, using a data acquisition system (AcqKnowledge®; Biopac MP100; Biopac Systems Inc., Goleta, CA, USA) as previously described.[31-33] Follow-up ERGs were recorded at P60 (chronic effect). Briefly, following a 12-hour period of dark-adaptation, the rats were weighed and then anesthetized with an intramuscular injection of ketamine (85 mg/kg) and xylazine (5 mg/kg). The pupils were dilated

using 1–2 drops of 1% tropicamide (Mydriacyl®; Alcon Canada Inc., Mississauga, ON, Canada), and the cornea was anesthetized with 1–2 drops of proparacaine hydrochloride (Alcaine®; Alcon Canada Inc., Mississauga, ON, Canada). The rats were then positioned on their sides inside a recording chamber. All procedures were carried out under a dim red light. Scotopic ERGs were evoked to flashes of increasing intensities ranging from -6.3 to 0.9 $log \cdot cd \cdot s \cdot m^{-2}$ (0.3 log unit increment; interstimulus interval, 10 seconds; averages, 3–5 flashes; bandwidth, 1–1000 Hz), while photopic ERGs were recorded after 20 minutes of light adaptation (background, 30 $cd \cdot m^{-2}$; stimulus intensity, 0.9 $log \cdot cd \cdot s \cdot m^{-2}$; interstimulus interval, 1 second; averages, 20 flashes).

The maximum mixed rod-cone a-wave (measured from the pre-stimulus baseline to the trough of the a-wave) and b-wave (the trough of the a-wave to peak of the b-wave) amplitudes and the photopic b-wave amplitude (baseline to b-wave peak) were measured using the AcqKnowledge® software (Biopac Systems Inc., Goleta, CA, USA). In cases where the peak of the b-wave could not be determined, the amplitude of the b-wave was considered as that measured at the time when the b-wave peaks in control animals. The maximal rod-mediated b-wave amplitude (referred to as rod V_{max}) was estimated using a sigmoidal fit of the luminance-response function curve as previously reported.[31,32,34]

To date, the ERG is the only objective mean to non-invasively assess retinal function. It is recognized that the ERG a-wave is generated by the photoreceptors (outer retina), while the b-wave represents electrical activities originating from the inner retina (most probably interactions between bipolar cells and Müller cells). Previous studies on ischemic retinopathy models, such as bilateral common carotid ligation or 4-vessel occlusion models, revealed an impaired inner retinal function (i.e., depressed b-wave) with relative sparing of the outer retinal function (i.e., the a-wave).[30] Previous studies using the Vannucci model showed variability in the severity of

brain injury.[21] Consequently, given that variability in retinal injury could potentially occur, we postulated that a complete destruction of inner retinal function would abolish the ERG b-wave and thus yield a b-wave amplitude to a-wave amplitude ratio (b/a-wave ratio) smaller than 1 (severe phenotype), while a b/a-wave ratio between 1 and 2 would suggest a mild phenotype given that the normal b/a-wave ratio is around 2. Following the same logic, ratios around 1 would identify an intermediate phenotype.

4. Retinocortical Function

After photopic ERG recordings (20 minutes of light-adaptation), visual evoked potentials (VEPs) were recorded with a subdermal needle electrode placed on the scalp over the occipital cortex (where the midline and interaural line cross) (background, 30 $cd \cdot m^{-2}$; stimulus intensity, 0.9 $log \cdot cd \cdot s \cdot m^{-2}$; interstimulus interval, 1 second; averages, 100 flashes). In control animals, only the left eye was stimulated (since equal VEP responses were assumed for the left and right eye stimulation). In HI animals, monocular VEP responses were obtained in order to compare the left and right retino-cortical pathways.

The P100 wave was identified as the most prominent positive peak occurring at a latency of approximately 100 msec, and its amplitude was measured from the trough immediately preceding the P100 to the peak of the P100.

5. Retinal Structure

After the ERG and VEP recordings at P60, the animals were euthanized with an intraperitoneal injection of sodium pentobarbital (100 mg/kg) and transcardially perfused with 0.1M phosphate buffered saline, followed by 4% paraformaldehyde. The left eyes of the HI and control animals

were enucleated and immediately immersed in 4% paraformaldehyde for 3 hours, prior to the removal of the cornea and lens. The eyecups thus obtained were re-immersed in 4% paraformaldehyde and left overnight at 4°C on an orbital shaker. On the following day, the eyecups were washed 3 x 5 minutes in 0.1M phosphate buffer. The eyecups were then incubated in a solution of 1% osmium tetroxide for 3 hours, followed by 3 x 5 minute washes in 0.1M phosphate buffer, and sequential immersions in 50, 80, 90, 95 and 100% ethanol, and propylene oxide prior to embedding (Epon resin, Mecalab, Montreal, QC, Canada). The embedded eyes were sectioned into 1 µm-thick sections along the superior-inferior axis at the level of the optic nerve head, collected on glass slides, and stained with 0.1% toluidine blue. Images were taken with a microscope equipped with a digital camera (Carl Zeiss Microscopy GmbH, Jena, Germany) combined with a 40x objective. The thicknesses of the total retina and of each retinal layer were measured at approximately 1000 µm from the optic nerve head in the inferior retina using AxioVision® software (Version 4.8.2.0; Carl Zeiss Microscopy GmbH, Jena, Germany).

For retinal reconstruction, retinal segments of 75 µm in width—taken at every 340 µm along the entire length of the superior and inferior retinas—were assembled side by side (Adobe Photoshop®, Adobe Systems Inc. San Jose, CA, USA) to yield a pan-retinal view. Then, the thickness was plotted against eccentricity to obtain the spider graphs, centered with the optic nerve head; the superior retina represented on the left of the optic nerve head and the inferior retina represented on the right of the optic nerve head.

6. Brain Structure

The brains were extracted after the perfusion described above and post-fixed in 4% paraformaldehyde solution overnight at 4°C, and then, they were cryoprotected in 30% sucrose

and serially sectioned into 16-μm coronal sections. Anterior sections were collected at -0.36mm from Bregma (anterior commissure area) and posterior sections at -2.16mm from Bregma (hippocampus area). After hematoxylin and eosin staining using standard protocol, brain morphology of posterior sections was examined with a light microscope (Leica DM4000B LED, Leica Microsystems, Wetzlar, Hessen, Germany) with a 5x objective. For each section, overlapping microphotographs were captured using a digital camera attached to the microscope (Leica DFC450C, Leica Microsystems, Wetzlar, Hessen, Germany). These pictures were then stitched together using a panoramic image stitching software (Microsoft Research Image Composite Editor) to obtain pictures of entire coronal section. Using ImageJ (Image Processing and Analysis in Java),[35] the surface of the left and right hemispheres were measured on two posterior sections and averaged to represent each animal.

7. Data Analysis

One-way ANOVA followed by Dunnett's post-hoc comparison tests (for significant ANOVA results) were performed to assess the differences between the control and experimental groups. Regression analyses were performed in order to assess the correlation between the left/right hemisphere surface area ratio (brain structure) and P100 amplitude (brain function), P100 and photopic b-wave amplitudes (retinal function), and the left/right hemisphere surface ratio (brain structure) and the total retinal thickness measured at 1000 μm from the optic nerve head (retinal structure). A p value < 0.05 was considered as statistically significant. All statistical analyses were performed with GraphPad Prism® (GraphPad Software Inc., San Diego, CA, USA).

RESULTS

1. Effect of Neonatal HI on Retinal Function

The rat pups exposed to hypoxia-ischemia at P10 presented with variable degrees of changes in their retinal function at P30 and P60. As shown in Figure 1A, compared to control animals, the mixed rod-cone ERGs of the ipsilateral (left) eye of the HI animals showed three distinct morphologies, namely: (1) the mild HI group with a b-wave to a-wave ratio (2.16 ± 0.28, $n = 3$) similar to the control (2.51 ± 0.07; i.e., b-wave being greater than the a-wave), (2) the moderate HI group with a b-wave to a-wave ratio close to 1 (i.e., b-wave being approximately equal to the a-wave; 1.04 ± 0.16, $n = 5$), and (3) the severe HI group with a b-wave to a-wave ratio less than 1 (i.e., b-wave being smaller than the a-wave; 0.44 ± 0.12, $n = 6$). All subsequent comparisons were made according to these subgroups. As illustrated in Figure 1A, the amplitudes of the rod mediated b-wave (rod V_{max}) and the photopic b-wave were either similar to those of the control animals (in the mild HI group) or reduced to varying extents, depending on the subgroup (in the moderate and severe HI groups), a finding which is best summarized with the data presented in Figure 1B or Table 1.

At P30, the ipsilateral (left) eyes of the ischemic and mild HI groups showed no significant difference in any of the ERG amplitudes measured compared to the control. In addition, no significant difference was found in the ERG amplitudes in the fellow (right) eyes of the HI animals except in the severe HI group, for which the amplitudes were significantly enhanced for the mixed rod-cone a-wave ($P < 0.05$), mixed rod-cone b-wave ($P < 0.05$) and rod V_{max} ($P < 0.01$) compared to the control. In contrast, the ipsilateral (left) eyes of the moderate and severe HI groups showed a significant attenuation of the amplitudes of the mixed rod-cone b-wave ($P < 0.001$), rod V_{max} ($P < 0.001$) and photopic b-wave ($P < 0.001$) for the moderate and

severe HI groups, while no difference was observed in the amplitude of the mixed rod-cone a-wave compared to the control.

The follow-up ERGs recorded at P60 appeared similar to those recorded at P30 (Fig. 2A). The HI animals remained in the same subgroups as initially categorized at P30 based on their mixed rod-cone ERG b-wave to a-wave ratio. At P60, the ERG amplitudes from the ipsilateral (left) eyes of the ischemic and mild HI groups remained unchanged compared to the control (Fig. 2B and Table 1). At this time, the fellow (right) eyes of the moderate and severe HI groups showed no significant difference in the ERG amplitudes, whereas the mild HI group showed a significant increase in the photopic b-wave amplitude compared to the control ($P < 0.01$). Similarly to P30, the ipsilateral (left) eyes of the moderate and severe HI groups showed a significant reduction in the b-wave amplitudes (i.e., mixed rod-cone b-wave, rod V_{max} and photopic b-wave, $P < 0.001$) but not the a-wave amplitude compared to control.

2. Effect of Neonatal HI on Retinal Structure

The HI-induced changes in the retinal function were accompanied by changes in the retinal structure in the left eyes of the HI animals (Fig. 3A). The total retinal thickness of the left eyes was significantly different between the groups (Fig. 3B). The moderate and severe HI groups showed a significant decrease in the total retinal thickness ($P < 0.001$) compared to the control. The mild HI group did not show a significant difference.

Analysis of the thicknesses of individual retinal layers also revealed significant differences between the groups. The inner retinal layers and the outer plexiform layer (OPL) were damaged to varying extents in the moderate and severe HI groups. That is, the moderate HI group showed a thinning of these layers, whereas the severe HI group showed a near complete

destruction of these layers with only one band of the inner nuclear layer (INL) cells remaining below the OPL (Fig. 3A). Aforementioned observations were supported by the data shown at Figure 3B and Table 2. Both the moderate and severe HI groups showed a significant decrease in the thickness of the inner retinal layers (i.e., INL, $P < 0.001$; inner plexiform layer [IPL], $P < 0.001$; retinal ganglion cell/fiber layer [RGC/FL], $P < 0.01$). These groups also showed a significant decrease in the thickness of the OPL ($P < 0.001$). The mild HI group showed no significant differences in the thickness of the inner retinal layers and the OPL compared to the control. In contrast, the thickness of the photoreceptor layers (i.e., the outer segment [OS], inner segment [IS], and outer nuclear layer [ONL]) did not change in the mild and moderate HI groups, but it increased significantly in the severe HI group ($P < 0.05$) compared to the control. Finally, the thickness of the retinal pigment epithelium (RPE) did not differ significantly between the groups ($P = 0.44$).

In addition, the distribution of inner retinal (or post-photoreceptor) injury was heterogeneous along the superior-inferior axis of the retina—the damage being more pronounced at the center and the far periphery compared to the mid-periphery (Fig. 4A). Again, the different HI groups showed variability in the degree of damage: the damaged areas expanded from the center (next to the ONH) and the far periphery (next to the ora serrata) towards the mid-periphery as the severity of the functional/structural impairment increased. Specifically, compared to the control, the mild HI group showed significant reduction in the thicknesses of IPL, RGC/FL, and OPL only at the peripheral margin of the superior retina (Fig. 4B). The moderate HI group showed significantly thinner INL, RGC/FL, and OPL in the central regions of the superior and inferior retinas, and significantly thinner INL and OPL at the far periphery of the superior retina as well. In the moderate HI group, the thickness of the IPL was reduced all

across the retina. The severe HI group showed significant decreases in the thicknesses of the INL, IPL, and RGC/FL across the entire retina (except at the peripheral margin of the inferior retina for the INL). In the severe HI group, only the OPL showed some regions in the mid-periphery that were not significantly different in thickness compared to the control.

3. Effect of Neonatal HI on the Brain

The HI animals showed a variable degree of injury on the left (ipsilateral to the carotid ligation) hemisphere (Fig. 5). The left-to-right hemisphere surface ratio was positively correlated with the P100 amplitude driven by the right eye ($r^2 = 0.48$, $P < 0.01$; Fig. 6A). There was no correlation between the P100 amplitude driven by the right eye and the b-wave amplitude of the left eye ($P = 0.83$, Fig. 6B), and between the left/right hemisphere surface ratio and the total retinal thickness of the left eye ($P = 0.61$, Fig. 6C).

DISCUSSION

This study demonstrates that rat pups exposed to hypoxia-ischemia at P10 developed a retinopathy. Hypoxia-ischemia induced a functional impairment of the inner retina (i.e., the layers of cells connecting the photoreceptors to the brain) while sparing the photoreceptor function, as demonstrated by a severely attenuated b-wave (i.e., activity of the inner retina) in the presence of a well-preserved a-wave (i.e., activity of the photoreceptors) of the mixed rod-cone ERG responses. Both rod- and cone-mediated inner retinal functions were compromised, as was demonstrated by the attenuated rod-mediated response (rod V_{max}) and photopic b-wave. The histology of these eyes confirmed that the retinal pigment epithelium and the photoreceptor layers (i.e., the OS, IS, and ONL) were intact, compared to the significantly damaged inner retina

(i.e., the OPL, INL, IPL, and RGC/FL). We also confirmed the presence of cerebral damage associated with impaired cerebral visual function as demonstrated by the reduced VEP P100 amplitude and injury on the left hemisphere on brain histology. Interestingly, however, the severity of retinal and cerebral injuries did not correlate, suggesting that visual impairments following hypoxia-ischemia could arise either from retinal injury, cerebral injury, or a combination of both. This is an important finding since much of the emphasis until now has been placed on the abnormalities in the intra-cerebral visual pathways to explain the visual deficits in human newborns with neonatal encephalopathy.[3-11]. To our knowledge, this is the first demonstration of such risk in a rat model of term neonatal hypoxic-ischemic encephalopathy. Previous animal studies have highlighted the risk of the retinopathy following hypoxia-ischemia, but in younger animals (i.e., at ages that correspond to human preterm infants in whom retina is well known to be susceptible to damages).[18-20] Kiss et al. reported a reduction in the thickness of the ONL and INL as well as ganglion cell loss in 6-week-old rat retinas following 15 minutes of asphyxia at P0.[18] In another study using a similar rat model, 20 minutes of asphyxia at P0 induced abnormal structural changes in the ganglion cell/fiber layer at P60, marked by neurodegeneration, neovascularization and gliosis.[19] A 2-hour exposure of P1 rats to 5% oxygen resulted in cell death in the inner nuclear layer and ganglion cell layer, Müller cell swelling, and increased permeability of the retinal blood vessels.[36] Of interest, Huang et al. used the Vannucci model at P7 and demonstrated substantial inner retinal damage (with apoptosis) and gliosis accompanied by a reduction in the ERG b-wave amplitude at P14–60,[20] consistent with our findings. However, they did not report a complete destruction of the inner plexiform layer and ganglion cell/fiber layer as observed in the severe HI group in our study. The discrepancies between different studies may represent a strain difference in retinal susceptibility to HI, as

similar strain difference has been reported in the oxygen-induced retinopathy model.[37] Alternatively, the discrepancies may be due to the difference in the age at which HI was induced. The neurodevelopmental stage of a P0 rat is equivalent to that of very preterm infant (24 weeks gestational age), P7 is equivalent to late-preterm (32-36 weeks gestational age), whereas P10 is considered closer to full-term (40 weeks gestational age).[26]

The degree of the abnormalities in the ERGs and histology of the HI animals varied. We also noted a variability in the degree of brain injury, at the functional and structural level, and which has been previously attributed, at least in part, to the inter-individual difference in the number or efficiency of collaterals in the Vannucci model.[21,38] Interestingly, however, the severity of retinal injury and cerebral injury did not correlate, suggesting that retinal and cerebral injuries may occur separately. Differences in local compensatory mechanisms, such as hemodynamics, may underlie this phenomenon. A significant inter-individual variability in outcome is evident also in human term newborns with neonatal encephalopathy.[39] Further investigations are needed to better understand the factors contributing to the individual differences in retinal susceptibility to HI.

The inner retina appeared more damaged at the center and the far periphery compared to the mid-periphery, which was observed in both the superior and inferior retinas. This finding suggests that some regions of the retina are more susceptible to hypoxia-ischemia compared to others. The topographic distribution of injury may arise from the regional differences in blood circulation.[40] Retinal blood flow is higher in the central region,[41,42] explaining why retinal cells in the central region may be more sensitive to a decrease in blood flow. In rats, the formation and remodeling of the retinal vasculature progresses from the center towards the periphery and from the superficial (at the level of the fiber layer) towards the deep plexus (at the level of the inner

nuclear layer) between birth and the third postnatal week.[43,44] The remodeling period is terminated once the newly formed blood vessels acquire a pericyte coating.[43] At P10, the superficial plexus fully covers the retina, with pericytes around its arterioles and primary branches, where a capillary-free zone forms.[43] In contrast, the deep plexus does not reach the edge of the retina until around P14.[44] The capillary-free zones around the optic disc may also explain the more pronounced damage to the central part of the retina compared to the mid-periphery. The fact that the far periphery is still not vascularized by the deep plexus and remains pericyte-free at P10 [43] may provide an additional explanation as to why the far periphery was more damaged than the mid-periphery. More investigations are needed to understand the changes in retinal blood vessel architecture following HI and how these changes vary with eccentricity. This may help elucidate the mechanisms involved in the development and progression of the retinopathy that follows HI at term.

The abnormalities in retinal function and structure could only be obtained if the rat pups were subjected to hypoxia following the unilateral carotid ligation, which emphasizes the crucial role played by the hypoxic event in addition to ischemia. One of the limitations of our study is a lack of true hypoxia-only control (hypoxia without carotid ligation). Previous studies showed that when hypoxia and ischemia were used separately, neither produced measurable cerebral injury.[21,45] This is not to say that the retina would react the same way as the brain in the presence of an ischemic or hypoxic event. However, a near absence of meaningful results from the contralateral eye (hypoxia-only retina) of the experimental group (ligation + hypoxia) or the ligation-only group suggests a minimal (if any) effect of hypoxia to the retinal structure and function at least until P60. Some contralateral eyes (the severe group at P30 and the mild group at P60), however, did show a slight yet significant supranormal ERG amplitudes and this may

represent such an effect, as it was previously shown that ischemia could yield supranormal ERGs in the ischemic or the fellow eye.[46-49]

The selective resistance of the photoreceptors to HI compared to the inner retina is intriguing especially since the photoreceptors are the cells that consume the most oxygen per gram of tissue weight in the body.[49,50] It may be explained by the high mitochondrial content of the photoreceptors that is needed to provide enough energy to meet their high metabolic demands.[30,50] Hypoxia has been shown to induce an enlargement of the mitochondria, which results in an increased resistance to apoptosis and survival.[5aew1] Furthermore, the photoreceptors are rich in neuroglobin, an oxygen-binding globin protein, which is known to play a neuroprotective role.[30,52,53] Photoreceptors have been shown to have a better ability to reach their metabolic demand anaerobically compared to the inner retina.[30,54,55] Photoreceptors are also more resistant to glutamate excitotoxicity,[56,57] which is known to be one of the main mechanisms underlying ischemic retinal injury.[30,58,59] The selective resistance of the photoreceptors may finally arise from the differences in the blood supplies between the photoreceptors and the inner retina. The photoreceptors are perfused by the choroidal artery and the choriocapillaries, which receive approximately 80% of the total blood supply to the eye, but have low oxygen extraction;[41,50,60] the inner retina is perfused by the branches of the retinal artery, which receives only 20% of the total blood supply to the eye, but has high oxygen extraction.[41,60] Integrity of the blood-retinal barrier is better preserved on the choroidal vasculature side compared to the retinal vasculature side after an hypoxia-ischemia.[61] Further investigations are needed to determine which of the abovementioned hypotheses is/are correct. Also, a long-term follow-up on retinal function and structure following neonatal HI is needed to rule out the possibility of a slower degeneration of the photoreceptors that is not yet evidenced at P60.

One could argue that a bilateral common carotid occlusion, which produces symmetrical brain injuries in rats, may have been a more representative model of the brain injuries encountered in human term asphyxiated newborns, since these injuries are usually bilateral and symmetrical. However, for this study, we chose the unilateral model so to examine the role of HI in the development of brain and retinal injuries, while also taking into account the role of reperfusion in the overall outcome. In addition, since the brain injury is located in the left hemisphere and more than 90% of the retinal fibers cross over at the optic chiasm to the opposite side of the brain in rats, studying the right eye in this model allowed us to distinguish visual impairments arising from the retina versus the brain. In our model, the visual pathway driven by the left eye was impaired due to reduced retinal output, whereas the visual pathway driven by the right eye was most probably impaired due to cerebral anomaly, given the absence of functional deficit at the retinal level. Thus, the animal model combining a unilateral carotid ligation with a 2-hour exposure to hypoxia in P10 rat pups gave us a unique opportunity to study the different impacts of cerebral versus retinal injuries on vision.

The maturity of the rat retina at P10 may be slightly behind that of humans at term. Although most retinal layers are present at P10, the first measurable ERGs do not appear until around P12,[62] which then matures up to P30.[33] Although the human retina is functional at term, it also undergoes rapid structural and functional maturation during first 3–4 months.[63-66] In addition, the visual system refines its connections through visual inputs up to 3 years of age. Another difference between the human and rat retinas is that humans have higher percentage of cones in comparison to rats, and the distribution of the cones is highly concentrated in the fovea within the macula, while the rats do not have a macula. The blood supplies to the retina are similar in humans and rats. The outer retina is supplied by the choroidal vasculature (middle and

posterior ciliary arteries), whereas the inner retina is supplied by the retinal vasculature (central retinal artery), with a similar developmental sequence (the choroidal circulation before the retinal circulation; center to periphery; superficial to deep plexus).[44,67] Further investigations are thus needed to determine if human asphyxiated term newborns develop similar functional and structural damages to the retina as observed in this study in the rat model. The results observed in the rat model may not be generalizable to human newborns with neonatal encephalopathy.

In conclusion, we found functional and structural anomalies in the retina following HI with or without the presence of brain injury. Specifically, these injuries were limited to the inner retina, while the photoreceptors were relatively spared. These findings suggest that retinal injuries, in addition to or independent of cerebral injuries, may contribute to visual impairments in term asphyxiated newborns, and warrant further studies in humans and animals to better understand the disease process underlying the retinal damages associated with neonatal asphyxia and their relation to brain injury. Distinguishing retinal injuries from cerebral injuries is a worthy challenge that will help with the planning of improved treatments for these newborns.

ACKNOWLEDGMENTS

The authors thank Aaron Johnstone for training Suna Jung in the surgical techniques, and Zehra Khoja for her help with the tissue collection.

Supported by the CIHR (Frederick Banting and Charles Best Canada Graduate Scholarship), the Research Institute of the McGill University Health Centre Foundation of Stars, and the McGill University Integrated Program in Neuroscience (SJ); by the CIHR (MOP 126082; PL); and by research grant funding from the Fonds de la Recherche en Santé Québec (FRQS) Clinical Research Scholar Career Award Junior 1, and a Canadian Institutes of Health Research (CIHR)

Operating Grant (PW). The authors alone are responsible for the content and writing of the paper.

Disclosure: **S. Jung**, None; **A. Polosa**, None; **P. Lachapelle**, None; **P. Wintermark**, None

REFERENCES

1. American Academy of Pediatrics. Relation between perinatal factors and neurological outcome. In: *Guidelines for Perinatal Care*. 3rd ed. Elk Grove Village, Il: American Academy of Pediatrics; 1992:221-234.
2. Al-Macki N, Miller SP, Hall N, Shevell M. The spectrum of abnormal neurologic outcomes subsequent to term intrapartum asphyxia. *Pediatr Neurol*. 2009; 41:399-405.
3. Foster A. Childhood blindness. *Eye*. 1988;2 Suppl:S27-36.
4. Eken P, de Vries LS, van der Graaf Y, Meiners LC, van Nieuwenhuizen O. Haemorrhagic-ischaemic lesions of the neonatal brain: correlation between cerebral visual impairment, neurodevelopmental outcome and MRI in infancy. *Dev Med Child Neurol*. 1995;37:41-55.
5. Huo R, Burden SK, Hoyt CS, Good WV. Chronic cortical visual impairment in children: aetiology, prognosis, and associated neurological deficits. *Br J Ophthalmol*. 1999;83:670-675.
6. Hoyt CS. Visual function in the brain-damaged child. *Eye*. 2003;17:369-384.
7. Hoyt CS. Brain injury and the eye. *Eye*. 2007;21:1285-1289.
8. Brodsky MC, Fray KJ, Glasier CM. Perinatal cortical and subcortical visual loss. *Ophthalmology*. 2002;109:85-94.

9. Mercuri E, Baranello G, Romeo DMM, Cesarini L, Ricci D. The development of vision. *Early Hum Dev*. 2007;83:795-800.

10. Salati R, Borgatti R, Giammari G, Jacobson L. Oculomotor dysfunction in cerebral visual impairment following perinatal hypoxia. *Dev Med Child Neurol*. 2002;44:542-550.

11. Van Hof-van Duin J, Mohn G. Visual defects in children after cerebral hypoxia. *Behav Brain Res*. 1984;14:147-155.

12. Nickel BL, Hoyt CS. The hypoxic retinopathy syndrome. *Am J Ophthalmol*. 1982;93:589-593.

13. McCulloch DL, Taylor MJ, Whyte HE. Visual evoked potentials and visual prognosis following perinatal asphyxia. *Arch Ophthalmol*. 1991;109:229-233.

14. Muttitt SC, Taylor MJ, Kobayashi JS, MacMillan L, Whyte HE. Serial visual evoked potentials and outcome in term birth asphyxia. *Pediatr Neurol*. 1991;7:86-90.

15. Flammer J, Konieczka K, Bruno RM, Virdis A, Flammer AJ, Taddei S. The eye and the heart. *Eur Heart J*. 2013;34:1270-1278.

16. Rivera JC, Sapieha P, Joyal JS et al. Understanding retinopathy of prematurity: update on pathogenesis. *Neonatology*. 2011;100:343-353.

17. Hellstrom A, Smith LE, Dammann O. Retinopathy of prematurity. *Lancet*. 2013;382:1445-1457.

18. Kiss P, Szogyi D, Reglodi D et al. Effects of perinatal asphyxia on the neurobehavioral and retinal development of newborn rats. *Brain Res*. 2009;1255:42-50.

19. Rey-Funes M, Ibarra ME, Dorfman VB et al. Hypothermia prevents the development of ischemic proliferative retinopathy induced by severe perinatal asphyxia. *Exp Eye Res*. 2010 90:113-120.

20. Huang HM, Huang CC, Hung PL, Chang YC. Hypoxic-ischemic retinal injury in rat pups. *Pediatr Res*. 2012;72:224-231.

21. Rice JE, 3rd, Vannucci RC, Brierley JB. The influence of immaturity on hypoxic-ischemic brain damage in the rat. *Ann Neurol*. 1981;9:131-141.

22. Vannucci RC. Experimental models of perinatal hypoxic-ischemic brain damage. *APMIS Suppl*. 1993;40:89-95.

23. Vannucci RC, Connor JR, Mauger DT et al. Rat model of perinatal hypoxic-ischemic brain damage. *J Neurosci Res*. 1999;55:158-163.

24. Vannucci RC, Vannucci SJ. Perinatal hypoxic-ischemic brain damage: evolution of an animal model. *Dev Neurosci*. 2005;27:81-86.

25. Northington FJ. Brief update on animal models of hypoxic-ischemic encephalopathy and neonatal stroke. *ILAR J*. 2006;47:32-38.

26. Patel SD, Pierce L, Ciardiello AJ, Vannucci SJ. Neonatal encephalopathy: pre-clinical studies in neuroprotection. *Biochem Soc Trans*. 2014;42:564-568.

27. Recker R, Adami A, Tone B et al. Rodent neonatal bilateral carotid artery occlusion with hypoxia mimics human hypoxic-ischemic injury. *J Cereb Blood Flow Metab*. 2009;29:1305-1316.

28. Fan X, van Bel F, van der Kooij MA, Heijnen CJ, Groenendaal F. Hypothermia and erythropoietin for neuroprotection after neonatal brain damage. *Pediatr Res*. 2013;73:18-23.

29. Fang AY, Gonzalez FF, Sheldon RA, Ferriero DM. Effects of combination therapy using hypothermia and erythropoietin in a rat model of neonatal hypoxia-ischemia. *Pediatr Res*. 2013;73:12-17.

30. Osborne NN, Casson RJ, Wood JP, Chidlow G, Graham M, Melena J. Retinal ischemia: mechanisms of damage and potential therapeutic strategies. *Progr Retin Eye Res*. 2004;23:91-147.

31. Dembinska O, Rojas LM, Varma DR, Chemtob S, Lachapelle P. Graded contribution of retinal maturation to the development of oxygen-induced retinopathy in rats. *Invest Ophthalmol Vis Sci*. 2001;42:1111-1118.

32. Dorfman AL, Dembinska O, Chemtob S, Lachapelle P. Structural and functional consequences of trolox C treatment in the rat model of postnatal hyperoxia. *Invest Ophthalmol Vis Sci*. 2006;47:1101-1108.

33. Dorfman A, Dembinska O, Chemtob S, Lachapelle P. Early manifestations of postnatal hyperoxia on the retinal structure and function of the neonatal rat. *Invest Ophthalmol Vis Sci*. 2008;49:458-466.

34. Dembinska O, Rojas LM, Chemtob S, Lachapelle P. Evidence for a brief period of enhanced oxygen susceptibility in the rat model of oxygen-induced retinopathy. *Invest Ophthalmol Vis Sci*. 2002;43:2481-2490.

35. Rasband WS. ImageJ. U.S. National Institutes of Health, Bethesda, Maryland, USA, http://imagej.nih.gov/ij/, 1997-2004

36. Kaur C, Sivakumar V, Foulds WS, Luu CD, Ling EA. Cellular and vascular changes in the retina of neonatal rats after an acute exposure to hypoxia. Invest *Ophthalmol Vis Sci*. 2009;50:5364-5374.

37. Dorfman AL, Chemtob S, Lachapelle P. Postnatal hyperoxia and the developing rat retina: beyond the obvious vasculopathy. *Doc Ophthalmol*. 2010;120:61-66.

38. Charriaut-Marlangue C, Bonnin P, Leger PL, Renolleau S. Brief update on hemodynamic responses in animal models of neonatal stroke and hypoxia-ischemia. *Exp Neurol.* 2013;248:316-320.

39. Barks JD. Current controversies in hypothermic neuroprotection. *Semin Fetal Neonatal Med.* 2008;13:30-34.

40. Klemp K, Lund-Andersen H, Sander B, Larsen M. The effect of acute hypoxia and hyperoxia on the slow multifocal electroretinogram in healthy subjects. *Invest Ophthalmol Vis Sci*. 2007;48:3405-3412.

41. Alm A, Bill A. Ocular and optic nerve blood flow at normal and increased intraocular pressures in monkeys (Macaca irus): a study with radioactively labelled microspheres including flow determinations in brain and some other tissues. *Exp Eye Res*. 1973;15:15-29.

42. Hill DW. The regional distribution of retinal circulation. *Ann R Coll Surg Engl*. 1977;59:470-475.

43. Benjamin LE, Hemo I, Keshet E. A plasticity window for blood vessel remodelling is defined by pericyte coverage of the preformed endothelial network and is regulated by PDGF-B and VEGF. *Development.* 1998;125:1591-1598.

44. Stone J, Itin A, Alon T et al. Development of retinal vasculature is mediated by hypoxia-induced vascular endothelial growth factor (VEGF) expression by neuroglia. *J Neurosci*. 1995;15:4738-4747.

45. Levine S. Anoxic-ischemic encephalopathy in rats. *Am J Pathol*. 1960;36:1-17.

46. Brunette JR, Olivier P, Galeano C, Lafond G. Hyper-response and delay in the electroretinogram in acute ischemia. *Can J Ophthalmol*. 1983;18:188-193.

47. Henkes HE. Electroretinography in circulatory disturbances of the retina. II. The electroretinogram in cases of occlusion of the central retinal artery or of its branches. *AMA Arch Ophthalmol*. 1954;51:42-53.

48. Sakaue H, Katsumi O, Hirose T. Electroretinographic findings in fellow eyes of patients with central retinal vein occlusion. *Arch Ophthalmol*. 1989;107:1459-1462.

49. Wangsa-Wirawan ND, Linsenmeier RA. Retinal oxygen: fundamental and clinical aspects. *Arch Ophthalmol*. 2003;121:547-557.

50. Bhutto I, Lutty G. Understanding age-related macular degeneration (AMD): relationships between the photoreceptor/retinal pigment epithelium/Bruch's membrane/choriocapillaris complex. *Mol Aspects Med*. 2012;33:295-317.

51. Mazure NM, Brahimi-Horn MC, Pouyssegur J. Hypoxic mitochondria: accomplices in resistance. *Bull Cancer*. 2011;98:40-46.

52. Schmidt M, Giessl A, Laufs T, Hankeln T, Wolfrum U, Burmester T. How does the eye breathe? Evidence for neuroglobin-mediated oxygen supply in the mammalian retina. *J Biol Chem*. 2003;278:1932-1935.

53. Yu Z, Liu N, Li Y, Xu J, Wang X. Neuroglobin overexpression inhibits oxygen-glucose deprivation-induced mitochondrial permeability transition pore opening in primary cultured mouse cortical neurons. *Neurobiol Dis*. 2013;56:95-103.

54. Winkler BS. The electroretinogram of the isolated rat retina. *Vision Res*. 1972;12:1183-1198.

55. Stone J, Maslim J, Valter-Kocsi K, Mervin K, Bowers F, Chu Y, Barnett N, Provis J, Lewis G, Fisher SK, Bisti S, Gargini C, Cervetto L, Merin S, Peer J. Mechanisms of

photoreceptor death and survival in mammalian retina. *Progr Retinal Eye Res*. 1999;18:689-735.

56. Lucas DR, Newhouse JP. The toxic effect of sodium L-glutamate on the inner layers of the retina. *AMA Arch Ophthalmol*. 1957;58:193-201.

57. Olney JW. Glutamate-induced retinal degeneration in neonatal mice. Electron microscopy of the acutely evolving lesion. *J Neuropathol Exp Neurol.* 1969;28:455-474.

58. Block F, Schwarz M. The b-wave of the electroretinogram as an index of retinal ischemia. *Gen Pharmacol.* 1998;30:281-287.

59. Kaur C, Foulds WS, Ling EA. Hypoxia-ischemia and retinal ganglion cell damage. *Clin Ophthalmol*. 2008;2:879-889.

60. Alm A, Bill A. Blood flow and oxygen extraction in the cat uvea at normal and high intraocular pressures. *Acta Physiol Scand.* 1970;80:19-28.

61. Kaur C, Foulds WS, Ling EA. Blood-retinal barrier in hypoxic ischaemic conditions: basic concepts, clinical features and management. *Prog Retin Eye Res*. 2008;27:622-647.

62. Weidman TA, Kuwabara T. Postnatal development of the rat retina. An electron microscopic study. *Arch Ophthalmol*. 1968;79:470-484.

63. Abramov I, Gordon J, Hendrickson A, Hainline L, Dobson V, LaBossiere E. The retina of the newborn human infant. *Science*. 1992;217:265-267.

64. Fulton AB, Hansen RM. Electroretinography: application to clinical studies of infants. *J Pediatr Ophthalmol Strabismus*. 1985;22:251-255.

65. Graven SNB, Joy V. Sensory development in the fetus, neonate, and infant: Introduction and overview. *Newborn and Infant Nursing Reviews*. 2008;8:169-172.

66. Kriss A, Russell-Eggitt I. Electrophysiological assessment of visual pathway function in infants. *Eye*. 1992;6(Pt 2):145-153.

67. Provis JM. Development of the primate pretinal vasculature. *Prog Retin Eye Res*. 2001;20:799-821.

FIGURE LEGENDS

Figure 1. Neonatal HI-induced functional impairments of the ipsilateral (*left*) retina at postnatal day 30 (P30). (**A**) Representative scotopic (mixed rod-cone and rod V_{max}) and photopic electroretinograms (ERGs). Horizontal and vertical calibrations in milliseconds (ms) and µVolts (µV), respectively. *Vertical arrows* correspond to stimulus onset. The a-wave and the b-wave are indicated by *a* and *b*, respectively. The ERGs from the left eyes (i.e., ipsilateral to the carotid ligation) (OS; solid line) of the HI animals presented three phenotypes: mild (mixed rod-cone b-wave > a-wave), moderate (mixed rod-cone b-wave ≈ a-wave) or severe (mixed rod-cone b-wave < a-wave). The ERGs from the right eyes (i.e., contralateral to the carotid ligation, *OD; dotted line*) of the HI animals and the left eyes of the ischemic animals appeared similar to those from the left eyes of the control animals. (**B**) Amplitude measurements of the ERG waves. *Clear bars*, left eyes (*OS*); *shaded bars*, right eyes (*OD*). Mean ± SD. The HI subgroups and ischemic group compared to the control group: * $P < 0.05$. Only the right eyes of the severe HI group showed a significant difference in the a-wave amplitude compared to the control. The amplitudes of the mixed rod-cone b-wave and rod V_{max} were significantly decreased in the left eyes of the moderate and severe HI groups, and increased in the right eyes of the severe HI group, but not different in the right eyes of the mild and moderate HI groups and in the left eyes of the ischemic group. The amplitude of the photopic b-wave was significantly decreased in the left eyes of the moderate and severe HI groups, but not in the other groups.

Figure 2. Neonatal HI-induced functional impairments of the ipsilateral retina at postnatal day 60 (P60). (**A**) Representative scotopic (mixed rod-cone and rod V_{max}) and photopic electroretinograms (ERGs). Horizontal and vertical calibrations in milliseconds (ms) and µVolts

(μV), respectively. *Vertical arrows* correspond to stimulus onset. The a-wave and the b-wave are indicated by *a* and *b*, respectively. The ERGs from the left eye (i.e., ipsilateral to the carotid ligation, *OS; solid line*) of the hypoxic-ischemic (HI) animals remained in the same subgroups as initially categorized at P30. The ERGs from the right eyes (i.e., contralateral to the carotid ligation, *OD; dotted line*) of the HI animals appeared similar to those of the left eyes of the control animals. (**B**) Amplitude measurements of the ERG waves. *Clear bars*, left eyes (*OS*); *shaded bars*, right eyes (*OD*). Mean ± SD. HI subgroups compared to the control group: * $P < 0.05$. No significant difference was found in the scotopic a-wave amplitude between the groups. The amplitudes of the mixed rod-cone b-wave and rod V_{max} were significantly decreased in the left eyes of the moderate and severe HI groups, but not in the left eyes of the mild HI group and the right eyes of all HI animals. The amplitude of the photopic b-wave was significantly decreased in the left eyes of the moderate and severe HI groups and increased in the right eyes of the mild HI group, but was not different in the other groups.

Figure 3. Neonatal HI-induced structural damages to the left retina at postnatal day 60 (P60). (**A**) Representative toluidine blue stained retinal cross sections from the left eyes (magnification, X40). Images were taken at approximately 1000 μm from the optic nerve head in the inferior retina. Variability was present in the severity of the injuries to the inner retina in the left eyes (i.e., ipsilateral to the carotid ligation) of the different HI subgroups, while the outer retina appeared relatively intact, compared to the control. (**B**) Thickness of the retinal layers from the left eyes. Mean ± SD. HI subgroups compared to the control group: * $P < 0.05$; ** $P < 0.01$; *** $P < 0.001$. The thickness of the total retina, OPL, INL, IPL, and RGC/FL were significantly

decreased in the moderate and severe HI groups, but not in the mild HI group, compared to the control. The severe HI group showed an increase in OS, IS, and ONL thicknesses.

Figure 4. Topographic distribution of the inner retinal injury. (**A**) Representative retinal sections from the left eyes along the superior-inferior axis at the level of the optic nerve head (magnification, X40). (**B**) Spider graphs depicting the variation in INL, IPL, RGC/FL and OPL thicknesses with eccentricity. Mean ± SD. HI subgroups compared to the control group: significance ($P < 0.05$) represented by *color-coded lines* representing each HI subgroup at the *top* of each graph. The mild HI group showed changes near the ora serrata in the superior retina. The moderate HI group showed damages near the optic nerve head and the ora serrata in the superior and inferior retinas. The severe HI group showed damages across the entire retina.

Figure 5. Brain HI injury and impairment of the retinocortical visual pathway function. The hematoxylin and eosin-stained brain sections are presented next to the visual evoked potentials (VEPs) driven by the left eye (i.e., ipsilateral to the carotid ligation, *OS; solid line*) and the right eye (i.e., contralateral to carotid ligation, *OD; dotted line*) of the same animal for comparison. HI severity grouping was based on the electroretinograms. VEPs: horizontal and vertical calibrations respectively in milliseconds (ms) and µVolts (µV); *vertical arrow* corresponds to stimulus onset.

Figure 6. Correlation between retinal and cerebral injuries. (**A**) The P100 amplitude driven by the right eye (i.e., contralateral to carotid ligation) was positively correlated with the left/right hemisphere surface area. (**B**) There was no correlation between the amplitudes of the photopic b-

wave of the left eye (i.e., ipsilateral to the carotid ligation) and the P100 driven by the right eye. (**C**) There was no correlation between the thickness of the retina of the left eye (i.e., ipsilateral to the carotid ligation) and the left/right hemisphere surface area.

FIGURES

Figure 1

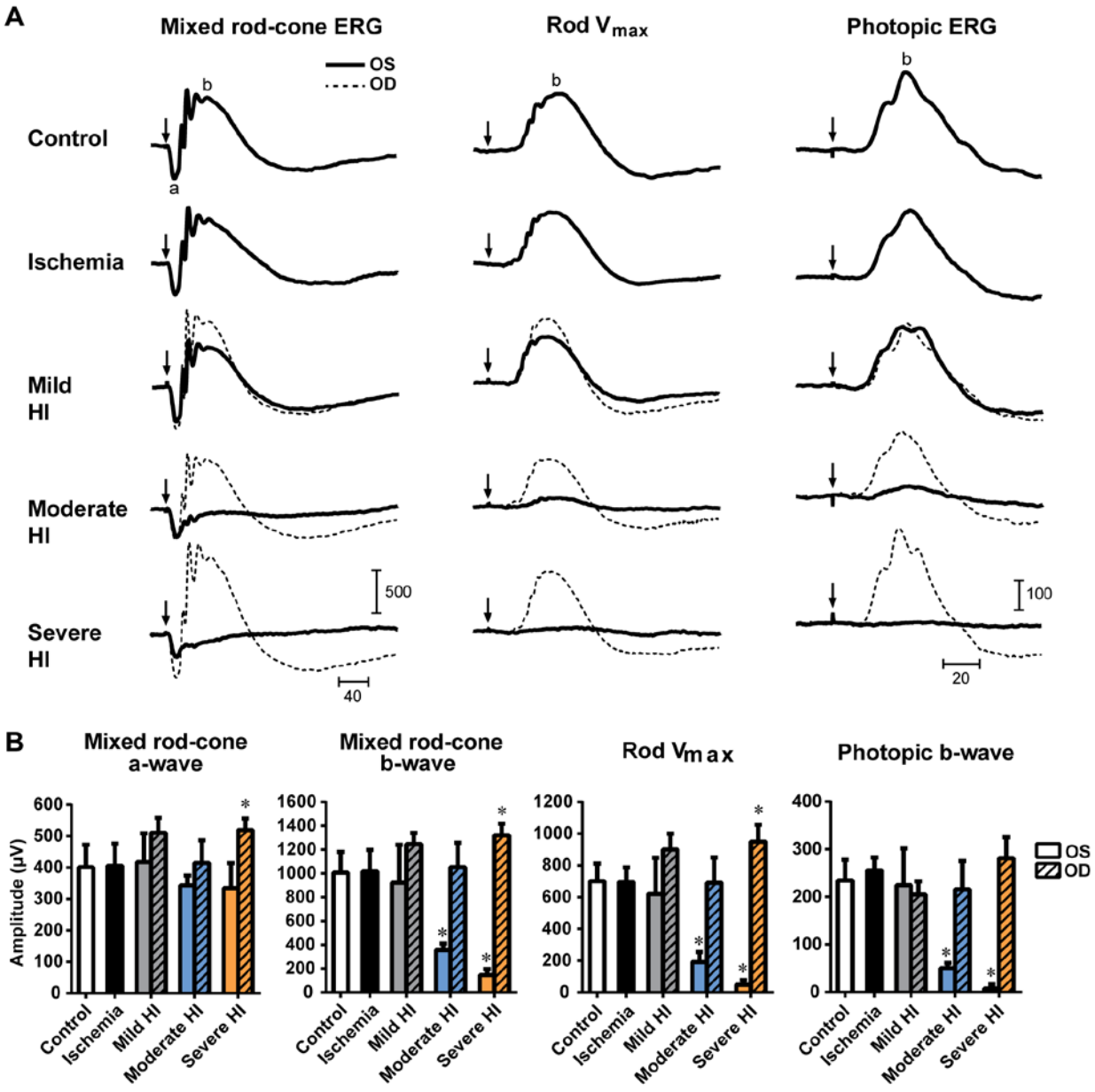

Figure 2

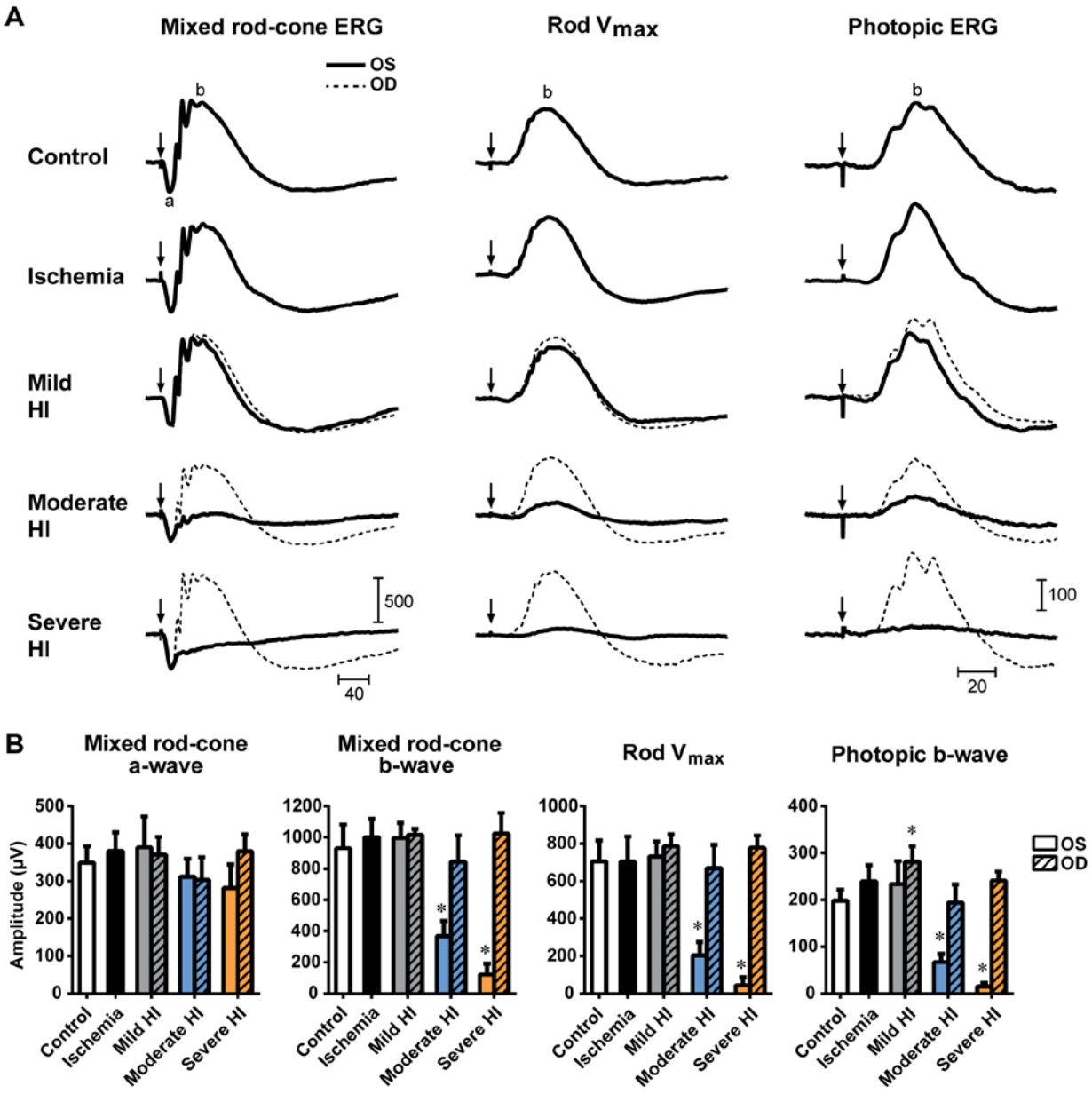
A
Mixed rod-cone ERG
Rod Vmax
Photopic ERG
OS
OD
Control
Ischemia
Mild HI
Moderate HI
Severe HI
a
b
500
40
100
20
B
Mixed rod-cone a-wave
Mixed rod-cone b-wave
Rod Vmax
Photopic b-wave
Amplitude (μV)
Control
Ischemia
Mild HI
Moderate HI
Severe HI
OS
OD

Figure 3

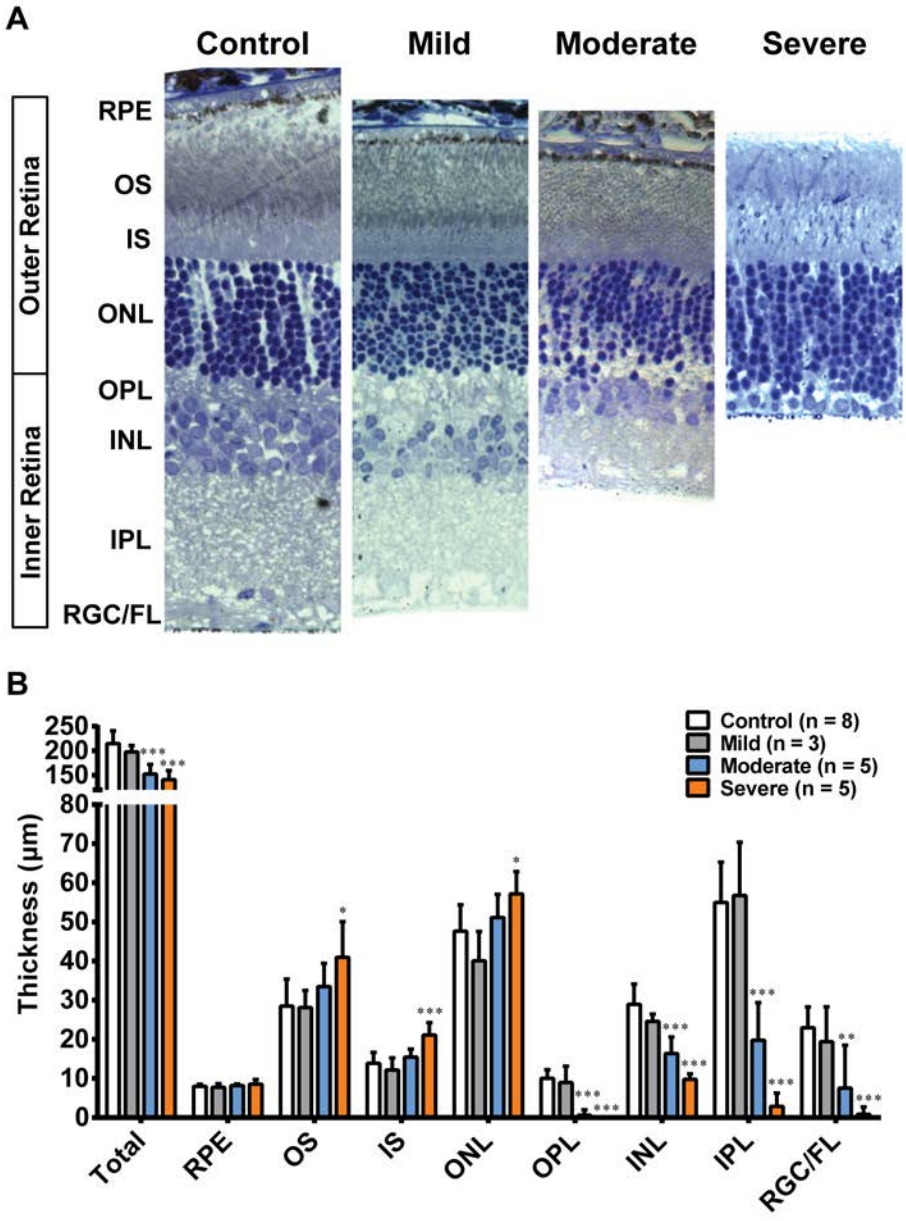
A
Control
Mild
Moderate
Severe
Outer Retina
Inner Retina
RPE
OS
IS
ONL
OPL
INL
IPL
RGC/FL
B
Control (n = 8)
Mild (n = 3)
Moderate (n = 5)
Severe (n = 5)
Thickness (µm)
250
200
150
80
70
60
50
40
30
20
10
0
Total
RPE
OS
IS
ONL
OPL
INL
IPL
RGC/FL

Figure 4

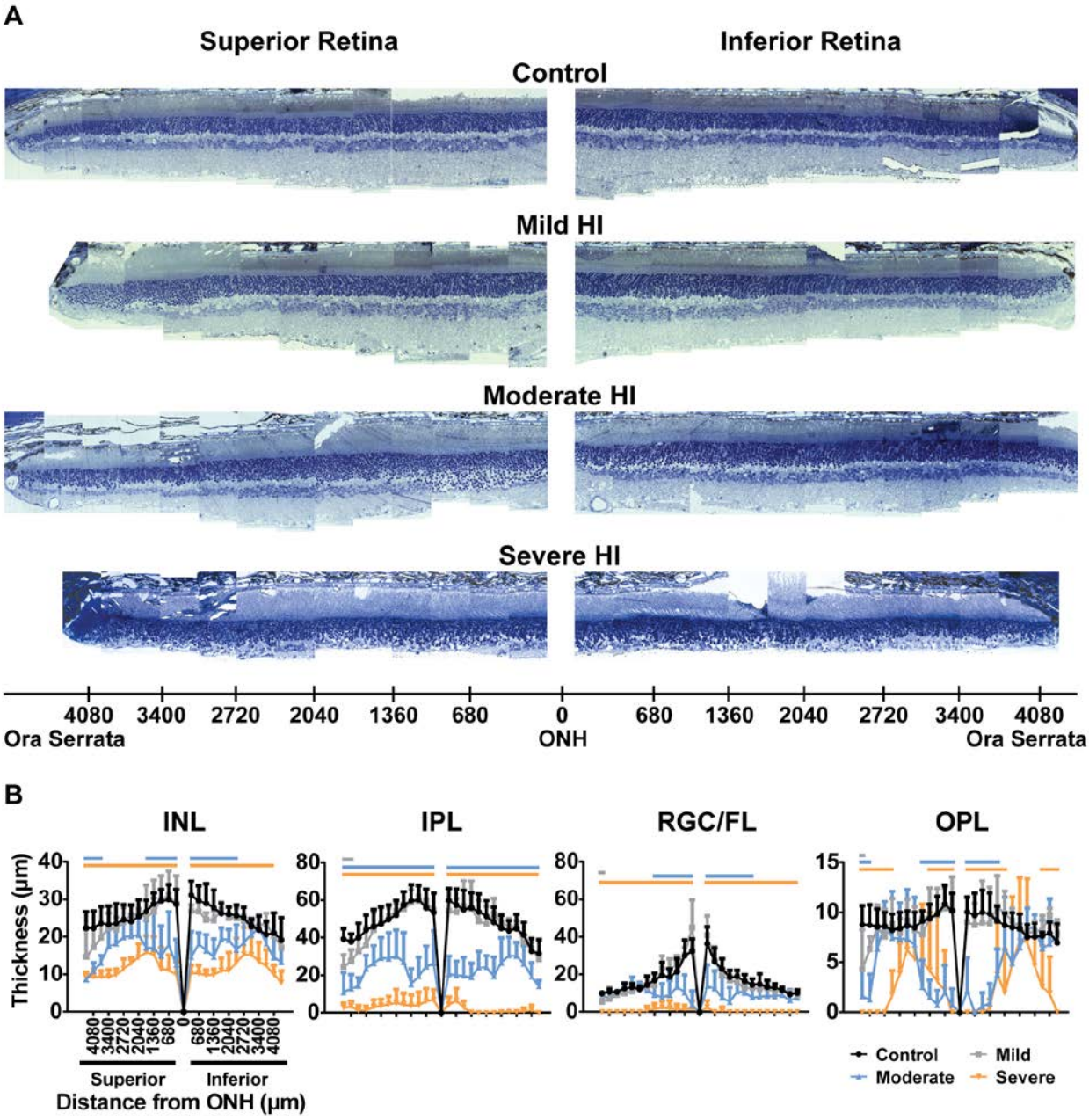
A
Superior Retina
Inferior Retina
Control
Mild HI
Moderate HI
Severe HI
4080 3400 2720 2040 1360 680 0 680 1360 2040 2720 3400 4080
Ora Serrata
ONH
Ora Serrata
B
INL
IPL
RGC/FL
OPL
Thickness (µm)
Superior
Inferior
Distance from ONH (µm)
Control
Mild
Moderate
Severe

Figure 5

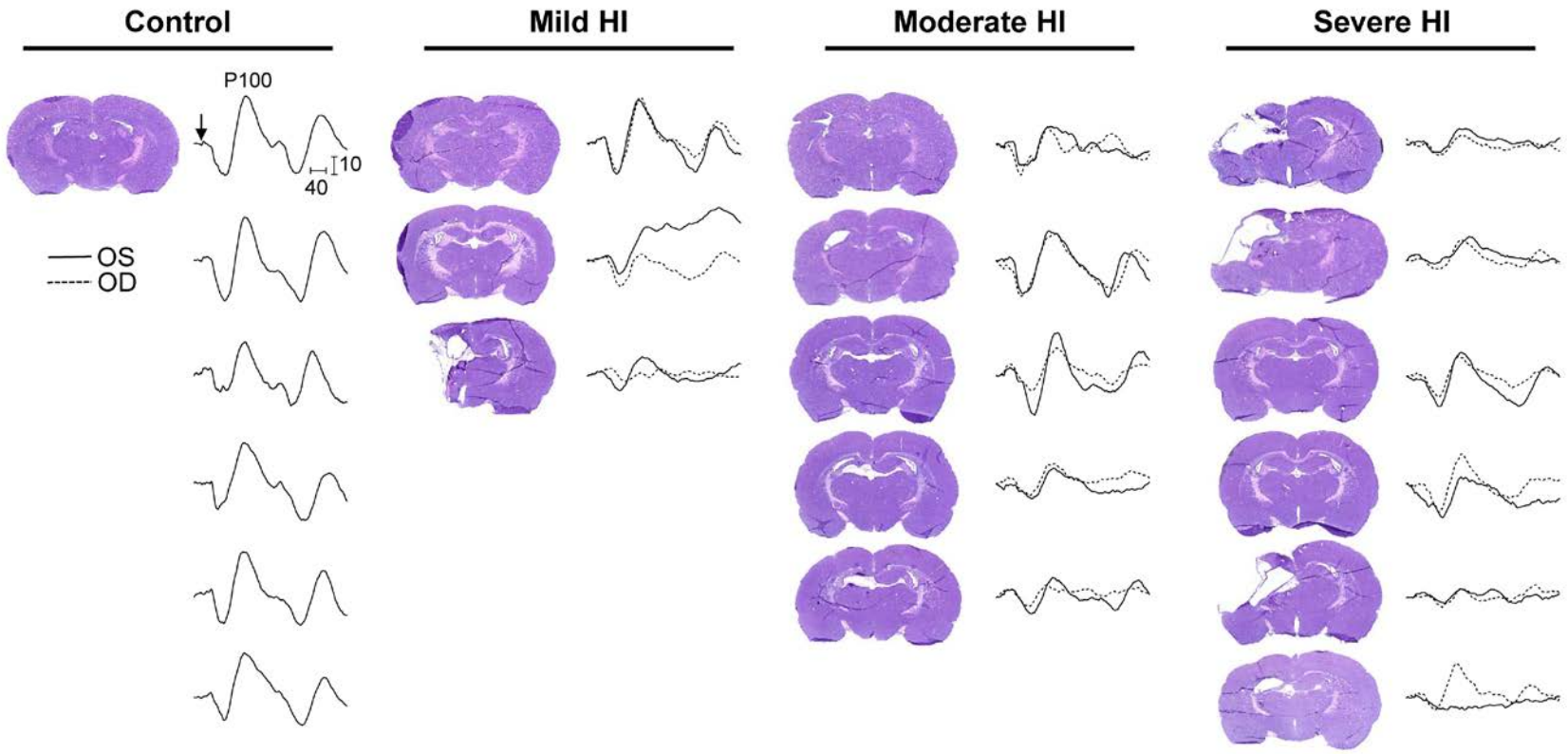

Figure 6

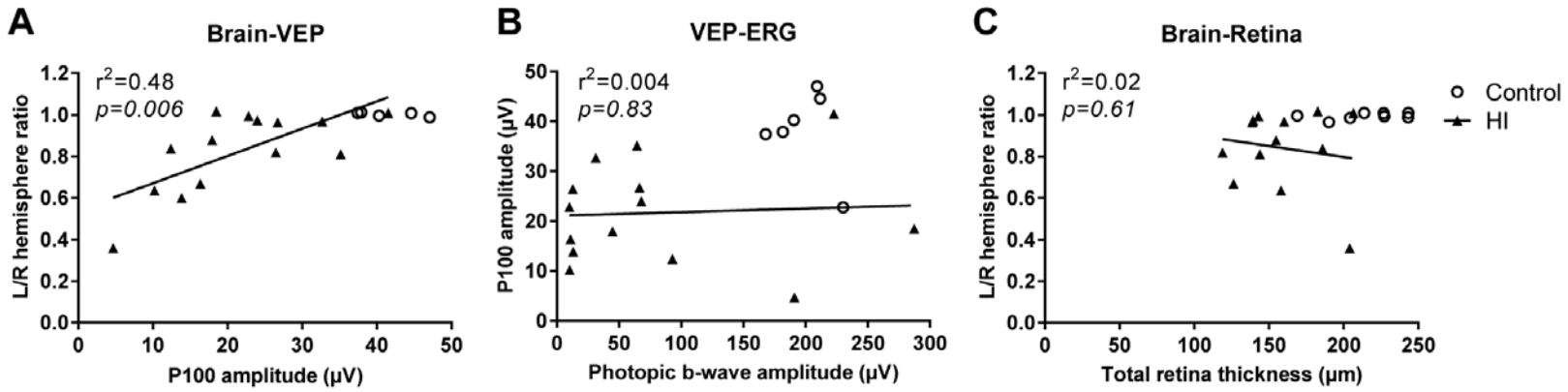
A
Brain-VEP
r²=0.48
p=0.006
L/R hemisphere ratio
P100 amplitude (μV)
B
VEP-ERG
r²=0.004
p=0.83
P100 amplitude (μV)
Photopic b-wave amplitude (μV)
C
Brain-Retina
r²=0.02
p=0.61
L/R hemisphere ratio
Total retina thickness (μm)
Control
HI

TABLES

Table 1. Electroretinogram Amplitudes

	Control *n* = 6	Ischemia *n* = 4	Mild HI *n* = 3		Moderate HI *n* = 5		Severe HI *n* = 6	
	OS	**OS**	**OS**	**OD**	**OS**	**OD**	**OS**	**OD**
P30								
Mixed rod-cone a-wave	401.20 ± 71.40	405.72 ± 70.33	417.82 ± 91.18	510.68 ± 47.36	343.23 ± 31.42	414.82 ± 71.81	334.53 ± 79.58	519.32 ± 36.72 *
Mixed rod-cone b-wave	1007.31 ± 173.85	1016.26 ± 181.17	921.42 ± 319.26	1245.83 ± 93.93	356.53 ± 54.19 ‡	1052.94 ± 204.53	147.65 ± 47.83 ‡	1320.05 ± 98.32 *
Rod V_{max}	701.13 ± 111.48	695.45 ± 91.62	620.47 ± 227.78	900.60 ± 99.99	191.50 ± 63.17 ‡	690.88 ± 160.00	48.37 ± 29.14 ‡	950.25 ± 107.35 †
Photopic b-wave	234.61 ± 43.22	255.54 ± 26.88	224.57 ± 76.94	204.98 ± 27.81	50.25 ± 10.89 ‡	215.75 ± 59.32	7.72 ± 8.58 ‡	281.04 ± 44.09
P60								
Mixed rod-cone a-wave	348.97 ± 43.83	379.63 ± 50.76	390.09 ± 82.58	370.79 ± 47.29	311.78 ± 48.07	303.36 ± 60.56	281.69 ± 63.30	378.87 ± 45.97
Mixed rod-cone b-wave	931.48 ± 150.87	1001.54 ± 115.57	995.49 ± 98.15	1016.44 ± 36.83	368.78 ± 95.54 ‡	842.42 ± 170.14	121.92 ± 68.24 ‡	1024.11 ± 132.66
Rod V_{max}	705.28 ± 110.64	702.90 ± 135.39	732.33 ± 77.97	786.20 ± 63.03	203.96 ± 70.61 ‡	669.80 ± 123.78	44.77 ± 41.45 ‡	778.75 ± 64.15
Photopic b-wave	198.60 ± 22.74	239.77 ± 33.90	233.76 ± 49.05	280.82 ± 33.46 †	67.26 ± 17.11 ‡	194.37 ± 38.41	14.74 ± 8.19 ‡	241.32 ± 19.24

OS, ipsilateral left eye; OD, contralateral right eye.

* $P < 0.05$.

† $P < 0.01$.

‡ $P < 0.001$ versus control.

Table 2. Thicknesses of the Retinal Layers

	Control *n* = 8	Mild HI *n* = 3	Moderate HI *n* = 5	Severe HI *n* = 5
Total thickness, μm	214.79 ± 26.03	197.75 ± 13.13	152.59 ± 19.68 ‡	141.31 ± 18.46 ‡
RPE thickness, μm	7.97 ± 0.19	7.75 ± 0.93	8.20 ± 0.41	8.57 ± 1.15
OS thickness, μm	28.47 ± 6.93	28.10 ± 4.39	33.48 ± 5.97	40.98 ± 9.07 *
IS thickness, μm	13.86 ± 2.80	12.15 ± 3.11	15.50 ± 2.03	21.09 ± 3.20 ‡
ONL thickness, μm	47.64 ± 6.75	40.05 ± 7.50	51.13 ± 5.93	57.20 ± 5.68 *
OPL thickness, μm	10.00 ± 2.23	8.96 ± 4.20	0.61 ± 1.36 ‡	0.00 ± 0.00 ‡
INL thickness, μm	28.93 ± 5.22	24.59 ± 1.84	16.35 ± 4.23 ‡	9.77 ± 1.39 ‡
IPL thickness, μm	54.99 ± 10.34	56.78 ± 13.58	19.79 ± 9.61 ‡	2.85 ± 3.41 ‡
RGC/FL thickness, μm	22.92 ± 5.35	19.39 ± 8.94	7.54 ± 10.93 †	0.84 ± 1.87 ‡

* $P < 0.05$.

† $P < 0.01$.

‡ $P < 0.001$ versus control.

PREFACE TO CHAPTER III

In the previous chapter, we demonstrated that neonatal HI produced irreversible damage to the inner retina while relatively sparing the outer retina up to P60 in rats. Current strategy against hypoxic-ischemic injury focuses on the neuroprotective strategies or ways to prevent neurons from dying. Such strategies that have been tested in animal models include hypoxia/ischemia pretreatment, glutamate receptor blockers, anti-inflammatory agents and free radical scavengers, which all had limited success in human trials. A relatively new approach is targeting neurorestorative pathways. In recent years, sildenafil, a phosphodiesterase type-5 (PDE5) inhibitor, has been studied for the latter role in animal models of stroke and neurodegenerative diseases and showed promising results. To our surprise, potential therapeutic role of sildenafil has not been studied extensively in retinal diseases. In the contrary, existing literature focuses on potential side effects of the sildenafil on the retina due to reported visual side effects. It is therefore important to determine if sildenafil has a beneficial effect on the retinal injury produced by neonatal HI, and if it is safe for the unaffected eye. In Chapter III, we show that sildenafil improves functional and structural outcome of the affected retina in the rats exposed to HI at term-equivalent age, without negative consequences (function) on the fellow retina or the retina of sham controls.

CHAPTER III

MANUSCRIPT 2

Suna Jung, Aaron Johnstone, Zehra Khoja, Emmanouil Rampakakis, Pierre Lachapelle, Pia Wintermark. Sildenafil Improves Functional and Structural Outcome of Retinal Injury Following Term Neonatal Hypoxia-Ischemia. Invest Ophthalmol Vis Sci. 2016; 57(10): 4306-4314.

ABSTRACT

Purpose: To investigate the effects of sildenafil on retinal injury following neonatal hypoxia-ischemia (HI) at term-equivalent age in rat pups.

Methods: HI was induced in male Long-Evans rat pups at postnatal day 10 (P10) by a left common carotid ligation followed by a 2-hour exposure to 8% oxygen. Sham operated rats served as the control group. Both groups were administered vehicle, 2, 10, or 50 mg/kg of sildenafil, twice daily for 7 consecutive days. Retinal function was assessed by flash electroretinograms (ERGs) at P29, and retinal structure was assessed by retinal histology at P30.

Results: HI caused significant functional (i.e., attenuation of the ERG a-wave and b-wave amplitudes and photopic negative response) and structural (i.e., thinning of the total retina, especially the inner retinal layers) retinal damage in the left eyes (i.e., ipsilateral to the carotid ligation). Treatment with the different doses of sildenafil led to a dose-dependent increase in the amplitudes of the ERG a- and b-waves and of the photopic negative response in HI animals, with higher doses associated with greater effect sizes. Similarly, a dose response was observed in terms of improvements in the retinal layer thicknesses.

Conclusions: HI at term-equivalent age induced functional and structural damage mainly to the inner retina. Treatment with sildenafil provided a dose-dependent recovery of retinal function and structure.

INTRODUCTION

Neonatal encephalopathy associated with birth asphyxia is one of the most important causes of pediatric visual impairments in developed countries.[1] Although visual impairments occurring in these newborns have been thought to be due primarily to brain injury, recent evidence suggests that retinal injury may also play a role.[2-6] In a rat model of premature neonatal hypoxic-ischemic encephalopathy (HIE), the function and structure of the inner retina were found to be damaged, while those of the outer retina relatively were spared;[2] recently, similar results were demonstrated in a rat model of term neonatal encephalopathy.[3] In both studies, no correlation was found between the degree of cerebral injury and retinal injury, which suggests that retinal injury may occur independently of cerebral injury as a result of neonatal hypoxia-ischemia (HI).[2, 3]

Sildenafil is a vasodilator that acts by inhibiting the phosphodiesterase type-5 (PDE5) enzyme, which breaks down cyclic guanosine monophosphate (cGMP). Sildenafil has been used widely to treat erectile dysfunction in adults[7] and pulmonary hypertension in both adults and newborns.[8, 9] More recently, the potential therapeutic role of sildenafil has been expanded beyond vasodilation, since an accumulating body of literature has demonstrated the neuroprotective and/or neurorestorative roles of sildenafil in animal models of neurologic diseases, such as ischemic stroke, multiple sclerosis, and Alzheimer's disease.[10-15] Surprisingly, neuroprotective and/or neurorestorative potential of sildenafil on retinal diseases have not been explored. Most available studies regarding the effect of sildenafil on the retina have investigated the risks of the side effects of sildenafil on retinal function or structure.[16-25] Recent studies have suggested that sildenafil may have direct effects on inner retinal cells,[17,26-27] since PDE5 is expressed in the inner nuclear layer and the ganglion cell layer in the human retina.[28] PDE5 also

is expressed in the choroidal and retinal blood vessels.[28] Furthermore, sildenafil also inhibits, but with a reduced efficiency, the PDE6 that is expressed in the outer segment of photoreceptors and is involved in phototransduction[16,19,21,29] and the survival of photoreceptors.[30] With respect to newborns, a concern has been raised over the possible link between the use of sildenafil and the exacerbation of retinopathy of prematurity in a case report based on one newborn;[22] however, the described newborn also was ventilated and septic, and presented with a severe problem of oxygenation before the use of sildenafil, so the causal link between sildenafil and retinopathy was not clear. A later study with larger number of newborns reported no adverse ocular findings in association with sildenafil.[20] In fact, one study suggested that vaso-obliteration and neovascularization, which are the hallmarks of retinopathy of prematurity, were decreased after sildenafil administration in a mouse model of retinopathy of prematurity.[31]

Thus, we hypothesized that sildenafil may be a therapeutic candidate to treat retinal injury induced by neonatal HI at term-equivalent age. In this study, we investigated the effects of neonatal HI on retinal function and structure, and whether different doses of sildenafil could alleviate the retinal anomalies induced by neonatal HI in a rat model of term neonatal encephalopathy.

MATERIALS AND METHODS

1. Animals

All experiments were conducted in accordance with the Association for Research in Vision and Ophthalmology Statement for the use of animals in ophthalmic and vision research, and were approved by the local animal care committee. Adult female Long-Evans rats with their male-only litters (Harlan Laboratories) were received in our animal facility, housed under standard

environment, and allowed food and water ad libitum. Rat pups remained with their mother until weaning at postnatal day 21 (P21).

2. Induction of Term Neonatal HIE

A well-established rat model of term neonatal HIE (Vannucci model),[32-35] combining a left common carotid artery ligation and a 2-hour exposure to 8% oxygen, was used with 10-day-old rat pups as previously described,[3] since this model mimics the patterns of brain injury observed in human term asphyxiated newborns[32-35] and produces concomitant retinal injury.[3] Rats undergoing both the ligation and hypoxia were considered the HI group. Sham operated rats (identical procedure as the HI group, but without ligation and hypoxia) served as the control group.

3. Sildenafil Administration

HI and sham rat pups were weighed daily and then randomized to sildenafil (Viagra®; Pfizer Canada Inc., Kirkland, QC, Canada) or vehicle (Ora-Blend® suspension media; Perrigo Company PLC, Minneapolis, MN, USA) twice daily by oral gavage, starting from 12 hours post-HI for 7 consecutive days. Different doses of sildenafil — i.e., low (2 mg/kg), medium (10 mg/kg), and high (50 mg/kg) — were used in the HI and sham rat pups (n = 4–7 animals/group).

4. Retinal Function

At P29, full-field flash electroretinograms (ERGs) (LKC Technologies, Inc., Gaithersburg, MD, USA) were recorded binocularly following a previously described protocol.[3] The maximum mixed rod-cone a-wave amplitude [36] was measured from the pre-stimulus baseline to the trough

of the a-wave, and the maximum mixed rod-cone b-wave amplitude [37, 38] was measured from the trough of the a-wave to the peak of the b-wave. The photopic b-wave amplitude was measured from the baseline to the b-wave peak, and the photopic negative response (PhNR)[39, 40] was measured from the baseline to the most negative trough following the photopic b-wave. Measurements were performed using EM for Windows® software (LKC Technologies, Inc., Gaithersburg, MD, USA). When the peak of the b-wave could not be determined, the amplitude of the b-wave was measured at the time when the b-wave peaked in the control animals.

5. Retinal Structure

At P30, the animals were sacrificed, and the eyes were enucleated. Retinal histology was performed as per a previously described protocol.[3] Using AxioVision® software (Version 4.8.2.0; Carl Zeiss Microscopy GmbH, Jena, Germany), the thicknesses of the different retinal layers were measured at approximately 1000 μm inferior from the optic nerve head, a region that showed the most prominent HI-induced damage.[3] For retinal reconstruction, retinal segments of 75 μm in width—taken at every 340 μm along the entire length of the superior and inferior retinas—were assembled side by side (Adobe Photoshop®, Adobe Systems Inc. San Jose, CA, USA) to yield a pan-retinal view. Then, the retinal layer thickness was plotted against eccentricity to obtain the spider graphs (see Fig. 3B).

6. Statistical Analysis

The HI and sham rat pups were subdivided into the following groups: vehicle (0 mg/kg) or sildenafil 2 mg/kg, 10 mg/kg, or 50 mg/kg. Differences in the ERG amplitudes and retinal thicknesses between the different doses of sildenafil and the vehicle group were assessed with

the respective effect sizes (non-standardized difference of the means) and corresponding 95% confidence intervals (CIs).

RESULTS

1. Sildenafil Improved the Retinal Function Outcome in the HI Rat Pups at P29

Hypoxia-ischemia caused impairment in the retinal function of the left eye (i.e., ipsilateral to the carotid ligation) of the rat pups treated with vehicle alone. HI induced an attenuation in the amplitude of the ERG mixed rod-cone b-wave, photopic b-wave, and PhNR, and to a lesser extent, of the mixed rod-cone a-wave, compared to the sham vehicle rat pups (Table 1; Fig. 1). Hypoxia-ischemia did not affect the ERGs recorded from the right eyes (i.e., contralateral to the carotid ligation).

The left eyes of the HI animals showed a dose-dependent improvement in all ERG parameters with treatment with different doses of sildenafil, where higher doses were associated with greater effect sizes (Table 1; Fig. 1). The 50 mg/kg dose of sildenafil induced significantly improved response in terms of all ERG parameters, whereas the 10 mg/kg of sildenafil induced significantly improved response in terms of the mixed rod-cone b-wave, the photopic b-wave, and the PhNR, but not the a-wave.

Interestingly, sildenafil had no significant effect on the ERG amplitudes of the right eyes of the HI rat pups (i.e., contralateral to the carotid ligation) and both eyes of the sham rat pups treated with the different doses of sildenafil.

2. Sildenafil Improved the Retinal Structure Outcome in the HI animals at P30

Considering the ERG results, retinal histology was performed only on the left eyes of the sham vehicle group and the HI groups treated with the different doses of sildenafil.

Hypoxia-ischemia induced damages to the retinal structure in the left eyes (i.e., ipsilateral to the carotid ligation) of the rat pups treated with vehicle (Fig. 2). The total retinal thickness was reduced in the HI vehicle rat pups, compared to the sham vehicle rat pups (Table 2; Fig. 2). Specifically, the HI vehicle rat pups showed a thinning of the inner retinal layers (i.e., inner nuclear layer [INL], inner plexiform layer [IPL], and retinal ganglion cell/fiber layer [RGC/FL]) and the outer plexiform layer (OPL), compared to the sham vehicle rat pups. In contrast, the thickness of the outer nuclear layer (ONL) was greater in the HI rat pups treated with the vehicle compared to the sham vehicle rat pups. No significant difference was found in the thickness of the retinal pigment epithelium (RPE), the outer segment (OS), and the inner segment (IS) between groups.

The thicknesses of the affected layers (total retina, ONL, OPL, INL, IPL, RGC/FL) in the HI animals showed a dose-dependent improvement with treatment with different doses of sildenafil. Again, higher doses were associated with greater effect sizes (Table 2; Fig. 2). The 10 mg/kg and the 50 mg/kg doses induced significantly improved response in terms of thicknesses of all the affected layers.

The pattern of retinal injury was not uniform along the superior-inferior axis of the retina (Fig. 3A). The spider graph revealed that the HI rat pups treated with vehicle had thinner INL, IPL, and RGC/FL, which spanned almost all retinal eccentricity, while the increase in ONL and the decrease in OPL thicknesses were detected mostly in the central retina (Fig. 3B). Treatment with the low-dose of sildenafil did not seem to reverse any of the HI-induced changes in retinal

thickness, except in the inferior retina, where the areas showing a thinning of the OPL were limited to a smaller portion of the central region, compared to the HI rat pups treated with the vehicle. In contrast, the HI rat pups treated with the medium and high doses of sildenafil disclosed a nearly normal inner retina at almost all retinal eccentricities along the superior-inferior axis.

DISCUSSION

Neonatal HI induced significant retinal damage, including a reduction in the ERG amplitudes and a thinning of the retina. As previously reported,[2,3] HI affected mostly the inner retina, both functionally (i.e., attenuation of the ERG b-wave and PhNR) and structurally (i.e., destruction of the INL, IPL, and RGC/FL). The photoreceptor function (attenuation of the ERG a-wave) also was affected, but to a lesser extent. Treatment with the different doses of sildenafil led to a dose-dependent improvement in the ERG amplitudes and in the retinal layer thicknesses, with higher doses associated with greater effect sizes. The 50 mg/kg dose of sildenafil induced significantly improved response in terms of all ERG parameters, whereas the 10 mg/kg of sildenafil induced significantly improved response in terms of the mixed rod-cone b-wave, the photopic b-wave, and the PhNR, but not the a-wave. The 10 mg/kg and the 50 mg/kg doses induced significantly improved response in terms of thicknesses of all the affected layers. Our study is the first to explore the therapeutic role of sildenafil on retinal injury induced by neonatal HI at term-equivalent age.

The underlying mechanisms, however, remain to be elucidated and most probably involve multiple pathways. One possible mechanism is through a vascular effect. The endothelial cells and the smooth muscles of the retinal vasculature, the choroidal vasculature, and the

ophthalmic artery express PDE5.[28] Sildenafil has been shown to increase the diameter of some of these blood vessels and consequently increase the ocular blood flow in porcine eyes as well as in healthy human subjects.[41-45] Thus, in the short-term, sildenafil may help restore the blood flow to the affected retina. In fact, Charriaut-Marlangue et al. have demonstrated a blood flow increase in the common carotid artery contralateral to the ligated side after a single administration of intraperitoneal sildenafil immediately following an HI insult in a premature rat model of neonatal HIE.[46] However, in our study, sildenafil was administered with a 12-hour delay and continued for 7 days; thus, a process other than acute vasodilation is likely involved. Another possible vascular effect of sildenafil is through the modulation of retinal angiogenesis.[47] Fawzi et al. reported that sildenafil administration in a neonatal mouse model of oxygen-induced retinopathy prevented the hyperoxia-induced retinal vaso-obliteration through HIF-α stabilization, which in turn prevented the retinal neovascularization known to take place when the pups are returned to normoxia.[31]

The beneficial effects of sildenafil may also arise from non-vascular mechanisms. Sildenafil has been shown to upregulate neurotrophic factors in adult rodent models of neurological diseases, reduce neuroinflammation, and activate pro-survival signalling pathways, which have resulted in reduced neuronal loss and synaptic damage, and enhanced neurogenesis.[10-15,48-52] In a premature rat model of brain injury, sildenafil has been shown to decrease neuronal apoptosis and microglial activation.[46] Since neuronal apoptosis has been shown to peak at 24 hours post-HI in the neonatal retina,[2] the sildenafil administered 12 hours post-HI may have limited apoptosis and further degeneration by its possible anti-apoptotic and anti-inflammatory effects, which have been observed in the adult rat brain.[11,15,48,49,51] Further

investigations are needed to determine the exact mechanisms underlying the beneficial effects of sildenafil on retinal function and structure.

Interestingly, the outer segment of photoreceptors expresses PDE6,[29] which is involved in photoreceptor survival[30] and phototransduction.[16] Selective inhibition of PDE6 has been shown to increase intracellular cGMP in the photoreceptors and lead to photoreceptor degeneration.[30,53] Sildenafil also inhibits PDE6, but with a reduced efficiency. In our study, sildenafil did not induce photoreceptor degeneration. In fact, treatment with sildenafil restored the function of the photoreceptors, which had been impaired following hypoxia-ischemia at term-equivalent age. Of note, a decrease in a-wave amplitude in HI vehicle animals was accompanied by an increase in ONL thickness. This discrepancy between function and structure is perplexing; however, on a closer observation, the increase in ONL thickness appeared to be a result of cells taking up more space (increased space between rows of cells) in the now absent inner retina (resulting from the absence of the structural support that the inner retina normally provides to the outer retina), as the number of rows in ONL remained similar across the different groups (13-14 rows). The stacking of the cells also appeared more disorganized in the HI vehicle rats compared to the sham vehicle rats. Hence, a decrease in a-wave amplitude can be a sign of functional anomaly of the photoreceptors that may precede the degeneration of the cells. Although there was no obvious loss of photoreceptors at this time point, it is possible that there were already some ultrastructural changes that affected the ERG a-wave. Secondly, a decrease in the a-wave amplitude could have resulted partly from the loss of inner retina. There is evidence that the off-bipolar cells contribute to the ERG a-wave in Long-Evans rats,[54,55,56] Our own data lends some support towards this possibility as the HI animals treated with the low-dose sildenafil showed a

trend towards improved OPL and INL thicknesses in some parts of the retina, along with a trend towards improved ERG a-wave amplitudes.

Sildenafil is already safely used in newborns with persistent pulmonary hypertension.[57-59] Studies of the neonatal population have shown no adverse ocular findings in association with sildenafil.[20] Our results from the sham groups confirm that sildenafil does not affect normal retinal function, as is demonstrated by the absence of a difference in the ERG amplitudes between the sham rat pups treated with different doses of sildenafil and the sham vehicle rat pups. Most importantly, our results from the HI animals suggest that sildenafil limited or repaired the retinal injury resulting from neonatal hypoxia-ischemia, with a substantial improvement of retinal function and structure compared to the untreated rat pups. Further research with larger sample size and additional screening for side effects is therefore warranted to determine if sildenafil can be used as a novel therapy to treat term asphyxiated newborns with retinal injury to significantly improve the potential future outcomes of these newborns.

In our study protocol, we chose to reproduce as much as possible what would be a feasible therapeutic approach for human term asphyxiated newborns. We administered sildenafil by oral route instead of the intraperitoneal or subcutaneous route described in most of the previous animal experiments,[14,16-17,31,46] since oral sildenafil is the most commonly used route with human newborns. It is safe to assume that oral sildenafil reaches the retina, as it has been demonstrated to transiently affect the ERG in healthy human subjects 1 hour after intake.[19,25] Oral sildenafil displays an adequate bioavailability (23% in male rats and 38% in humans).[60,61] Sildenafil is metabolized faster in male rats compared to humans, with the elimination half-life of respectively 0.4 and 3.7 hours, after an oral administration.[61] Dosages in the present study were chosen so that they correspond somewhat to the equivalent recommended amount for

human newborns ranging from low doses that are usually initially used to maximal described doses.[62] In addition, we started the sildenafil administration 12 hours after the hypoxic-ischemic event, taking into consideration the delay that it would take to identify human newborns at risk of developing injury despite the hypothermia treatment. Finally, we repeated the treatment for 7 days so that it would potentially continue acting on the cascades of chemical reactions triggered following hypoxia-ischemia.

The fact that sildenafil had a beneficial effect even when started 12 hours after the HI insult highlights the probable neurorestorative role of sildenafil in the retina, with a wider treatment window compared to neuroprotective strategies.[63] Other neuroprotective therapies (such as N-methyl-d-aspartate [NMDA] blocker, antioxidants, and anti-inflammatory agents) were found effective only when given before or during the HI insult in adult rat models of ischemic retinopathy.[64,65] Hypothermia treatment during HI in P0 rats prevented the development of retinopathy;[6,66] however, the effect of delayed hypothermia treatment was not tested. With respect to the brain, hypothermia treatment started 12 hours post-HI in a P7 Vannucci model offered no benefit to animals with moderate HI injury and was even deleterious to animals with severe HI injury.[67] Our results strongly suggest that sildenafil holds promise for the treatment of retinal injury following HI at term-equivalent age.

For technical reasons (i.e., different embedding techniques for retinal histology or retinal immunohistochemistry), the same retinas that were used for retinal histology with toluidine blue could not be used for immunohistochemistry, explaining why we only investigated the impact of retinal function and structure in the present study. Additional animal experiments for immunohistochemistry and western blot are needed to further understand the mechanism involved with these beneficial effects. It will also be important to further test the potential sex

difference in response to treatment, as the experiments described here were only performed in male rat pups. And further studies also need to assess whether the beneficial effects of sildenafil on the retina persist at long-term as the rats mature.

In conclusion, hypoxia-ischemia at term-equivalent age induced functional and structural damages mainly in the inner retina in rats. Treatment with oral sildenafil provided a dose-dependent beneficial effect on the function and structure of the retina in a rat model of term neonatal encephalopathy. In addition, treatment with sildenafil had no adverse effect on normal retinal function. These results highlight the potential therapeutic role of sildenafil for retinal injury induced by neonatal hypoxia-ischemia at term-equivalent age. Neurorestorative mechanisms of sildenafil on the retina remain to be elucidated.

ACKNOWLEDGMENTS

The authors thank Wayne Ross Egers for his professional English correction of the manuscript and Laura Dale and Laurel Stephens for technical support.

Supported by studentship support from the Canadian Institutes of Health Research (CIHR) (Frederick Banting and Charles Best Canada Graduate Scholarship), the Research Institute of the McGill University Health Centre Foundation of Stars, and the McGill University Integrated Program in Neuroscience (all to SJ). This work was funded through an operating grant (MOP-133707) awarded by CIHR to PW and PL, as well as a CIHR grant (MOP 126082) to PL and a Clinical Research Scholar Career Award Junior 1 and 2 awarded by the Fonds de recherche en Santé Québec to PW. The authors alone are responsible for the content and writing of the paper.

Disclosure: **S. Jung**, None; **A. Johnstone**, None; **Z. Khoja**, None; **E. Rampakakis**, None; **P. Lachapelle**, None; **P. Wintermark**, None

REFERENCES

1. Hoyt CS. Brain injury and the eye. *Eye.* 2007;21:1285-1289.
2. Huang HM, Huang CC, Hung PL, Chang YC. Hypoxic-ischemic retinal injury in rat pups. *Pediatr Res.* 2012;72:224-231.
3. Jung S, Polosa A, Lachapelle P, Wintermark P. Visual Impairments Following Term Neonatal Encephalopathy: Do Retinal Impairments Also Play a Role? *Invest Ophthalmol Vis Sci.* 2015;56:5182-5193.
4. Kiss P, Szogyi D, Reglodi D, et al. Effects of perinatal asphyxia on the neurobehavioral and retinal development of newborn rats. *Brain Res.* 2009;1255:42-50.
5. Nickel BL, Hoyt CS. The hypoxic retinopathy syndrome. *Am J Ophthalmol.* 1982;93:589-593.
6. Rey-Funes M, Ibarra ME, Dorfman VB, et al. Hypothermia prevents the development of ischemic proliferative retinopathy induced by severe perinatal asphyxia. *Exp Eye Res.* 2010;90:113-120.
7. Goldstein I, Lue TF, Padma-Nathan H, Rosen RC, Steers WD, Wicker PA; Sildenafil Study Group. Oral sildenafil in the treatment of erectile dysfunction. *N Engl J Med.* 1998;338:1397-1404.
8. Barnett CF, Machado RF. Sildenafil in the treatment of pulmonary hypertension. *Vasc Health Risk Manag.* 2006;2:411-422.
9. Shah PS, Ohlsson A. Sildenafil for pulmonary hypertension in neonates. *Cochrane Database Syst Rev.* 2011;CD005494.
10. Bednar MM. The role of sildenafil in the treatment of stroke. *Curr Opin Investig Drugs.* 2008;9:754-759.

11. Chen XM, Wang NN, Zhang TY, Wang F, Wu CF, Yang JY. Neuroprotection by sildenafil: neuronal networks potentiation in acute experimental stroke. *CNS Neurosci Ther*. 2014;20:40-49.

12. Nunes AK, Raposo C, Luna RL, Cruz-Hofling MA, Peixoto CA. Sildenafil (Viagra®) down regulates cytokines and prevents demyelination in a cuprizone-induced MS mouse model. *Cytokine.* 2012;60:540-551.

13. Zhang L, Zhang RL, Wang Y, et al. Functional recovery in aged and young rats after embolic stroke: treatment with a phosphodiesterase type 5 inhibitor. *Stroke.* 2005;36:847-852.

14. Zhang RL, Chopp M, Roberts C, et al. Sildenafil enhances neurogenesis and oligodendrogenesis in ischemic brain of middle-aged mouse. *PloS One.* 2012;7:e48141.

15. Zhang J, Guo J, Zhao X, et al. Phosphodiesterase-5 inhibitor sildenafil prevents neuroinflammation, lowers beta-amyloid levels and improves cognitive performance in APP/PS1 transgenic mice. *Behav Brain Res.* 2013;250:230-237.

16. Behn D, Potter MJ. Sildenafil-mediated reduction in retinal function in heterozygous mice lacking the gamma-subunit of phosphodiesterase. *Invest Ophthalmol Vis Sci.* 2001;42:523-527.

17. Nivison-Smith L, Zhu Y, Whatham A, et al. Sildenafil alters retinal function in mouse carriers of retinitis pigmentosa. *Exp Eye Res.* 2014;128:43-56.

18. Balacco Gabrieli C, Regine F, Vingolo EM, Rispoli E, Isidori A. Acute electroretinographic changes during sildenafil (Viagra) treatment for erectile dysfunction. *Doc Ophthalmol.* 2003;107:111-114.

19. Laties A, Zrenner E. Viagra (sildenafil citrate) and ophthalmology. *Progr Retin Eye Res.* 2002;21:485-506.

20. Kehat R, Bonsall DJ, North R, Connors B. Ocular findings of oral sildenafil use in term and near-term neonates. *J AAPOS.* 2010;14:159-162.

21. Kinoshita J, Iwata N, Shimoda H, Kimotsuki T, Yasuda M. Sildenafil-induced reversible impairment of rod and cone phototransduction in monkeys. *Invest Ophthalmol Vis Sci.* 2015;56:664-673.

22. Marsh CS, Marden B, Newsom R. Severe retinopathy of prematurity (ROP) in a premature baby treated with sildenafil acetate (Viagra) for pulmonary hypertension. *Br J Ophthalmol.* 2004;88:306-307.

23. Pierce CM, Petros AJ, Fielder AR. No evidence for severe retinopathy of prematurity following sildenafil. *Br J Ophthalmol.* 2005;89:250.

24. Vatansever HS, Kayikcioglu O, Gumus B. Histopathologic effect of chronic use of sildenafil citrate on the choroid & retina in male rats. *Indian J Med Res.* 2003;117:211-215.

25. Vobig MA, Klotz T, Staak M, Bartz-Schmidt KU, Engelmann U, Walter P. Retinal side-effects of sildenafil. *Lancet.* 1999;353:375.

26. Luke M, Luke C, Hescheler J, Schneider T, Sickel W. Effects of phosphodiesterase type 5 inhibitor sildenafil on retinal function in isolated superfused retina. *J Ocul Pharmacol Ther.* 2005;21:305-314.

27. Martins J, Kolomiets B, Caplette R, et al. Sildenafil acutely decreases visual responses in ON and OFF retinal ganglion cells. *Invest Ophthalmol Vis Sci.* 2015;56:2639-2648.

28. Foresta C, Caretta N, Zuccarello D, et al. Expression of the PDE5 enzyme on human retinal tissue: new aspects of PDE5 inhibitors ocular side effects. *Eye (Lond).* 2008;22:144-149.

29. Wallis RM, Corbin JD, Francis SH, Ellis P. Tissue distribution of phosphodiesterase families and the effects of sildenafil on tissue cyclic nucleotides, platelet function, and the contractile responses of trabeculae carneae and aortic rings in vitro. *Am J Cardiol.* 1999;83:3C-12C.

30. Paquet-Durand F, Sahaboglu A, Dietter J, et al. How long does a photoreceptor cell take to die? Implications for the causative cell death mechanisms. *Adv Exp Med Biol.* 2014;801:575-581.

31. Fawzi AA, Chou JC, Kim GA, Rollins SD, Taylor JM, Farrow KN. Sildenafil attenuates vaso-obliteration and neovascularization in a mouse model of retinopathy of prematurity. *Invest Ophthalmol Vis Sci.* 2014;55:1493-1501.

32. Patel SD, Pierce L, Ciardiello AJ, Vannucci SJ. Neonatal encephalopathy: pre-clinical studies in neuroprotection. *Biochem Soc Trans.* 2014;42:564-568.

33. Patel SD, Pierce L, Ciardiello A, et al. Therapeutic hypothermia and hypoxia-ischemia in the term-equivalent neonatal rat: characterization of a translational preclinical model. *Pediatr Res.* 2015;78:264-271.

34. Recker R, Adami A, Tone B, et al. Rodent neonatal bilateral carotid artery occlusion with hypoxia mimics human hypoxic-ischemic injury. *J Cereb Blood Flow Metab.* 2009;29:1305-1316.

35. Rice JE, 3rd, Vannucci RC, Brierley JB. The influence of immaturity on hypoxic-ischemic brain damage in the rat. *Ann. Neurol.* 1981;9:131-141.

36. Hood DC, Birch DG. The A-wave of the human electroretinogram and rod receptor function. *Invest Ophthalmol Vis Sci.* 1990;31:2070-2081.

37. Miller RF, Dowling JE. Intracellular responses of the Müller (glial) cells of mudpuppy retina: their relation to b-wave of the electroretinogram. *J Neurophysiol.* 1970;33:323-341.

38. Stockton RA, Slaughter MM. B-wave of the electroretinogram. A reflection of ON bipolar cell activity. *J Gen Physiol.* 1989;93:101-122.

39. Li B, Barnes GE, Holt WF. The decline of the photopic negative response (PhNR) in the rat after optic nerve transection. *Doc Ophthalmol*. 2005;111:23-31.

40. Machida S, Raz-Prag D, Fariss RN, Sieving PA, Bush RA. Photopic ERG negative response from amacrine cell signaling in RCS rat retinal degeneration. *Invest Ophthalmol Vis Sci*. 2008;49:442-452.

41. Koksal M, Ozdemir H, Kargi S, et al. The effects of sildenafil on ocular blood flow. *Acta Ophthalmol Scand.* 2005;83:355-359.

42. Dundar SO, Dundar M, Kocak I, Dayanir Y, Ozkan SB. Effect of sildenafil on ocular haemodynamics. *Eye (Lond)*. 2001;15:507-510.

43. Pache M, Meyer P, Prunte C, Orgul S, Nuttli I, Flammer J. Sildenafil induces retinal vasodilatation in healthy subjects. *Br J Ophthalmol.* 2002;86:156-158.

44. Polak K, Wimpissinger B, Berisha F, Georgopoulos M, Schmetterer L. Effects of sildenafil on retinal blood flow and flicker-induced retinal vasodilatation in healthy subjects. *Invest Ophthalmol Vis Sci.* 2003;44:4872-4876.

45. Yuan Z, Hein TW, Rosa RH, Jr., Kuo L. Sildenafil (Viagra) evokes retinal arteriolar dilation: dual pathways via NOS activation and phosphodiesterase inhibition. *Invest Ophthalmol Vis Sci.* 2008;49:720-725.

46. Charriaut-Marlangue C, Nguyen T, Bonnin P, et al. Sildenafil mediates blood-flow redistribution and neuroprotection after neonatal hypoxia-ischemia. *Stroke.* 2014;45:850-856.

47. Pyriochou A, Zhou Z, Koika V, et al. The phosphodiesterase 5 inhibitor sildenafil stimulates angiogenesis through a protein kinase G/MAPK pathway. *J Cell Physiol.* 2007;211:197-204.

48. Barros-Minones L, Martin-de-Saavedra D, Perez-Alvarez S, et al. Inhibition of calpain-regulated p35/cdk5 plays a central role in sildenafil-induced protection against chemical hypoxia produced by malonate. *Biochim Biophys Acta.* 2013;1832:705-717.

49. Caretti A, Bianciardi P, Ronchi R, Fantacci M, Guazzi M, Samaja M. Phosphodiesterase-5 inhibition abolishes neuron apoptosis induced by chronic hypoxia independently of hypoxia-inducible factor-1alpha signaling. *Exp Biol Med (Maywood).* 2008;233:1222-1230.

50. Dias Fiuza Ferreira E, Valerio Romanini C, Cypriano PE, Weffort de Oliveira RM, Milani H. Sildenafil provides sustained neuroprotection in the absence of learning recovery following the 4-vessel occlusion/internal carotid artery model of chronic cerebral hypoperfusion in middle-aged rats. *Brain Res Bull.* 2013;90:58-65.

51. Pifarre P, Gutierrez-Mecinas M, Prado J, et al. Phosphodiesterase 5 inhibition at disease onset prevents experimental autoimmune encephalomyelitis progression through immunoregulatory and neuroprotective actions. *Exp Neurol.* 2014;251:58-71.

52. Romanini CV, Schiavon AP, Ferreira ED, de Oliveira RM, Milani H. Sildenafil prevents mortality and reduces hippocampal damage after permanent, stepwise, 4-vessel occlusion in rats. *Brain Res Bull.* 2010;81:631-640.

53. Lolley RN, Farber DB, Rayborn ME, Hollyfield JG. Cyclic GMP accumulation causes degeneration of photoreceptor cells: simulation of an inherited disease. *Science.* 1977;196:664-666.

54. Dang TM, Tsai TI, Vingrys AJ, Bui BV. Post-receptoral contributions to the rat scotopic electroretinogram a-wave. *Doc Ophthalmol*. 2011;122:149-156.

55. Shiells RA, Falk G. Contribution of rod, on-bipolar, and horizontal cell light responses to the ERG of dogfish retina. *Vis Neurosci*. 1999;16:503-511.

56. Hanitzsch R, Karbaum R, Lichtenberger T. Do horizontal cells contribute to the rabbit ERG? *Doc Ophthalmol*. 1999;97:57-66.

57. Abman SH. Recent advances in the pathogenesis and treatment of persistent pulmonary hypertension of the newborn. *Neonatology.* 2007;91:283-290.

58. Baquero H, Soliz A, Neira F, Venegas ME, Sola A. Oral sildenafil in infants with persistent pulmonary hypertension of the newborn: a pilot randomized blinded study. *Pediatrics.* 2006;117:1077-1083.

59. Steinhorn RH, Kinsella JP, Pierce C, et al. Intravenous sildenafil in the treatment of neonates with persistent pulmonary hypertension. *J Pediatr.* 2009;155:841-847 e841.

60. Mukherjee A, Dombi T, Wittke B, Lalonde R. Population pharmacokinetics of sildenafil in term neonates: evidence of rapid maturation of metabolic clearance in the early postnatal period. *Clin Pharmacol Ther.* 2009;85:56-63.

61. Walker DK, Ackland MJ, James GC, et al. Pharmacokinetics and metabolism of sildenafil in mouse, rat, rabbit, dog and man. *Xenobiotica.* 1999;29:297-310.

62. Wintermark P. Current controversies in newer therapies to treat birth asphyxia. *Int J Pediatr.* 2011;2011:848413.

63. Sola A, Baquero H. Oral sildenafil in neonatal medicine: "tested in adults also used in neonates". *An Pediatr (Barc).* 2007;66:167-176.

64. Osborne NN, Casson RJ, Wood JP, Chidlow G, Graham M, Melena J. Retinal ischemia: mechanisms of damage and potential therapeutic strategies. *Prog Retin Eye Res.* 2004;23:91-147.

65. Block F, Schwarz M. The b-wave of the electroretinogram as an index of retinal ischemia. *Gen Pharmacol.* 1998;30:281-287.

66. Rey-Funes M, Dorfman VB, Ibarra ME, et al. Hypothermia prevents gliosis and angiogenesis development in an experimental model of ischemic proliferative retinopathy. *Invest Ophthalmol Vis Sci.* 2013;54:2836-2846.

67. Sabir H, Scull-Brown E, Liu X, Thoresen M. Immediate hypothermia is not neuroprotective after severe hypoxia-ischemia and is deleterious when delayed by 12 hours in neonatal rats. *Stroke.* 2012;43:3364-3370.

FIGURE LEGENDS

Figure 1. Flash electroretinograms of the sham and HI rat pups treated with different doses of sildenafil. Veh, vehicle; HI, hypoxia-ischemia; 2mg/kg, sildenafil 2 mg/kg; 10mg/kg, sildenafil 10 mg/kg; 50mg/kg, sildenafil 50 mg/kg. (**A, B**) Representative scotopic (**A**) and photopic (**B**) ERG waveforms obtained from the left (i.e., ipsilateral to the carotid ligation) (*solid line*) and right (i.e., contralateral to the carotid ligation) (*dashed line*) eyes. *Vertical arrows* denote the stimulus onset. *Double-headed arrows* display how the amplitudes were measured. The units of horizontal and vertical scale bars are respectively in milliseconds and microvolts. (**C–F**) Amplitude measurements of the ERG waves. Mean ± SE. (**C**) Mixed rod-cone a-wave amplitude. (**D**) Mixed rod-cone b-wave amplitude. (**E**) Photopic b-wave amplitude. (**F**) Photopic negative response (PhNR) amplitude.

Figure 2. Retinal structure in the left eyes of the sham vehicle rat pups and the HI rat pups treated with different doses of sildenafil. Veh, vehicle; HI, hypoxia-ischemia; 2mg/kg, sildenafil 2 mg/kg; 10mg/kg, sildenafil 10 mg/kg; 50mg/kg, sildenafil 50 mg/kg. (**A**) Representative toluidine blue stained retinal cross sections (magnification: 40X). Images were taken at 1000 μm inferior to the optic nerve head. (**B**) Thicknesses of the different retinal layers. Solid horizontal line represents the mean of the sham vehicle group. Mean ± SE.

Figure 3. Topographic distribution of the inner retinal injury in the left eyes of the sham vehicle rat pups and the HI rat pups treated with different doses of sildenafil. Veh, vehicle; 2mg/kg, sildenafil 2 mg/kg; 10mg/kg, sildenafil 10 mg/kg; 50mg/kg, sildenafil 50 mg/kg. (**A**) Reconstruction of the retina along the superior-inferior axis at the level of the ONH

(magnification: 40X). (**B**) Spider graphs representing the thickness of retinal layers with respect to eccentricity. Mean ± SE.

FIGURES

Figure 1

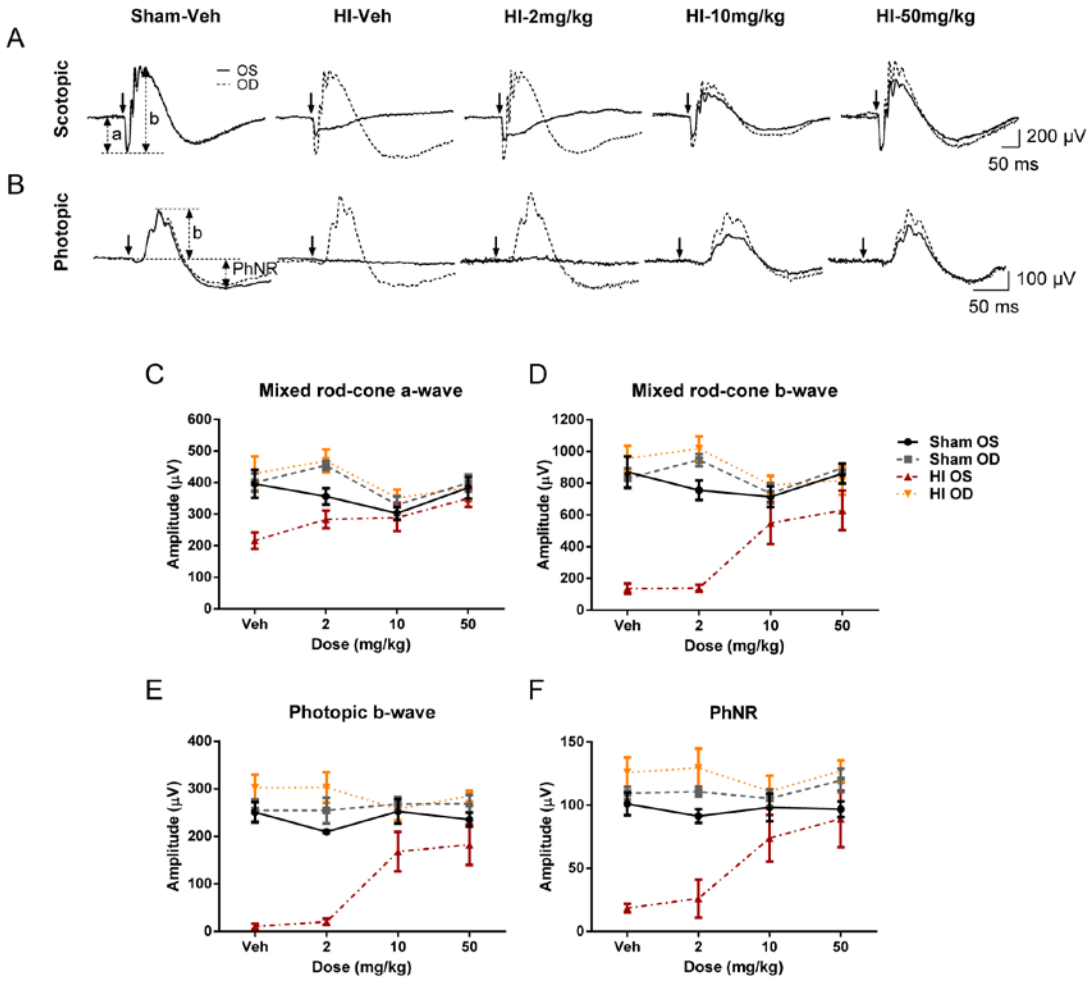

Figure 2

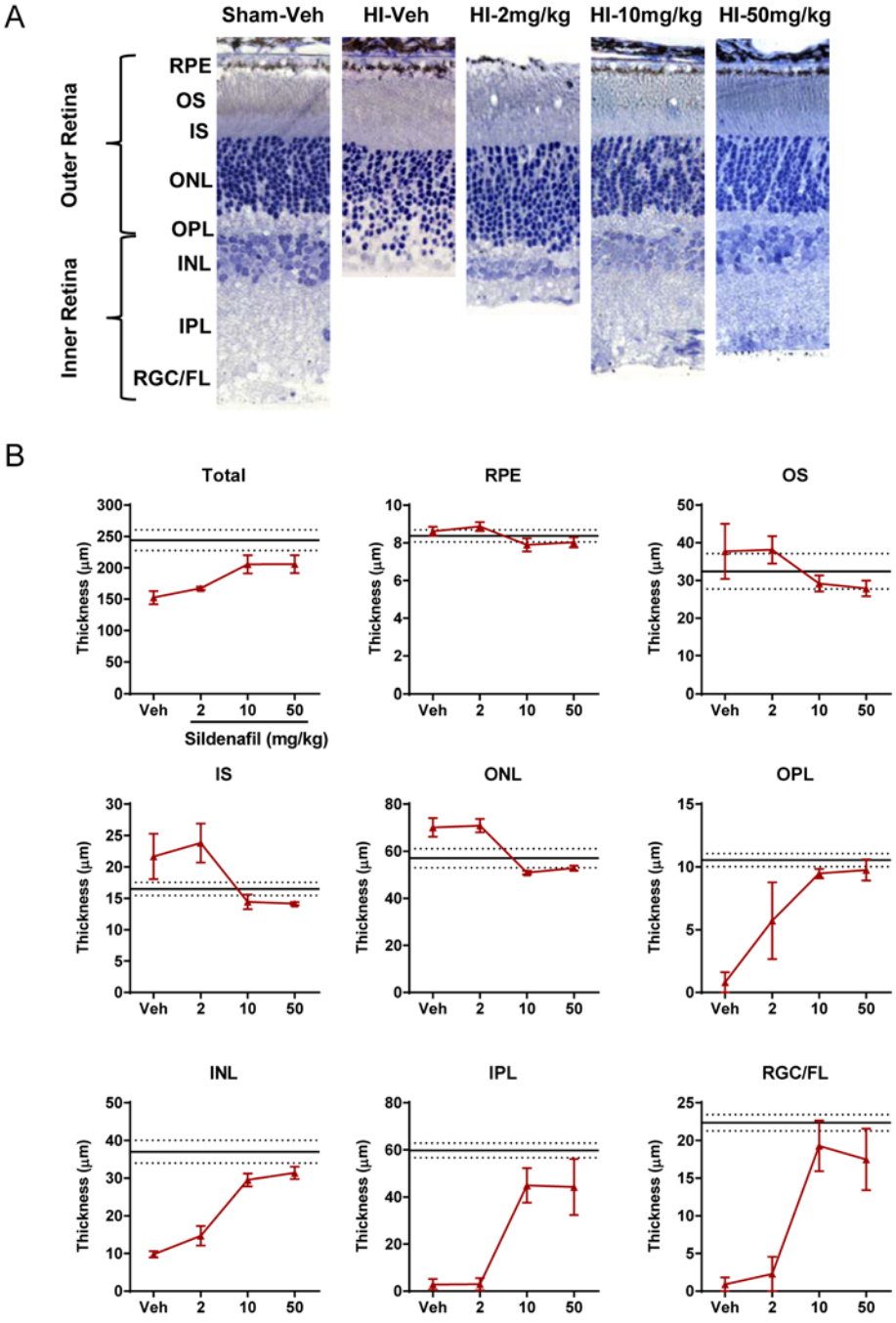
A
Sham-Veh
HI-Veh
HI-2mg/kg
HI-10mg/kg
HI-50mg/kg
Outer Retina
Inner Retina
RPE
OS
IS
ONL
OPL
INL
IPL
RGC/FL
B
Total
RPE
OS
IS
ONL
OPL
INL
IPL
RGC/FL
Thickness (µm)
Veh
2
10
50
Sildenafil (mg/kg)

Figure 3

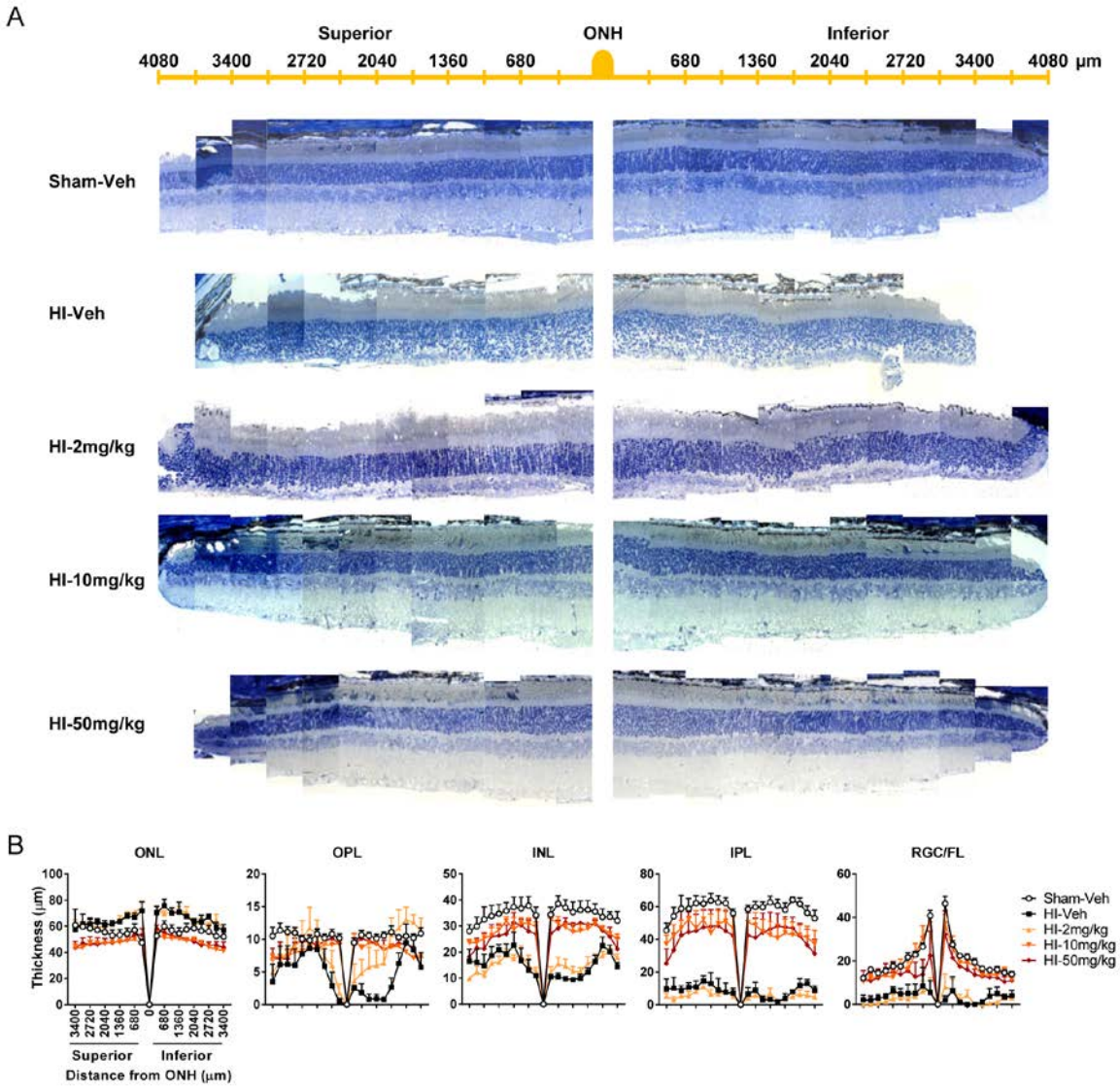
A
Superior
ONH
Inferior
4080 3400 2720 2040 1360 680 680 1360 2040 2720 3400 4080 μm
Sham-Veh
HI-Veh
HI-2mg/kg
HI-10mg/kg
HI-50mg/kg
B
ONL
OPL
INL
IPL
RGC/FL
Thickness (μm)
Superior
Inferior
Distance from ONH (μm)
Sham-Veh
HI-Veh
HI-2mg/kg
HI-10mg/kg
HI-50mg/kg

TABLES

Table 1. Electroretinogram Amplitudes

Electroretinogram Parameters	Sham-Veh *n* = 7	Sham-Sild 2mg/kg *n* = 5	Sham-Sild 10mg/kg *n* = 7	Sham-Sild 50mg/kg *n* = 6
OS				
Mixed rod-cone a-wave, µV	395.97 ± 44.90	356.22 ± 25.73	302.64 ± 19.39	383.13 ± 33.82
Effect size (95% CI)		-39.75 (-168.85, 89.34)	-93.33 (-199.89, 13.24)	-12.84 (-140.19, 114.52)
Mixed rod-cone b-wave, µV	870.51 ± 96.79	755.50 ± 60.68	714.80 ± 65.07	860.93 ± 62.52
Effect size (95% CI)		-115.01 (-396.99, 166.96)	-155.71 (-409.83, 98.40)	-9.58 (-273.44, 254.28)
Photopic b-wave, µV	250.69 ± 21.51	209.54 ± 2.67	252.53 ± 25.47	235.05 ± 14.33
Effect size (95% CI)		-41.15 (-98.86, 16.57)	1.84 (-70.80, 74.48)	-15.64 (76.69, 43.42)
PhNR, µV	100.89 ± 9.00	91.36 ± 5.42	98.24 ± 11.07	96.83 ± 6.21
Effect size (95% CI)		-9.53 (-35.57, 16.52)	-2.64 (-33.72, 28.43)	-4.05 (-28.97, 20.87)
OD				
Mixed rod-cone a-wave, µV	400.29 ± 28.35	454.30 ± 14.54	329.26 ± 26.30	398.62 ± 26.75
Mixed rod-cone b-wave, µV	829.76 ± 63.30	946.16 ± 38.24	735.33 ± 61.79	896.70 ± 24.97
Photopic b-wave, µV	254.49 ± 23.01	254.36 ± 27.18	267.71 ± 15.35	268.82 ± 17.95
PhNR, µV	109.44 ± 5.01	110.62 ± 3.98	105.24 ± 7.06	119.45 ± 9.32

Table 1. Extended

Electroretinogram Parameters	HI-Veh *n* = 6	HI-Sild 2mg/kg *n* = 5	HI-Sild 10mg/kg *n* = 6	HI-Sild 50mg/kg *n* = 4
OS				
Mixed rod-cone a-wave, µV	216.28 ± 25.99	283.38 ± 27.62	288.92 ± 43.38	349.73 ± 27.14
Effect size (95% CI)		67.1 (-18.95, 153.14)	72.63 (-40.04, 185.31)	133.44 (43.66, 223.22)
Mixed rod-cone b-wave, µV	135.18 ± 32.67	138.68 ± 20.89	548.88 ± 132.35	628.83 ± 124.89
Effect size (95% CI)		3.5 (-88.67, 95.66)	413.7 (109.95, 717.45)	493.64 (247.26,740.02)
Photopic b-wave, µV	10.38 ± 5.90	20.26 ± 6.46	167.90 ± 41.53	182.38 ± 42.41
Effect size (95% CI)		9.88 (-9.93, 29.68)	157.52 (64.05, 250.98)	171.99 (92.83, 251.15)
PhNR, µV	18.45 ± 3.36	26.04 ± 15.07	73.78 ± 18.57	89.03 ± 22.35
Effect size (95% CI)		7.56 (-24.32, 39.50)	55.33 (13.29, 97.38)	70.58 (28.70, 112.45)
OD				
Mixed rod-cone a-wave, µV	429.20 ± 53.69	468.34 ± 36.85	351.50 ± 25.93	383.08 ± 36.96
Mixed rod-cone b-wave, µV	955.78 ± 79.43	1017.4 ± 78.19	788.42 ± 58.46	815.50 ± 88.48
Photopic b-wave, µV	302.07 ± 27.54	302.76 ± 32.30	257.62 ± 24.06	284.73 ± 11.08
PhNR, µV	125.83 ± 11.70	129.36 ± 15.27	110.98 ± 12.24	126.93 ± 8.49

Effect size: calculated compared to the vehicle rat pups. CI, confidence interval of the effect size; OS, ipsilateral left eye; OD, contralateral right eye; PhNR, photopic negative response; sild, sildenafil; veh, vehicle.

Table 2. Thicknesses of the Retinal Layers

Retinal Layers	Sham–Veh	HI–Veh	HI–Sild 2mg/kg	HI–Sild 10mg/kg	HI–Sild 50mg/kg
Total thickness, μm	244.14 ± 16.56	152.55 ± 10.48	167.28 ± 2.63	205.64 ± 14.20	205.80 ± 14.22
Effect size (95% CI)			14.72 (-11.71, 41.16)	53.09 (9.24, 96.94)	53.25 (10.02, 96.47)
RPE thickness, μm	8.38 ± 0.32	8.62 ± 0.23	8.88 ± 0.24	7.89 ± 0.35	8.03 ± 0.27
Effect size (95% CI)			0.25 (-0.51, 1.02)	-0.73 (-1.69, 0.24)	-0.59 (-1.43, 0.25)
OS thickness, μm	32.45 ± 4.70	37.74 ± 7.28	38.14 ± 3.66	29.18 ± 2.14	27.87 ± 2.09
Effect size (95% CI)			0.40 (-19.53, 20.33)	-8.55 (-24.72, 7.62)	-9.86 (-28.39, 8.66)
IS thickness, μm	16.50 ± 1.04	21.67 ± 3.61	23.83 ± 3.12	14.43 ± 1.15	14.16 ± 0.25
Effect size (95% CI)			2.16 (-9.52, 13.84)	-7.24 (-15.35, 0.88)	-7.50 (-16.37, 1.36)
ONL thickness, μm	57.08 ± 4.02	70.17 ± 4.01	70.88 ± 2.88	50.95 ± 0.76	52.81 ± 1.06
Effect size (95% CI)			0.71 (-11.36, 12.79)	-19.22 (-27.79, -10.64)	-17.36 (-27.51, -7.21)
OPL thickness, μm	10.55 ± 0.52	0.81 ± 0.81	5.72 ± 3.05	9.48 ± 0.38	9.76 ± 0.84
Effect size (95% CI)			4.91 (-2.81, 12.63)	8.67 (6.70, 10.63)	8.95 (6.11, 11.79)
INL thickness, μm	37.03 ± 3.02	9.76 ± 0.83	14.71 ± 2.57	29.50 ± 1.70	31.42 ± 1.66
Effect size (95% CI)			4.94 (-1.68; 11.57)	19.74 (14.85; 24.62)	21.65 (17.11; 26.19)
IPL thickness, μm	59.79 ± 3.08	2.85 ± 2.31	2.95 ± 2.60	44.93 ± 7.35	44.25 ± 11.86
Effect size (95% CI)			0.11 (-8.40, 8.61)	42.08 (21.79, 62.37)	41.40 (11.85, 70.96)
RGC/FL thickness, μm	22.37 ± 1.09	0.91 ± 0.91	2.28 ± 2.28	19.28 ± 3.36	17.50 ± 4.07
Effect size (95% CI)			1.37 (-4.63, 7.37)	18.37 (9.16, 27.58)	16.59 (6.38, 26.80)

Effect size: calculated compared with the HI vehicle rat pups.

CHAPTER IV

GENERAL DISCUSSION

AND

CONCLUSION

SUMMARY OF FINDINGS

Using a rat model of term neonatal HIE, I demonstrated that:

1) Neonatal HI induced functional and structural damage to the inner retina, while relatively sparing the outer retina until 2 months following the insult.
2) The extent of injury to the inner retina varied with retinal eccentricity. Specifically, the centre and periphery were more affected than the mid-periphery.
3) There was inter-individual variability in the severity of retinal injury among rats exposed to HI, a finding also reported for the brain injury component of this model. However, the severity of retinal injury did not correlate with the severity of brain injury.
4) Oral sildenafil administered 12 hours following HI improved the functional and structural outcome of retinal injury in a dose-dependent manner.
5) Sildenafil did not have an adverse effect on the development of normal retinal function as assessed with the ERGs.

These findings constitute the first detailed characterization of a retinopathy induced by neonatal HI at term-equivalent age, and demonstrate for the first time a therapeutic potential of sildenafil to treat such retinopathy. Although cellular and molecular mechanisms underlying these findings remain to be elucidated, the findings themselves provide some clues as to what might be happening and raise several interesting questions for future research. The following section discusses these in detail.

COMPREHENSIVE DISCUSSION

1. Outer Retina vs. Inner Retina Susceptibility to HI

The inner retina suffered a much greater damage compared to the outer retina both functionally and structurally at P30 and P60, despite the fact that common carotid ligation and hypoxia should have disrupted the blood flow to both the choroid and retinal circulation. Although we did not explore the mechanisms underlying this discrepancy, it is possible that it involves similar processes as the ones proposed in other animal models of retinal hypoxia/ischemia. A greater susceptibility of the inner retina to hypoxia and/or ischemia has been well documented in adult rodent models of retinal hypoxia/ischemia (Osborne et al., 2004; Block and Schwarz, 1998), as well as in premature rodent models of hypoxia/ischemia (Kaur et al., 2008, 2009; Kiss et al., 2009; Rey-Funes et al., 2010; Huang et al., 2012) and retinal ischemia secondary to hyperoxia-induced vaso-obliteration in the OIR model (Dorfman et al., 2008; Sapieha et al., 2010). An increased susceptibility of the inner retinal cells or the selective resistance of photoreceptors to HI may stem from the differences in the characteristics of the cells themselves or the blood supply.

Photoreceptors have high metabolic demands, and it is probable that they are better equipped to meet their needs when the supply is reduced or to deal with stress. For instance, high mitochondrial content of photoreceptors may protect photoreceptors from apoptosis during hypoxia (Osborne et al., 2004; Bhutto et al., 2012; Mazure et al., 2011). Neuroglobin, an oxygen-binding globin protein which is enriched in photoreceptors, is also known to play an anti-apoptotic role during hypoxia (Schmidt et al., 2003; Yu et al., 2013). Furthermore, photoreceptors have been shown to have a better ability to produce energy by anaerobic metabolism compared to the inner retina (Winkler, 1972; Stone et al., 1999). Photoreceptors are

also more resistant to glutamate excitotoxicity (Lucas et al., 1957; Olney, 1969), an important mechanism underlying ischemic retinal injury (Block and Schwarz, 1998; Kaur et al., 2008). The abundant expression of glutamate receptors on bipolar and ganglion cells, in turn, may explain their increased susceptibility to HI (Osborne et al., 2004).

The photoreceptors and the inner retina are supplied by the choroidal and retinal vasculatures, respectively. The choroidal circulation accounts for approximately 80% of the total blood supply to the eye but has low oxygen extraction, while the retinal circulation receives only 20% of the total blood supply to the eye but has high oxygen extraction (Alm and Bill, 1970, 1973). The large volume of choroidal blood supply may protect photoreceptors when the blood flow is reduced. The maturation status of the two blood supplies also differs. At the time of HI insult (i.e., P10), the choroid and choriocapillaries are already well established whereas the retinal vessels, particularly the deep and intermediate capillary plexuses are still developing (Marneros et al., 2005; Stone et al., 1995). The immaturity of blood vessels may make the inner retinal cells more vulnerable to the insult. Finally, HI may induce a breakdown of the inner BRB, which can further exacerbate inner retina injury while the outer BRB is relatively better preserved (Kaur et al., 2008b). Further investigations are needed to determine which of the abovementioned hypotheses is/are correct.

The next question that arises is whether the initial resistance of photoreceptors will be maintained over time. It has been shown in the OIR model that the photoreceptors, which like in our model, appear unaffected at short-term, degenerate over a longer period of time (P60–P210) (Shao et al., 2011; Zhou et al., 2016). Our results also hint at the possibility of delayed degeneration of the photoreceptors. Although ERG and histology did not reveal significant attenuation of photoreceptor function and structure in chapter 2, and showed a significant but

milder deficit compared to the inner retina in chapter 3, there was some evidence pointing to abnormality both in function and structure. At the level of function, we observed a trend of decreasing ERG a-wave amplitudes with severity at P30 and P60 in chapter 2. In chapter 3, we observed a significant attenuation of the a-wave amplitude at P29, which was restored with an increasing dose of sildenafil. These findings may be signs of damage that is underway. At the level of histology, we observed an increasing thickness of the photoreceptor layers, namely OS, IS and ONL, with severity at P60, which reached a statistical significance in the severe HI group. At P30, the thickness of IS and ONL were significantly increased in the HI group, which again was reversed with higher doses of sildenafil. At first glance, this increase in photoreceptor layer thickness and the decreased a-wave amplitude appear counterintuitive; however, on a closer look, the number of ONL layers appeared to be similar across groups. Therefore, the increased thickness could be due to the loss of support from the inner retina, leading to more loosely packed photoreceptor cell bodies taking up more space. Elongated outer segments may be a sign of underlying RPE dysfunction. The RPE and outer segment of the photoreceptors interact closely, and the RPE is crucial for maintaining the proper length of the outer segment by engulfing the shed membranes during the renewal process (Strauss, 2005). When this function is impaired, outer segments can accumulate in the subretinal space leading to an increased thickness (Strauss, 2005; Matsumoto et al., 2008). Alternatively, inflammation and edema in the subretina could also lead to a thickening of the photoreceptor layers (Yu et al., 2014; Sun et al., 2015).

On retinal histology, we did not find any changes in the RPE thickness in HI animals compared to control at P30 and P60. In order to investigate further, we stained RPE/choroid/sclera flatmount with phalloidin-rhodamine and isolectin B4-FITC at P60.

Phallodin allows visualization of the hexagonal array of the RPE cells, while isolectin B4 stains the endothelial cells and microglia. According to our preliminary data, the HI animals displayed disruption of the RPE cells, as well as infiltration of microglia in the subretinal space (Appendix 1). These findings provide support for the outer retinal damage by HI, which may eventually lead to photoreceptor degeneration. This indeed turned out to be true in our long-term study, which showed progressive loss of the ERG a-wave amplitude over time, and a significant loss of ONL at P360 in rats exposed to HI at P10 (Appendix 2). It will be interesting to study whether choroidal involution plays a role in delayed photoreceptor degeneration in our model, as it did in the OIR model.

2. Susceptibility with Respect to Retinal Eccentricity

A pan-retinal view of retinal histology and the spider graph of retinal layer thickness revealed that the extent of inner retinal damage was uneven across retinal eccentricity. Specifically, at both P30 and P60, the centre and periphery were more severely damaged than the mid-periphery. This is in contrast with the OIR model, in which the central retina is damaged while the periphery appears normal (Shao et al., 2011). According to the literature on retinal development, the rats should have had differentiated retinal layers at the time of insult, along with the fully vascularized superficial plexus and partially vascularized deep plexus reaching approximately 2/3 of the retina from the optic disc; the intermediate plexus would have just begun to form (Stone et al., 1995; Usui et al., 2015). Based on this, it is reasonable to suspect that during HI, the inner retina at the periphery, which is not yet vascularized, did not get enough blood and oxygen for the cells to survive. What could explain the vulnerability of the central retina? Under the physiological condition, the central retina receives the greatest perfusion (Alm and Bill, 1973;

Hill, 1977). Hence, it may be more sensitive to the drop in blood flow. Also, like the blood vessels, the neuroretina matures from centre to periphery and hence the cells in the central retina may be more metabolically active compared to the peripheral cells at the time of insult and therefore have a greater energy demand. One may then propose at least two gradients of vulnerability: 1) Increasing vulnerability from centre to periphery due to decreasing maturity of blood vessels, and 2) Increasing vulnerability from periphery to centre due to increasing maturity of retinal neurons requiring a greater amount of energy. This model could result in a sweet spot in the mid-periphery where the decreased blood flow still meets the metabolic need of the cells to survive.

In order to test if the regional differences in blood supply could explain the pattern of injury we observed in our model, we performed retinal flatmounts and stained the blood vessels using isolectin B4 conjugated to FITC. At P60, the retina of HI rats showed a blood vessel loss that was non-uniform across retinal depth and eccentricity – a pattern similar to what we observed for retinal cytoarchitecture (Appendix 3). Specifically, we observed a near complete drop out of the deep and intermediate plexuses in the retinal periphery in rats exposed to HI at P10. This could mean that following HI the retina failed to vascularize the periphery, which may have rendered that part of the retina hypoxic/ischemic even after the insult. Although the periphery showed the most robust change, the centre and mid-periphery also showed decreased vascularization of the deeper plexuses, and in the severe HI group, the central retina was also nearly devoid of the deeper vessels. Such absence is presumably the result of vaso-obliteration following the death of the inner retinal cells, as horizontal and amacrine cells have been shown to play a crucial role for the maintenance of the deeper vessels (Usui et al., 2015). Our preliminary data are not sufficient to draw any conclusion about the causal relationship.

However, one can appreciate the interaction between the retinal vasculature and the cells that they supply, and gain insight into the involvement of the retinal vasculature in the pathophysiology of the disease.

3. Brain vs. Retina

We confirmed the presence of cerebral damage on the left hemisphere by brain histology, and an associated impaired cerebral visual function by flash VEP. Interestingly, however, the severity of retinal and cerebral injuries did not correlate at the level of the function or structure, suggesting that visual impairments following HI could arise either from retinal injury and/or cerebral injury. This is an important finding since, to date, visual deficits in human newborns with neonatal encephalopathy have been attributed primarily to the abnormalities in the intra-cerebral visual pathways.

It was particularly interesting to note an animal with a close to normal retina showing severe brain injury (1 out of 3 mild HI) and animals with severe retinal injury showing no apparent brain injury (2 out of 6 severe HI). It may have something to do with the way blood flow is redistributed during HI or the individual differences in the anatomy and/or function of the blood vessels, such as the collaterals or the anastomoses (Yamamoto et al., 2004; Costa et al., 1998). In adult animal models, the retina has been reported to be more resistant to HI than the brain, partially due to the ability of the retina to utilize glucose reserve in the vitreous (Osborne et al., 2004; Kuwabara and Cogan, 1961). In our study, at least at the gross anatomical level (histology), a greater number of animals developed a retinal injury compared to a brain injury. This again suggests that retinal injury may play a significant role in visual impairments following HI.

4. Therapeutic Role of Sildenafil in HI Retinal Injury

We demonstrated for the first time that oral sildenafil given with a 12-hour delay following HI had beneficial effects on the outcome of functional and structural retinal injury. The effects were dose-dependent, and the highest dose we tested (50 mg/kg) was able to bring the ERG parameters and layer thicknesses to the values similar to those of control. We also confirmed that sildenafil used at our dose range and duration did not have any adverse effect on the function of the control or the fellow retina, in line with the findings reported in previous studies using adult mice (Behn and Potter, 2001; Nivison-Smith et al., 2014). Given the absence of functional anomaly, we chose not to investigate the retinal histology from the eyes of the control rats and the fellow eyes of the HI rats treated with sildenafil at this time. Based on the previous study (Nivison-Smith et al., 2014), we reasoned that it would be unlikely to see any significant changes at the histological level in these retinas.

Our study did not investigate the possible mechanistic pathways of sildenafil action. According to the literature on the brain neurodegeneration models, sildenafil exerts its effects through multiple pathways, including decreasing apoptosis, decreasing pro-inflammatory signals, and promoting angiogenesis, neurogenesis and synaptogenesis (Bednar et al., 2008; Pyriochou et al., 2007; Caretti et al., 2008; Pifarre et al., 2014; Zhang et al., 2012; Nunes et al., 2012). The net effect appears to be a combination of cell death prevention and the promotion of repair and regenerative mechanisms. Sildenafil has been shown to decrease infarct size and improve motor outcome in the P7 Vannucci model (Charriaut-Marlangue et al., 2014). In their study, a single intraperitoneal injection of sildenafil was given immediately following HI, and the authors argued that the protective effect was through the increased cerebral blood flow after sildenafil (Charriaut-Marlangue et al., 2014). Recently, two groups have looked at the therapeutic role of

sildenafil in an increased intraocular pressure (IOP) model of retinal ischemic/reperfusion injury in adult male Lewis rats (Zanoni et al., 2017; Ezra-Elia et al., 2017). While Zanoni et al. showed a protective effect of sildenafil on the RGCs, Ezra-Elia et al. did not find any significant difference in the RGC counts between sildenafil and placebo treated groups, nor did they find any functional (ERG) improvement. Both studies, however, showed evidence of protection against apoptosis at the gene expression level. The only differences between the two studies were the age of the animals at which increased IOP was induced (6 months for the former and 4 months for the latter), and the route of sildenafil administration (oral for the former and i.p. for the latter). Perhaps the dose they used (1 mg/kg) was not high enough to yield more robust changes. One study looked at the drug's therapeutic role in the mouse OIR model (Fawzi et al., 2014). In their study, sildenafil prevented vaso-obliteration by stabilizing HIF-α, and as a result less neovascularization ensued. Taken together, sildenafil could be exerting its beneficial effects through vascular and non-vascular effects. The fact that sildenafil targets multiple pathways is interesting for our model, as the HI retinopathy most likely involves several of the pathways sildenafil is known to have an effect on – retinal vasculature, inflammation, apoptotic pathways, and synapses (plexiform layers are decreased in thickness in the retina of the HI animals). Further studies are needed in order to elucidate which molecular pathways are involved.

Our results are promising for several reasons. Sildenafil can target both brain and retinal injury at the same time. The fact that sildenafil was effective when given with a 12-hour delay may mean a longer treatment window, compared to neuroprotective strategies, such as NMDA blockers, free radical scavengers, anti-inflammatory agents, and hypothermia (Osborne et al., 2004; Block and Schwarz, 1998; Sabir et al,. 2012). This will be useful in the clinical setting, as therapeutic hypothermia, which is the only available therapy for the asphyxiated newborns with

encephalopathy, needs to be administered within 6 hours of life. Sildenafil, if proven useful in improving neurologic and potentially ophthalmic outcomes in human asphyxiated newborns, can be implemented with ease, due to its low cost, easiness of administration (oral) and relative safety (already being used to treat newborns with persistent pulmonary hypertention) (Shah et al., 2011).

5. Clinical Relevance

We have shown that HI induces severe retinal and cortical visual impairments, and retinal vascular impairment in the rat model of neonatal HIE. An obvious question one might ask is whether human term asphyxiated infants are at risk of developing retinal injury. Few studies exist on this topic. Nickel and Hoyt (1982) reported a hypoxic-ischemic retinopathy syndrome marked by a transient reduction in the ERG amplitudes in three infants of the age 7 to 12 months, who experienced asphyxia at birth. Whyte's group did not find any ERG anomalies in the early postnatal days of asphyxiated infants; however, later some of them developed retinal atrophy, optic nerve atrophy or optic nerve hypoplasia (McCulloch et al., 1991). Due to the timing of the exam, they could not conclude whether the later findings were due to primary injury or retrograde degeneration secondary to brain injury.

We conducted our own study to address this question. We recruited term newborns who had birth asphyxia and were treated with hypothermia. The presence or absence of brain injury was assessed by brain MRI on day of life 10. An ophthalmic exam along with flash ERG and flash VEP recordings were performed on day of life 10, 30, and/or 90 in unsedated infants. Age-matched healthy term newborns were recruited as our control group. Our preliminary data suggest that there may be mild retinal functional anomaly in asphyxiated infants without obvious

structural damage in the retina or the brain (Appendix 4). A greater number of control, as well as a long-term follow-up are needed in order to gain more insight.

6. Limitations and Future Directions

There are some limitations to the model we used. One of these is the age at which HI was induced. As far as the brain is concerned, which is what the Vannucci model was originally developed for, P10 represents a term-equivalent age (Patel et al., 2014). From the retina point-of-view, this age is still slightly premature, in terms of the development of retinal function, structure and vasculature. However, induction of HI by the Vannucci model in P14 (timing of the eye-opening) and P24 (when retinal function reaches the peak of maturation) rats results in the same pattern of retinal injury as seen in rats exposed to HI at P10 (Ghabraie et al., 2016). This confirms the relevance of our findings in the context of term asphyxiated newborns as far as the age is concerned.

Another limitation of the model is the variability in the severity of injury. This variability was already known for the brain part (Rice et al., 2981), and we showed that the severity of the retinal injury also varied. This is important to keep in mind for a treatment study. Some studies have tried to control for the variability factor prior to the administration of the therapy by confirming the presence of brain injury with the MRI (Park et al., 2015) or by measuring the blood flow in the contralateral common carotid artery as a proxy for estimating the risk of developing brain injury (Charriaut-Marlangue et al., 2014). It is currently unclear what causes such a wide range of outcomes in the rats subjected to the same procedure. Human asphyxiated newborns with similar stories also can develop very different outcomes. There are probably genetic components to the varied outcomes. Notwithstanding the above, we did not check for the

presence of retinal injury before sildenafil treatment in our study. However, there was a clear dose-response effect noted in the sildenafil treated animals. Also, we did not observed the most severe presentation of HI retinopathy in the rats treated with the two highest doses of sildenafil. Taken together, we are confident that the beneficial effects we saw were most likely due to the effect of sildenafil.

We did not investigate the possible cellular and/or molecular mechanisms behind HI induced retinopathy or its rescue with sildenafil. As mentioned earlier in the discussion, HI probably sets in motion multiple cascades of reactions that affect the retinal neurons, glia, microglia, and the vasculatures, resulting in cellular dysfunction and death within the weeks (for the inner retina) or months (for the outer retina) following the HI insult. It is possible that sildenafil prevented cellular apoptosis through its effects on pro-survival/anti-apoptotic pathways early on (hours to days); its anti-inflammatory effects could have salvaged the cells from further damage in the days to weeks or months following the insult; its neurorestorative effects (angiogenesis, neurogenesis, synaptogenesis) could have helped provide trophic and vascular supports to help with the repair processes of surviving cells. Evidence for the regenerative potential of mammalian retina is somewhat limited and has only begun to emerge recently (Wohl et al., 2012; Ooto et al., 2004; Close et al., 2006; Engelhardt et al., 2004). More studies are needed in order to elucidate the mechanisms of retinal injury in our model, as well as the mechanisms underlying the beneficial effects of sildenafil.

Hypothermia is the current standard therapy for asphyxiated newborns with neonatal encephalopathy. We did not evaluate the effect of hypothermia on the retina after HI injury in the present thesis. Future studies should be aimed at comparing the effect of hypothermia, sildenafil,

or a combination of both to determine if they offer synergistic benefits to treat the retinopathy resulting from neonatal HI.

In our studies, we only used male rats to eliminate the potential effect of sex. However, sex difference is an important factor to consider in biomedical research. With respect to human term newborns with HIE, males are reported to have a higher incidence and more severe neurodevelopmental outcomes compared to females (Hill and Fitch, 2012). Similar discrepancies were shown also in the rodent models of neonatal HIE (Smith et al., 2014); the differences in sex hormones and genetics were suggested as possible contributing factors to differential response of neurons to an HI insult, such as the neuroprotective effect of estrogen (Hill and Fitch, 2012). Furthermore, the extent and type of benefits offered by hypothermia also appear to differ by sex in rats subjected to the P7 Vannucci model (Smith et al., 2015). There is also evidence of sex difference in retinal function (Chaychi et al., 2015). Taken together, it would be important that future studies compare the effects of HI (and efficacy of treatment with sildenafil or otherwise) on the retina of both sexes.

Another factor that would be interesting to consider in future studies is the strain difference. Different strains of rats have been shown to display different levels of retinal susceptibility to oxidative stress induced by exposure to light (Polosa et al., 2016) or hyperoxia (Dorfman et al., 2009). For example, following postnatal exposure to hyperoxia (to mimic human retinopathy of prematurity) the structure and function of the retina were more severely damaged in pigmented Long-Evans rats compared to albino Sprague-Dawley rats (Dorfman et al., 2009).

CONCLUSION

The present thesis demonstrates that neonatal HI causes permanent retinal injury in a rat model of term neonatal HIE. In addition, a lack of correlation between the severity of retinal and brain injury suggests a possible contribution of retinal injury to the development of visual impairments following birth asphyxia, independent of brain injury. This finding adds to the current understanding of visual impairments in asphyxiated newborns, which was thought to be limited to cerebral damage. The detailed description of the retinopathy at the histological and functional level, and some preliminary data provided in the discussion give us some clues to understand the complexity of this disease process, one that likely involves interactions between retinal cytoarchitecture, function and blood supply. The second part of this thesis demonstrates that sildenafil, a phosphodiesterase type-5 inhibitor, administered post-HI improved all affected ERG parameters and retinal layer thicknesses in a dose-dependent manner, thus showing a promising therapeutic effect of the drug to treat HI-induced retinopathy. Currently, a detailed eye exam including electrophysiological assessments is not part of the standard of care of asphyxiated newborns. Our findings in the animal model as well as the preliminary results in our human study warrant future studies with a greater number of patients and healthy newborns, where their retinal function will be assessed and followed in long-term. Furthermore, sildenafil could potentially be an alternative or additional treatment that could be offered to asphyxiated newborns with neonatal encephalopathy, especially those who might not benefit from hypothermia. A randomized double-blind placebo controlled clinical trial is currently ongoing in our laboratory, and more are needed in order to assess the safety and efficacy of sildenafil in this population. It remains to be determined whether our discovery at the bench will translate to bedside. Nonetheless, these findings lay the ground work for the future studies to build on to

advance our knowledge of brain and retinal diseases in children, which could ultimately lead to the improvement of follow-up, treatment and outcomes of these children. In a broader context, we showed that the Vannucci model can be used as a model to study retinal diseases, and the findings from my thesis can be extended to increase our understanding of other retinal or brain diseases.

CHAPTER V

REFERENCES

REFERENCES

Abman SH (2007) Recent advances in the pathogenesis and treatment of persistent pulmonary hypertension of the newborn. Neonatology 91:283–290.

Alm A, Bill A (1970) Blood flow and oxygen extraction in the cat uvea at normal and high intraocular pressures. Acta Physiol Scand 80:19–28.

Alm A, Bill A (1973) Ocular and optic nerve blood flow at normal and increased intraocular pressures in monkeys (Macaca irus): a study with radioactively labelled microspheres including flow determinations in brain and some other tissues. Exp Eye Res 15:15–29.

Al-Macki N, Miller SP, Hall N et al. (2009) The spectrum of abnormal neurologic outcomes subsequent to term intrapartum asphyxia. Pediatr Neurol 41:399–405.

American Academy of Pediatrics (1992) Relation between perinatal factors and neurological outcome. In: Guidelines for Perinatal Care. 3rd ed. Elk Grove Village, Ill: American Academy of Pediatrics 221–234.

Aminoff MJ, Goodin DS (1994) Visual evoked potentials. J Clin Neurophysiol 11:493–499.

Azzopardi DV, Strohm B, Edwards AD et al. (2009) Moderate hypothermia to treat perinatal asphyxia encephalopathy. N Engl J Med 361:1349–1358.

Barnett CF, Machado RF (2006) Sildenafil in the treatment of pulmonary hypertension. Vasc Health Risk Manag 2: 411–422.

Bednar MM (2008) The role of sildenafil in the treatment of stroke. Curr Opin Investig Drugs 9:754–759.

Behn D, Potter MJ (2001) Sildenafil-mediated reduction in retinal function in heterozygous mice lacking the gamma-subunit of phosphodiesterase. Invest Ophthalmol Vis Sci 42(2):523–527.

Benjamin LE, Hemo I, Keshet E (1998) A plasticity window for blood vessel remodelling is defined by pericyte coverage of the preformed endothelial network and is regulated by PDGF-B and VEGF. Development 125:1591–1598.

Berrones D, Salcedo-Villanueva G, Morales-Canton V, Velez-Montoya R (2017) Changes in retinal and choroidal vascular blood flow after oral sildenafil: An optical coherence tomography angiography Study. J Ophthalmol 2017:1–5.

Bhutto I, Lutty G (2012) Understanding age-related macular degeneration (AMD): relationships between the photoreceptor/retinal pigment epithelium/Bruch's membrane/choriocapillaris complex. Mol Aspects Med 33:295–317.

Block F, Schwarz M (1998) The b-wave of the electroretinogram as an index of retinal ischemia. Gen Pharmacol 30:281–287.

Braekevelt CR, Hollenberg MJ (1970) The development of the retina of the albino rat. Am J Anat 127:281–301.

Brown KT (1968) The electroretinogram: its components and their origins. Vision Res 8:633–677.

Caretti A, Bianciardi P, Ronchi R, Fantacci M, Guazzi M, Samaja M (2008) Phosphodiesterase-5 inhibition abolishes neuron apoptosis induced by chronic hypoxia independently of hypoxiainducible factor-1alpha signaling. Exp Biol Med (Maywood) 233:1222–1230.

Cilio MR, Ferriero DM (2010) Synergistic neuroprotective therapies with hypothermia. Semin Fetal Neonatal Med 15(5): 293–298.

Chan-Ling T, Stone J (1993) Retinopathy of prematurity: its origin in the architecture of the retina. Prog Retinal Res 12:155–178.

Charriaut-Marlangue C, Nguyen T, Bonnin P, Duy AP, Leger PL, Csaba Z, Pansiot J, Bourgeois T, Renolleau S, Baud O (2014) Sildenafil mediates blood-flow redistribution and neuroprotection after neonatal hypoxia-ischemia. Stroke 45(3):850–856.

Chaychi S, Polosa A, Lachapelle P (2015) Differences in retinal structure and function between aging male and female Sprague-Dawley rats are strongly influenced by the estrus cycle. PLoS One 10(8):e0136056.

Chen J, Smith LE (2007) Retinopathy of prematurity. Angiogenesis 10(2):133–140.

Chen XM, Wang NN, Zhang TY, Wang F, Wu CF, Yang JY (2014) Neuroprotection by sildenafil: neuronal networks potentiation in acute experimental stroke. CNS Neurosci Ther 20: 40–49.

Close JL, Liu J, Gumuscu B, Reh TA (2006) Epidermal growth factor receptor expression regulates proliferation in the postnatal rat retina. Glia 54:94–104.

Costa VP1, Kuzniec S, Molnar LJ, Cerri GG, Puech-Leão P, Carvalho CA (1998) Collateral blood supply through the ophthalmic artery: a steal phenomenon analyzed by color Doppler imaging. Ophthalmology 105(4):689–693.

Cuaycong M, Engel M, Weinstein SL, Salmon E, Perlman JM, Sunderam S, Vannucci, SJ (2011) A novel approach to the study of hypoxia–ischemia-induced clinical and subclinical seizures in the neonatal rat. Dev Neurosci 33 : 241–250.

Di Russo F, Martinez A, Sereno MI et al. (2001) Cortical sources of the early components of the visual evoked potential. Hum Brain Mapp 15:95–111.

Dorfman A, Dembinska O, Chemtob S et al. (2008) Early manifestations of postnatal hyperoxia on the retinal structure and function of the neonatal rat. Invest Ophthalmol Vis Sci 49:458–466.

Dorfman AL, Polosa A, Joly S, Chemtob S, Lachapelle P (2009) Functional and structural changes resulting from strain differences in the rat model of oxygen-induced retinopathy. Invest Ophthalmol Vis Sci 50:2436–2450.

Dorfman AL, Chemtob S, Lachapelle P (2010) Postnatal hyperoxia and the developing rat retina: beyond the obvious vasculopathy. Doc Ophthalmol 120:61–66.

Dorfman AL, Cuenca N, Pinilla I et al. (2011) Immunohistochemical evidence of synaptic retraction, cytoarchitectural remodeling, and cell death in the inner retina of the rat model of oxygen-induced retinopathy (OIR). Invest Ophthalmol Vis Sci 52:1693–1708.

Dündar SO, Dündar M, Koçak I, Dayanir Y, Ozkan SB (2001) Effect of sildenafil on ocular haemodynamics. Eye (Lond) 15(Pt 4):507–10.

Edwards AD, Brocklehurst P, Gunn AJ, Halliday H, Juszczak E, Levene M, Strohm B, Thoresen M, Whitelaw A, Azzopardi D (2010) Neurological outcomes at 18 months of age after moderate hypothermia for perinatal hypoxic ischaemic encephalopathy: synthesis and meta-analysis of trial data. BMJ 340:c363.

Eken P, de Vries LS, van der Graaf Y et al. (1995) Hemorrhagic- ischemic lesions of the neonatal brain: Correlation between cerebral visual impairment, neurodevelopmental outcomes, and MIR in infancy. Dev Med Child Neurol 37:41–55.

Engelhardt M, Wachs FP, Couillard-Despres S, Aigner L (2004) The neurogenic competence of progenitors from the postnatal rat retina in vitro. Exp Eye Res 78:1025–1036.

Engels J, Elting N, Braun L, Bendix I, Herz J, Felderhoff-Müser U, Dzietko M (2017) Sildenafil enhances quantity of immature neurons and promotes functional recovery in the developing ischemic mouse brain. Dev Neurosci 39(1-4):287–297.

Ezra-Elia R, Alegro da Silva G, Zanoni DS, Laufer-Amorim R, Vitor Couto do Amaral A, Laus JL, Ofri R (2017) Functional and structural evaluation of sildenafil in a rat model of acute retinal ischemia/reperfusion injury. Curr Eye Res 42(3):452–461.

Fan X, van Bel F, van der Kooij MA et al. (2013) Hypothermia and erythropoietin for neuroprotection after neonatal brain damage. Pediatr Res 73:18–23.

Fang AY, Gonzalez FF, Sheldon RA et al. (2013) Effect of combination therapy using hypothermia and erythropoietin in a rat model of neonatal hypoxia-ischemia. Pediatr Res 73:12–17.

Fang AY, Guy KJ, König K (2013) The effect of sildenafil on retinopathy of prematurity in very preterm infants. J Perinatol 33(3):218–221.

Fawzi AA, Chou JC, Kim GA, Rollins SD, Taylor JM, Farrow KN (2014) Sildenafil attenuates vaso-obliteration and neovascularization in a mouse model of retinopathy of prematurity. Invest Ophthalmol Vis Sci 55(3):1493–501.

Flammer J, Konieczka K, Bruno RM, Virdis A, Flammer AJ, Taddei S (2013) The eye and the heart. Eur Heart J 34:1270–1278.

Foresta C, Caretta N, Zuccarello D, et al. (2008) Expression of the PDE5 enzyme on human retinal tissue: new aspects of PDE5 inhibitors ocular side effects. Eye (Lond) 22:144–149.

Foster A (1988) Childhood blindness. Eye 2(suppl):27–36.

Fruttiger M. (2007) Development of the retinal vasculature. Angiogenesis 10(2):77–88.

Fulton AB, Hansen RM (1985) Electroretinography: application to clinical studies of infants. J Pediat Ophthalmol Strab 22:251–255.

Fuwa K, Hosono S, Nagano N, Takahashi S, Nakashima M (2017) Retinopathy of prematurity after sildenafil treatment. Pediatr Int 59(3):360–361.

Gabrieli CB, Regine F, Vingolo EM, Rispoli E, Fabbri A, Isidori A (2001) Subjective visual halos after sildenafil (Viagra) administration: Electroretinographic evaluation. Ophthalmology 108(5):877–881.

Galli-Resta L, Leone P, Bottari D, Ensini M, Rigosi E, Novelli E (2008) The genesis of retinal architecture : an emerging role for mechanical interactions? Prog Retin Eye Res 27(3):260–283.

Ghabraie M, Jung S, Wintermark P, Lachapelle P (2016) Age and strain modulate the severity of the term neonatal hypoxic-ischemic retinopathy in rodents. Doc Ophthalmol 133 Suppl 1:9–41.

Gluckman PD, Wyatt JS, Azzopardi D, Ballard R, Edwards AD, Ferriero DM, et al. (2005) Selective head cooling with mild systemic hypothermia after neonatal encephalopathy: multicentre randomised trial. Lancet 365:663–70.

Goldstein I, Lue TF, Padma-Nathan H, Rosen RC, Steers WD, Wicker PA (1998) Sildenafil Study Group. Oral sildenafil in the treatment of erectile dysfunction. N Engl J Med 338: 1397–1404.

Granit R (1933) The components of the retinal action potential in mammals and their relation to the discharge in the optic nerve. J Physiol 77:207–239.

Granit R, Riddel LA (1934) The electrical responses of light- and dark-adapted frog’s eyes to rhythmic and continuous stimuli. J Physiol 81:l–28.

Harris A, Kagemann L, Ehrlich R, Ehrlich Y, López CR, Purvin VA (2008) The effect of sildenafil on ocular blood flow. Br J Ophthalmol 92(4):469–473.

Hill CA, Fitch RH (2012) Sex differences in mechanisms and outcome of neonatal hypoxia-ischemia in rodent models: implications for sex-specific neuroprotection in clinical neonatal practice. Neurol Res Int 2012:867531.

Hill DW (1977) The regional distribution of retinal circulation. Ann R Coll Surg Engl 59:470–475.

Hood DC, Birch DG (1990) The a-wave of the human electroretinogram and rod receptor function. Invest Ophthalmol Vis Sci 31:2070–2081.

Horsten GPM, Winkelman JE (1962) Electrical activity of the retina in relation to histological differentiation in infants born prematurely and at full-term. Vision Res 2:269–276.

Hoyt CS (2003) Visual function in the brain-damaged child. Eye 17:369–384.

Hoyt CS (2007) Brain injury and the eye. Eye (Lond) 21:1285–1289.

Huo R, Burden S, Hoyt CS et al. (1999) Chronic cortical visual impairment in children: etiology, prognosis, and associated neurological deficits. Br J Ophthalmol 83:670–675.

Huang HM, Huang CC, Hung PL et al. (2012) Hypoxic-ischemic retinal injury in rat pups. Pediatr Res 72:224–231.

Jacobs SE, Berg M, Hunt R, Tarnow-Mordi WO, Inder TE, Davis PG (2013) Cooling for newborns with hypoxic ischaemic encephalopathy. Cochrane Database Syst Rev (1):CD003311.

Jägle H, Jägle C, Sérey L, Yu A, Rilk A, Sadowski B, Besch D, Zrenner E, Sharpe LT (2004). Visual short-term effects of Viagra: double-blind study in healthy young subjects. Am J Ophthalmol 137(5):842–849.

Jägle H, Jägle C, Sèrey L, Sharpe LT (2005) Dose-dependency and time-course of electrophysiologic short-term effects of VIAGRA: a case study. Doc Ophthalmol 110(2-3):247–254.

Kaur C, Foulds WS, Ling EA (2008) Hypoxia-ischemia and retinal ganglion cell damage. Clin Ophthalmol 2:879–889.

Kaur C, Foulds WS, Ling EA (2008b) Blood-retinal barrier in hypoxic ischaemic conditions: basic concepts, clinical features and management. Prog Retin Eye Res 27:622–647.

Kaur C, Sivakumar V, Foulds WS et al. (2009) Cellular and vascular changes in the retina of neonatal rats after an acute exposure to hypoxia. Invest Ophthalol Vis Sci 50:5364–5374.

Kehat R, Bonsall DJ, North R, Connors B (2010) Ocular findings of oral sildenafil use in term and near-term neonates. J AAPOS 14(2):159–162.

Kim DY, Silverman RH, Chan RV, Khanifar AA, Rondeau M, Lloyd H, Schlegel P, Coleman DJ (2013) Measurement of choroidal perfusion and thickness following systemic sildenafil (Viagra®). Acta Ophthalmol 91(2):183–188.

Kinoshita J, Iwata N, Shimoda H, Kimotsuki T, Yasuda M (2015) Sildenafil-induced reversible impairment of rod and cone phototransduction in monkeys. Invest Ophthalmol Vis Sci 56(1):664–673.

Kiss P, Szogyi D, Reglodi D et al. (2009) Effects of perinatal asphyxia on the neurobehavioral and retinal development of newborn rats. Brain Res 1255:42–50.

Knapp AG, Schiller PH (1984) The contribution of on-bipolar cells to the electroretinogram of rabbits and monkeys. A study using 2-amino-4-phosphonobutyrate (APB). Vision Res 24(12):1841–1846.

Kriss A, Russell-Eggitt I (1992) Electrophysiological assessment of visual pathway function in infants. Eye 6:145–153.

Kurinczuk JJ, White-Koning M, Badawi N (2010) Epidemiology of neonatal encephalopathy and hypoxic-ischaemic encephalopathy. Early Hum Dev 86:329–338.

Kuwabara T, Cogan D (1961) Retinal glycogen. Arch Ophthalmol 66: 96–104.

Lai MC, Yang SN (2011) Perinatal hypoxic-ischemic encephalopathy. J Biomed Biotechnol 2011:609813.

Laties A, Zrenner E (2002) Viagra (sildenafil citrate) and ophthalmology. Progr Retin Eye Res 21:485–506.

Lees KR (2001) Advances in neuroprotection trials. Eur Neurol 45:6–10.

Levine S (1960) Anoxic-ischemic encephalopathy in rats. Am J Pathol 36:1–17.

Loidl CF, Gavilanes AW, Van Dijk EH et al. (2000) Effects of hypothermia and gender on survival and behavior after perinatal anoxia in rats. Physiol Behav 68:263–269.

Lucas DR, Newhouse JP (1957) The toxic effect of sodium L-glutamate on the inner layers of the retina. AMA Arch Ophthalmol 58:193–201.

Lüke M, Lüke C, Hescheler J, Schneider T, Sickel W (2005) Effects of phosphodiesterase type 5 inhibitor sildenafil on retinal function in isolated superfused retina. J Ocul Pharmacol Ther 21(4):305–314.

Luu JK, Chappelow AV, McCulley TJ, Marmor MF (2001) Acute effects of sildenafil on the electroretinogram and multifocal electroretinogram. Am J Ophthalmol 132(3):388–394.

Marneros AG, Fan J, Yokoyama Y et al. (2005) Vascular endothelial growth factor expression in the retinal pigment epithelium is essential for choriocapillaris development and visual function. Am J Pathol 167:1451–1459.

Marsh CS, Marden B, Newsom R (2004) Severe retinopathy of prematurity (ROP) in a premature baby treated with sildenafil acetate (Viagra) for pulmonary hypertension. Br J Ophthalmol 88:298–315.

Martins J, Kolomiets B, Caplette R, Sahel JA, Castelo-Branco M, Ambrósio AF, Picaud S. (2015) Sildenafil acutely decreases visual responses in ON and OFF retinal ganglion cells. Invest Ophthalmol Vis Sci 56:2639–2648.

Matsumoto H, Kishi S, Otani T, Sato T (2008) Elongation of photoreceptor outer segment in central serous chorioretinopathy. Am J Ophthalmol 145(1):162–168.

Mazure NM, Brahimi-Horn MC, Pouyssegur J (2011) Hypoxic mitochondria: accomplices in resistance. Bull Cancer 98:40–46.

McCulloch DL, Taylor MJ, Whyte HE (1991) Visual evoked potentials and visual prognosis following perinatal asphyxia. Arch Ophthalmol 109:229–233.

Michaelson IC (1948) The mode of development of the vascular system of the retina with some observations on its significance for certain retinal diseases. Trans Ophthalmol Soc UK 68:137–180.

Miller RF (1973) Generation of b-wave of electroretinogram. J Neurophysiol 36:28–38.

Moretti R, Leger PL, Besson VC, Csaba Z, Pansiot J, Di Criscio L, Gentili A, Titomanlio L, Bonnin P, Baud O, Charriaut-Marlangue C (2016) Sildenafil, a cyclic GMP phosphodiesterase inhibitor, induces microglial modulation after focal ischemia in the neonatal mouse brain. J Neuroinflammation 13(1):95.

Moschos MM, Nitoda E (2016) Pathophysiology of visual disorders induced by phosphodiesterase inhibitors in the treatment of erectile dysfunction. Drug Des Devel Ther 8:3407–3413.

Mukherjee A, Dombi T, Wittke B et al. (2009) Population pharmacokinetics of sildenafil in term neonates: evidence of rapid maturation of metabolic clearance in the early postnatal period. Clin Pharmacol Ther 85:56–63.

Muttitt SC, Taylor MJ, Kobayashi JS et al. (1991) Serial visual evoked potentials and outcome in term birth asphyxia. Pediatr Neurol 7:86–90.

Nickel BL, Hoyt CS (1982) The hypoxic retinopathy syndrome. Am J Ophthalmol 93:589–593.

Nivison-Smith L, Zhu Y, Whatham A, Bui BV, Fletcher EL, Acosta ML, Kalloniatis M (2014) Sildenafil alters retinal function in mouse carriers of retinitis pigmentosa. Exp Eye Res 128:43–56.

Nunes AK, Raposo C, Luna RL, Cruz-Hofling MA, Peixoto CA (2012) Sildenafil (Viagra®) down regulates cytokines and prevents demyelination in a cuprizone-induced MS mouse model. Cytokine 60:540–551.

Olney JW (1969) Glutamate-induced retinal degeneration in neonatal mice. Electron microscopy of the acutely evolving lesion. J Neuropathol Exp Neurol 28:455–474.

Ooto S, Akagi T, Kageyama R, et al (2004) Potential for neural regeneration after neurotoxic injury in the adult mammalian retina. Proc Natl Acad Sci U S A 101:13654–13659.

Osborne NN, Block F, Sontag KH (1991) Reduction in ocular blood flow results in GFAP expression in rat retinal Müller cells. Visual Neurosci 7:637–639.

Osborne NN, Casson RJ, Wood JPM et al. (2004) Retinal ischemia: mechanisms of damage and potential therapeutic strategies. Prog Retin Eye Res 23:91–147.

Pache M, Meyer P, Prünte C, Orgül S, Nuttli I, Flammer J (2002) Sildenafil induces retinal vasodilatation in healthy subjects. Br J Ophthalmol 86(2):156–158.

Paris G, Sponsel WE, Sandoval SS, Elliott WR, Trigo Y, Sanford DK, Harison JM (2001) Sildenafil increases ocular perfusion. Int Ophthalmol 23(4-6):355–358.

Park WS, Sung SI, Ahn SY, Yoo HS, Sung DK, Im GH, et al. (2015) Hypothermia augments neuroprotective activity of mesenchymal stem cells for neonatal hypoxic-ischemic encephalopathy. PLoS ONE 10(3):e0120893.

Patel SD, Pierce L, Ciardiello AJ, Vannucci SJ (2014) Neonatal encephalopathy: pre-clinical studies in neuroprotection. Biochem Soc Trans 42(2):564–568.

Penn RD, Hagins WA (1969) Signal transmission along retinal rods and the origin of the electroretinographic a-wave. Nature 223:201–205.

Pifarre P, Gutierrez-Mecinas M, Prado J, et al. (2014) Phosphodiesterase 5 inhibition at disease onset prevents experimental autoimmune encephalomyelitis progression through immunoregulatory and neuroprotective actions. Exp Neurol 251:58–71.

Polak K, Wimpissinger B, Berisha F, Georgopoulos M, Schmetterer L (2003) Effects of sildenafil on retinal blood flow and flicker-induced retinal vasodilatation in healthy subjects. Invest Ophthalmol Vis Sci 44(11):4872–4876.

Polosa A, Bessaklia H, Lachapelle P (2016) Strain Differences in Light-Induced Retinopathy. PLoS One 11(6):e0158082.

Pyriochou A, Zhou Z, Koika V, et al. (2007) The phosphodiesterase 5 inhibitor sildenafil stimulates angiogenesis through a protein kinase G/MAPK pathway. J Cell Physiol 211:197–204.

Rapaport DH, Wong LL, Wood ED, Ysumura D, LaVail MM (2004) Timing and topography of cell genesis in the rat retina. J Comp Neurol 474(2):304–324.

Recker R, Adami A, Tone B et al. (2009) Rodent neonatal bilateral carotid artery occlusion with hypoxia mimics human hypoxic-ischemic injury. J Cereb Blood Flow Metab 29:1305–1316.

Reese BE (2011) Development of the retina and optic pathway. Vision Res 51(7):613–632.

Rey-Funes M, Ibarra ME, Dorfman VB et al. (2010) Hypothermia prevents the development of ischemic proliferative retinopathy induced by severe perinatal asphyxia. Exp Eye Res 90:113–120.

Rey-Funes M, Ibarra ME, Dorfman VB et al. (2011) Hypothermia prevents nitric oxide system changes in retina induced by severe perinatal asphyxia. J Neurosci Res 89:729–743.

Rey-Funes M, Dorfman VB, Ibarra ME et al. (2013) Hypothermia prevents gliosis and angiogenesis development in an experimental model of ischemic proliferative retinopathy. Invest Ophthalmol Vis Sci 54:2836–2846.

Rice JE 3rd, Vannucci RC, Brierley JB (1981) The influence of immaturity on hypoxic-ischemic brain damage in the rat. Ann Neurol 9:131–141.

Scher M (2001) Perinatal asphyxia: timing and mechanisms of injury in neonatal encephalopathy. Curr Neurol Neurosci Rep 1:175–184.

Romijn HJ, Hofman MA, Gramsbergen A (1991) At what age is the developing cerebral cortex of the rat comparable to that of the full-term newborn human baby? Early Hum Dev 26:61–67.

Sabir H, Scull-Brown E, Liu X, Thoresen M (2012) Immediate hypothermia is not neuroprotective after severe hypoxia-ischemia and is deleterious when delayed by 12 hours in neonatal rats. Stroke 43:3364–3370.

Samiee-Zafarghandy S, van den Anker JN, Laughon MM, Clark RH, Smith PB, Hornik CP; Pharmaceuticals for Children Act – Pediatric Trials Network Administrative Core Committee (2016) Sildenafil and retinopathy of prematurity risk in very low birth weight infants. J Perinatol 36(2):137–140.

Sapieha P, Joyal JS, Rivera JC, Kermorvant-Duchemin E, Sennlaub F, Hardy P, Lachapelle P, Chemtob S (2010) Retinopathy of prematurity: understanding ischemic retinal vasculopathies at an extreme of life. J Clin Invest 120(9):3022–3032.

Schmidt M, Giessl A, Laufs T, Hankeln T, Wolfrum U, Burmester T (2003) How does the eye breathe? Evidence for neuroglobin-mediated oxygen supply in the mammalian retina. J Biol Chem 278:1932–1935.

Shah PS (2010) Hypothermia: a systematic review and meta-analysis of clinical trials. Semin Fetal Neonatal Med 15(5):238–246.

Shah PS, Ohlsson A (2011) Sildenafil for pulmonary hypertension in neonates. Cochrane Database Syst Rev CD005494.

Shankaran S, Laptook AR, Ehrenkranz RA et al. (2005) Whole-body hypothermia for neonates with hypoxic-ischemic encephalopathy. N Eng J Med 353:1574–1584.

Shankaran S (2012) Hypoxic-ischemic encephalopathy and novel strategies for neuroprotection. Clin Perinatol 39:919–929.

Shao Z, Dorfman AL, Seshadri S, Djavari M, Kermorvant-Duchemin E, Sennlaub F, Blais M, Polosa A, Varma DR, Joyal JS, Lachapelle P, Hardy P, Sitaras N, Picard E, Mancini J, Sapieha P, Chemtob S (2011) Choroidal involution is a key component of oxygen-induced retinopathy. Invest Ophthalmol Vis Sci 52(9):6238–6248.

Siegel J, Gayle D, Sharma A et al. (1996) The locus of origin of augmenting and reducing of visual evoked potentials in rat brain. Physiol Behav 60:287–291.

Smith AL, Alexander M, Rosenkrantz TS, Sadek ML, Fitch RH (2014) Sex differences in behavioral outcome following neonatal hypoxia ischemia: insights from a clinical meta-analysis and a rodent model of induced hypoxic ischemic brain injury. Exp Neurol 254:54–67.

Smith AL, Garbus H, Rosenkrantz TS, Fitch RH (2015) Sex differences in behavioral outcomes following temperature modulation during induced neonatal hypoxic ischemic injury in rats. Brain Sci 5(2):220–240.

Stockton RA, Slaughter MM (1989) B-wave of the electroretinogram: a reflection of ON bipolar cell activity. J Gen Physiol 93:101–122.

Stone J, Itin A, Alon T et al. (1995) Development of retinal vasculature is mediated by hypoxia-induced vascular endothelial growth factor (VEGF) expression by neuroglia. J Neurosci 15:4738–4747.

Stone J, Maslim J, Valter-Kocsi K, Mervin K, Bowers F, Chu Y, Barnett N, Provis J, Lewis G, Fisher SK, Bisti S, Gargini C, Cervetto L, Merin S, Peer J (1999) Mechanisms of photoreceptor death and survival in mammalian retina. Progr Retinal Eye Res 18:689–735.

Strauss O (2005) The retinal pigment epithelium in visual function. Physiol Rev 85(3):845–881.

Sun JK, Radwan SH, Soliman AZ, Lammer J, Lin MM, Prager SG, Silva PS, Aiello LB, Aiello LP (2015) Neural retinal disorganization as a robust marker of visual acuity in current and resolved diabetic macular edema. Diabetes 64(7):2560–2570.

Terrett NK, Bell AS, Brown D, Ellis P (1996) Sildenafil (Viagra^{TM}), a potent and selective inhibitor of type 5 cGMP phosphodiestrase with utility for the treatment of male erectile dysfunction. Bioorganic Med Chem Lett 6:1819–1824.

Tessier-Lavigne M (2000) Visual processing by the retina. In: Principles of neural science (Kandel ER, Schwartz JH, Jessell TM, eds), pp507–522. Now York: McGraw-Hill.

Towfighi J, Mauger D, Vannucci RC, Vannucci SJ (1997) Influence of age on the cerebral lesions in an immature rat model of cerebral hypoxia–ischemia: a light microscopic study. Brain Res Dev Brain Res 100:149–160.

Traudt CM, McPherson RJ, Bauer LA, Richards TL, Burbacher TM, McAdams RM, Juul SE (2013) Concurrent erythropoietin and hypothermia treatment improve outcomes in a term nonhuman primate model of perinatal asphyxia. Dev Neurosci 35: doi:10.1159/000355460.

Tucker AM, Aquilina K, Chakkarapani E, Hobbs CE, Thoresen M (2000) Development of amplitude-integrated electroencephalography and interburst interval in the rat. Pediatr Res 65: 62–66.

Usui Y, Westenskow PD, Kurihara T et al. (2015) Neurovascular crosstalk between interneurons and capillaries is required for vision. J Clin Invest 125(6):2335–2346.

Vannucci RC, Towfighi J, Vannucci SJ (1998) Hypoxic preconditioning and hypoxic–ischemic brain damage in the immature rat: pathologic and metabolic correlates. J Neurochem 71:1215–1220.

Vatansever HS, Kayikcioglu O, Gumus B (2003) Histopathologic effect of chronic use of sildenafil citrate on the choroid & retina in male rats. Indian J Med Res 117:211–215.

Weidman TA, Kuwabara T (1968) Postnatal development of the rat retina. Arch Ophthalmol 79:470–484.

Winkler BS (1972) The electroretinogram of the isolated rat retina. Vision Res 12:1183–1198.

Wintermark P (2011) Current controversies in newer therapies to treat birth asphyxia. Int J Pediatr 2011:1–5.

Wohl SG, Schmeer CW, Isenmann S (2012) Neurogenic potential of stem/progenitor-like cells in the adult mammalian eye. Progr Retin Eye Res 31:213–242.

Wu YW, Mathur AM, Chang T, McKinstry RC, Mulkey SB, Mayock DE, Van Meurs KP, Rogers EE, Gonzalez FF, Comstock BA, Juul SE, Msall ME, Bonifacio SL, Glass HC, Massaro AN, Dong L, Tan KW, Heagerty PJ, Ballard RA (2016) High-dose erythropoietin and hypothermia for hypoxic-ischemic encephalopathy: a phase II trial. Pediatrics 137(6). pii: e20160191. doi: 10.1542/peds.2016-0191.

Wurtz RH, Kandel ER (2000) Central visual pathways. In: Principles of neural science (Kandel ER, Schwartz JH, Jessell TM, eds), pp523–547. Now York: McGraw-Hill.

Xiong T, Qu Y, Mu D, Ferriero D (2011) Erythropoietin for neonatal brain injury: opportunity and challenge. Int J Dev Neurosci 29:583–591.

Yamamoto T, Mori K, Yasuhara T, Tei M, Yokoi N, Kinoshita S, Kamei M (2004) Ophthalmic artery blood flow in patients with internal carotid artery occlusion. Br J Ophthalmol 88:505–508.

Yan F, Zhang M, Meng Y, Li H, Yu L, Fu X, Tang Y, Jiang C (2016) Erythropoietin improves hypoxic-ischemic encephalopathy in neonatal rats after short-term anoxia by enhancing angiogenesis. Brain Res 1651:104–113.

Yazdani A, Khoja Z, Johnstone A, Dale L, Rampakakis E, Wintermark P (2016) Sildenafil Improves Brain Injury Recovery following Term Neonatal Hypoxia-Ischemia in Male Rat Pups. Dev Neurosci 38(4):251–263.

Yi X, Mai LC, Uyama M (1998) Time-course expression of vascular endothelial growth factor as related to the development of the retinochoroidal vasculature in rats. Exp Brain Res 118:155–160.

Yu C, Ho JK, Liao YJ (2014) Subretinal fluid is common in experimental non-arteritic anterior ischemic optic neuropathy. Eye (Lond) 28(12):1494–1501.

Yu Z, Liu N, Li Y, Xu J, Wang X (2013) Neuroglobin overexpression inhibits oxygen-glucose deprivation-induced mitochondrial permeability transition pore opening in primary cultured mouse cortical neurons. Neurobiol Dis 56:95–103.

Zanoni DS, Da Silva GA, Ezra-Elia R, Carvalho M, Quitzan JG, Ofri R, Laus JL, Laufer-Amorim R (2017) Histological, morphometric, protein and gene expression analyses of rat retinas with ischaemia-reperfusion injury model treated with sildenafil citrate. Int J Exp Pathol 98(3):147–157.

Zhang L, Zhang RL, Wang Y et al. (2005) Functional recovery in aged and young rats after embolic stroke: treatment with a phosphodiesterase type 5 inhibitor. Stroke 36:847–852.

Zhang RL, Chopp M, Roberts C, et al. (2012) Sildenafil enhances neurogenesis and oligodendrogenesis in ischemic brain of middle-aged mouse. PLoS One 7:e48141.

Zhang J, Guo J, Zhao X, et al. (2013) Phosphodiesterase-5 inhibitor sildenafil prevents neuroinflammation, lowers beta-amyloid levels and improves cognitive performance in APP/PS1 transgenic mice. Behav Brain Res 250:230–237.

Zhou TE, Rivera JC, Bhosle VK, Lahaie I, Shao Z, Tahiri H, Zhu T, Polosa A, Dorfman A, Beaudry-Richard A, Costantino S, Lodygensky GA, Lachapelle P, Chemtob S (2016) Choroidal involution is associated with a progressive degeneration of the outer retinal function in a model of retinopathy of prematurity: early role for IL-1β. Am J Pathol 186(12):3100–3116.

Zoumalan CI, Zamanian RT, Doyle RL, Marmor MF (2009) ERG evaluation of daily, high-dose sildenafil usage. Doc Ophthalmol 118(3):225–231.

CHAPTER VI

APPENDICES

LEGENDS

Appendix 1. Neonatal HI induced RPE impairment and microglia infiltration at P60. The RPE (*red*) was labelled with phalloidin-rhodamine, and the microglia (*green*) was labelled with isolectin B4-FITC on RPE/choroid/sclera complex flatmounts. 20X. Scale bar, 50 μm.

Appendix 2. Long-term degeneration of the photoreceptor function and structure. (**A**) Representative mixed rod-cone ERG waveforms recorded from the left eyes (ipsilateral to the ligation) of the control and HI rats over time. Calibration: vertical, 500 μV; horizontal, 80 ms. *Arrows*, stimulus onset; *a*, a-wave; *b*, b-wave. (**B**) The amplitudes of the mixed rod-cone a- and b-waves in the control and HI rats over time. Mean ± SD. (**C**) Progressive loss of the a-wave over time in the severe HI animal. (**D**) Retinal histology at P350 showing a thinning of the ONL as well as the inner retinal layers in HI animals. The loss of the ONL thickness was most pronounced at the periphery and centre, while the mid-periphery showed a relative preservation. 40X. Scale bar, 50 μm. (**E**) Spider graph representation of the retinal layer thickness at P350. Mean ± SD.

Appendix 3. Neonatal HI induced retinal vascular impairment at P60. (**A**) Representative confocal Z-stack images of retinal flatmount stained with isolectin B4-FITC, showing the superficial (*blue*), intermediate (*green*), and deep (*red*) vessels. The *schematic* shows the approximate sampling locations. *S*, superior; *T*, temporal; *N*, nasal; *I*, inferior. 20X. Scale bar, 50 μm. (**B**) The number of branching point in superficial and deeper vessels at different eccentricities. Mean ± SD. **, $P < 0.01$ between brackets; ***, $P < 0.001$ vs. control; ###, $P < 0.001$ vs. Moderate HI. $n = 2–4$.

Appendix 4. Evidence of ERG anomalies in term asphyxiated newborns treated with hypothermia. Photopic ERG waveforms from the right (*solid lines*) and left (*dotted lines*) eyes of an asphyxiated newborn with brain injury (patient 1) and one without brain injury (patient 2) are shown. Control waveforms represent the averaged responses of healthy term newborns at the respective ages. Patient 1 (brain injury, normal fundus) showed attenuated and delayed ERG responses on DOL10 and 30. Patient 2 (no brain injury, mild optic disc pallor on DOL10 and 30) showed delayed ERG b-wave peak time on DOL10 and 30. Both patients showed normalized responses on DOL90. *Arrows*, stimulus onset; *a*, a-wave; *b*, b-wave; calibration: vertical, 20 μV; horizontal, 20 ms.

Appendix 1

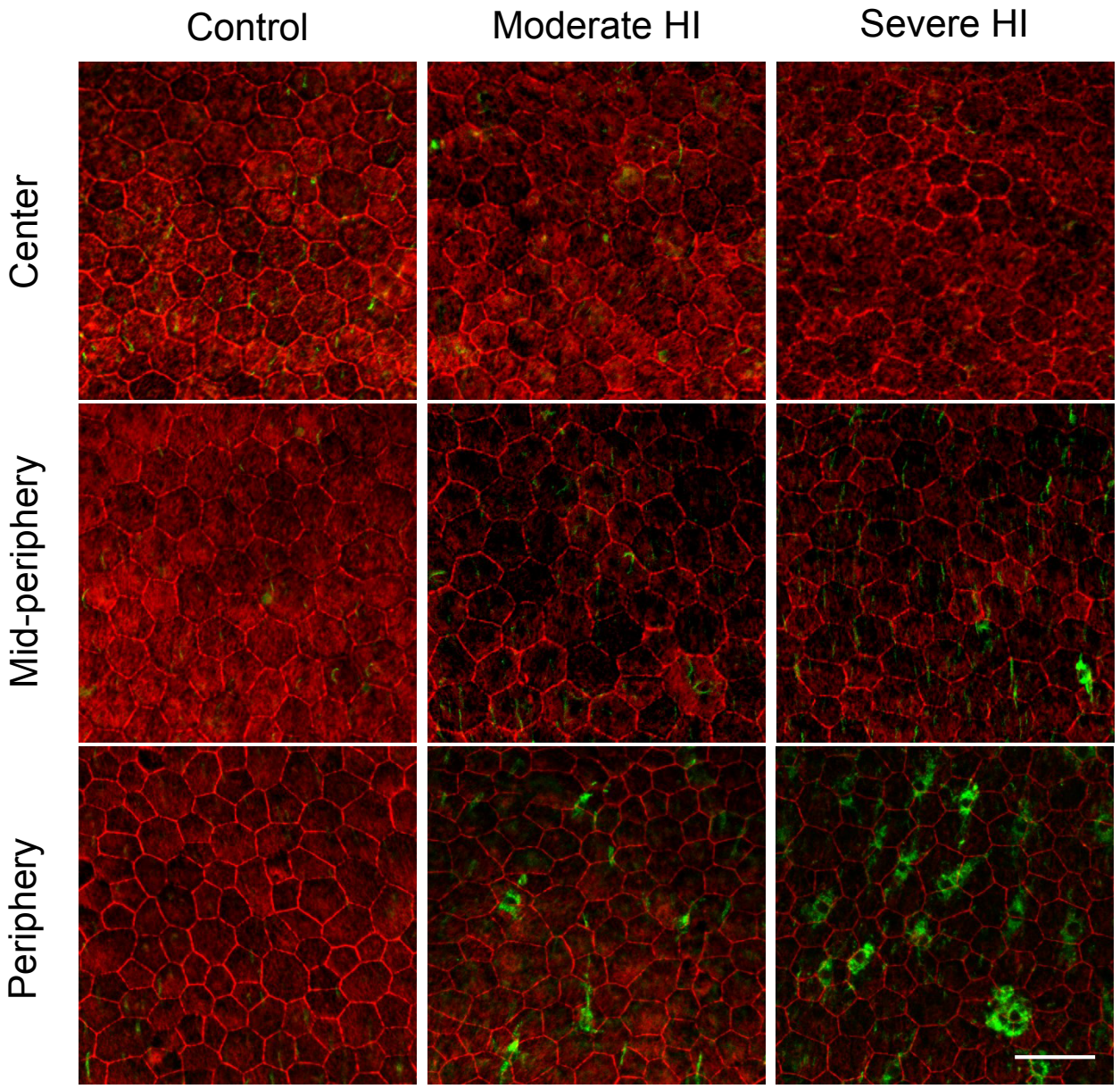
Control
Moderate HI
Severe HI
Center
Mid-periphery
Periphery

Appendix 2

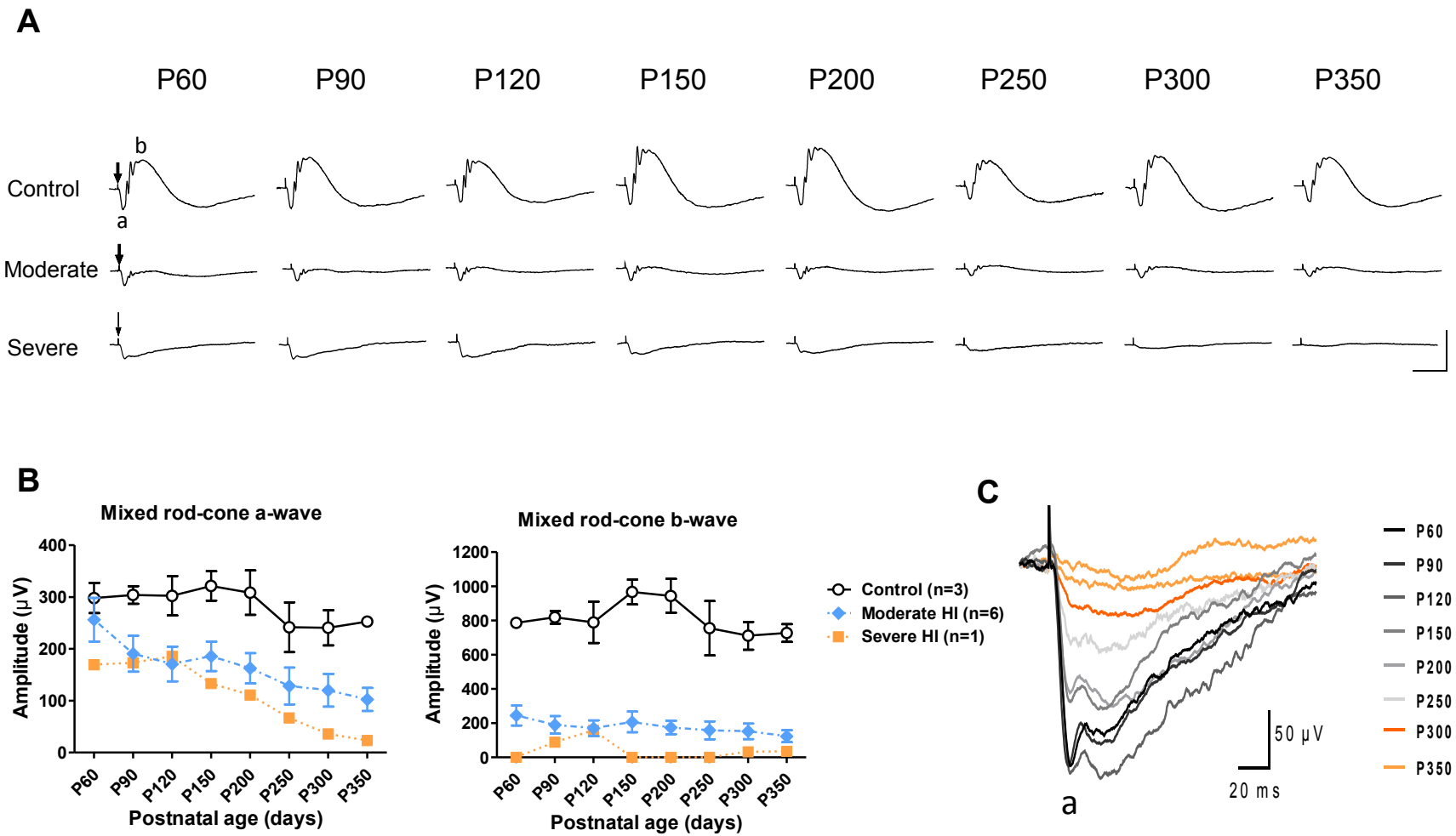
A
P60
P90
P120
P150
P200
P250
P300
P350
Control
Moderate
Severe
b
a
B
Mixed rod-cone a-wave
Amplitude (µV)
Postnatal age (days)
Mixed rod-cone b-wave
Amplitude (µV)
Postnatal age (days)
Control (n=3)
Moderate HI (n=6)
Severe HI (n=1)
C
50 µV
20 ms
a

Appendix 2 (con't)

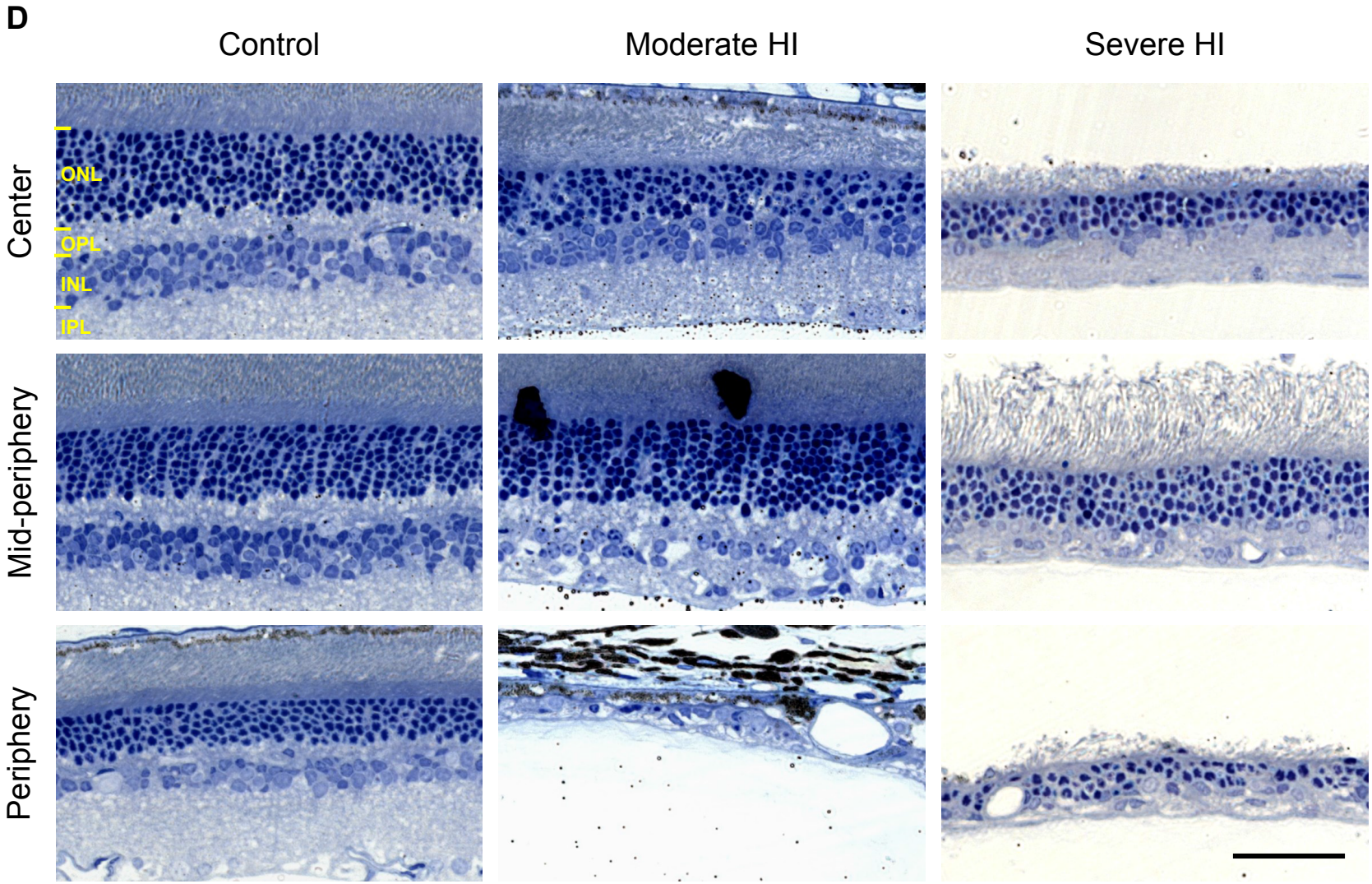

Appendix 2 (con't)

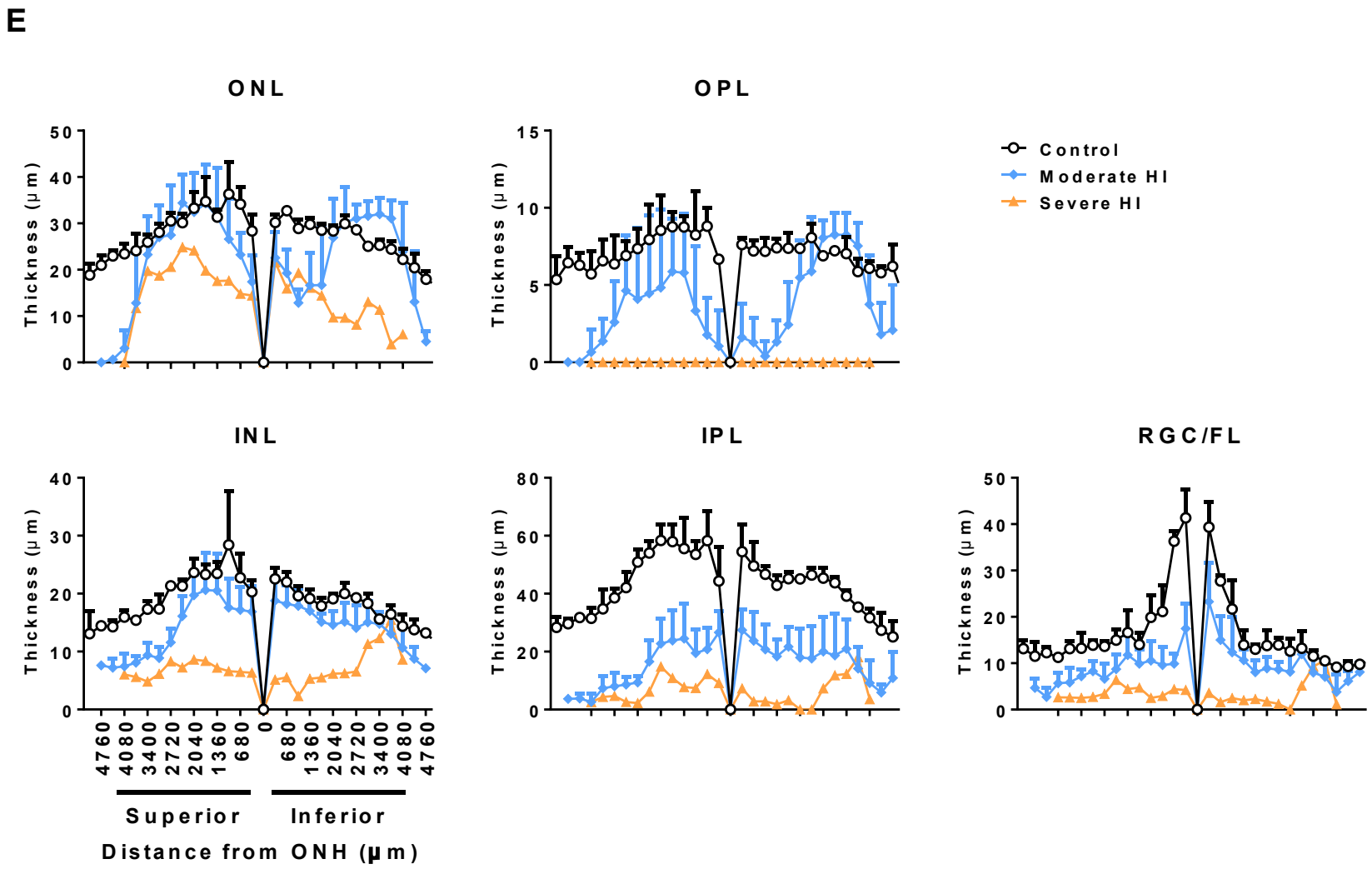

Appendix 3

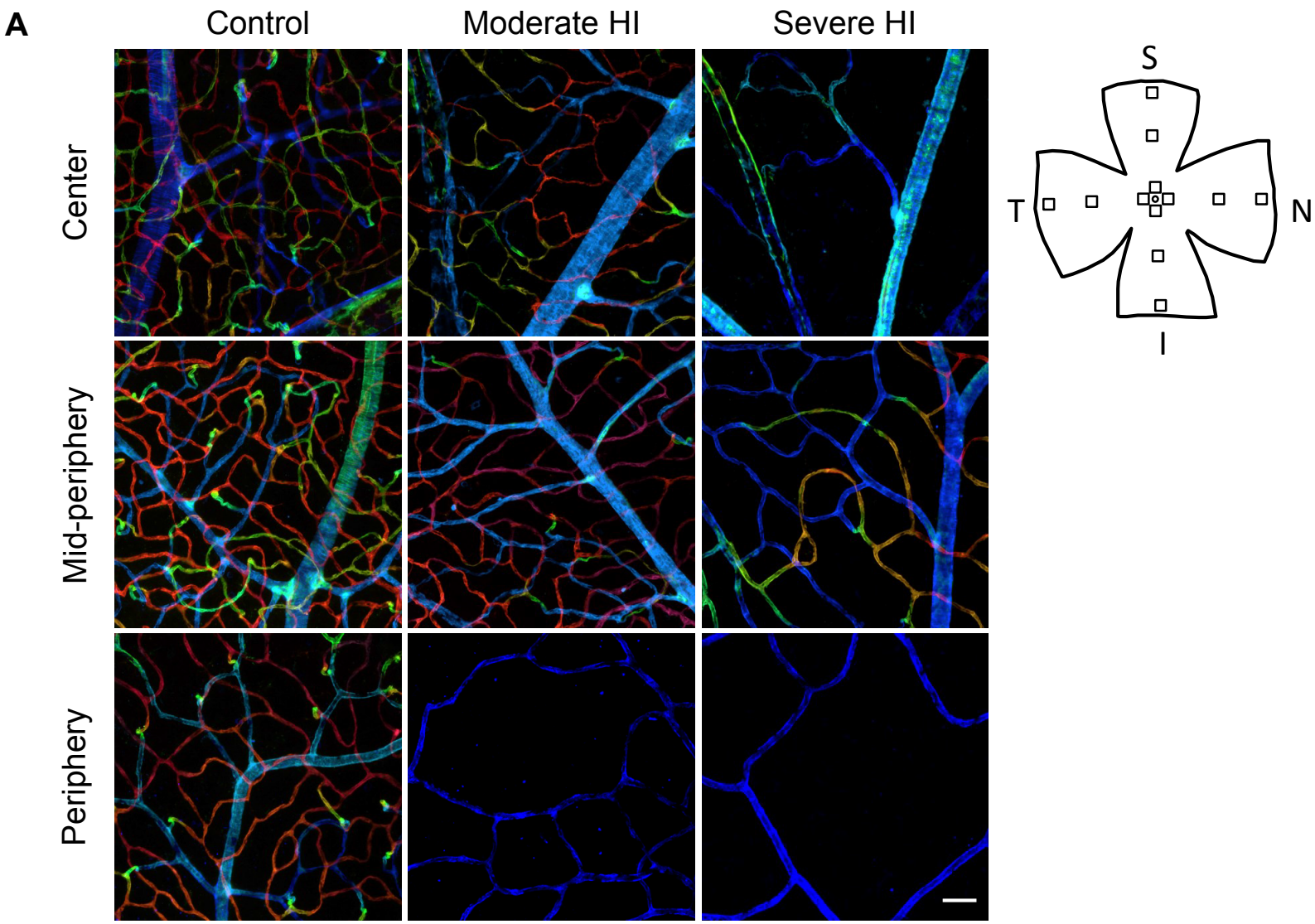
A
Control
Moderate HI
Severe HI
Center
Mid-periphery
Periphery
S
T
N
I

Appendix 3 (con't)

B

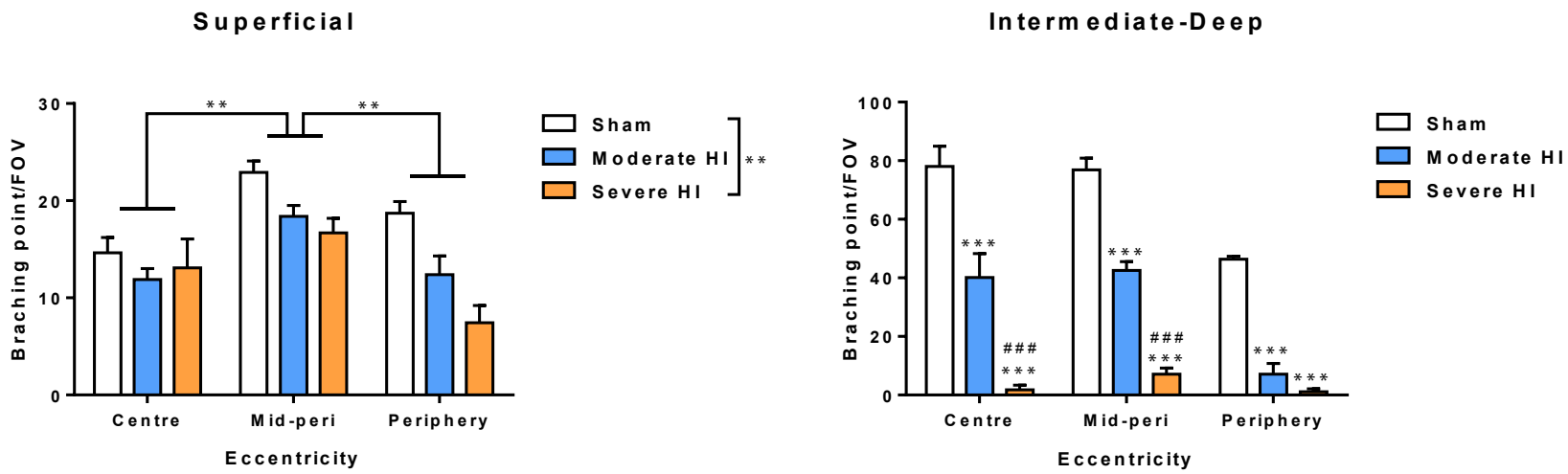

Appendix 4